General Disclaimer

One or more of the Following Statements may affect this Document

- This document has been reproduced from the best copy furnished by the organizational source. It is being released in the interest of making available as much information as possible.

- This document may contain data, which exceeds the sheet parameters. It was furnished in this condition by the organizational source and is the best copy available.

- This document may contain tone-on-tone or color graphs, charts and/or pictures, which have been reproduced in black and white.

- This document is paginated as submitted by the original source.

- Portions of this document are not fully legible due to the historical nature of some of the material. However, it is the best reproduction available from the original submission.

HCMM HYROLOGICAL ANALYSIS IN UTAH

By

Dr. A. Woodruff Miller, Associate Professor

Civil Engineering Department
Brigham Young University
Provo, Utah 84602

Final Report
May 1982

Prepared for
National Aeronautics and Space Administration
Goddard Space Flight Center
Greenbelt, Maryland 20771

Contract No. NAS5--26473

Original photography may be purchased from EROS Data Center Sioux Falls, SD 57198

TABLE OF CONTENTS

LIST OF TABLES

LIST OF FIGURES

1. INTRODUCTION

Studies of water resources have relied upon traditional methods of data collection. These types of data collection are cumbersome and expensive and result in, at best, a representative sample of a given system. The application of remote sensing to the study of the earth's surface has given the researcher an inexpensive tool for the collection of masses of data. These data are not a representative sample, but represent the entire area of study. The increasing sophistication of the instruments make possible the routine application of remotely sensed data to the study of the environment.

Throughout 1978 and 1979 an extensive study was made of Utah Lake, by the Eyring Research Institute, for the Bureau of Reclamation. At this time the National Aeronautics and Space Administration was also collecting data using the Heat Capacity Mapping Mission (HCMM) Satellite. A grant was obtained from NASA to apply the satellite data to the study of Utah Lake. The Heat Capacity Mapping Mission (HCMM) was the first of a planned series of Applications Explorer Missions that involve the placement of small, dedicated spacecraft in special orbits to satisfy mission-unique data acquisition requirements (NASA, 1980). The HCMM supports exploratory scientific investigations to establish the feasibility of utilizing thermal infrared remote sensor-derived temperature measurements of the earth's surface.

The HCMM spacecraft was launched on April 26, 1978, into a nearly sun-synchronous 620 km circular orbit. Local times of equator crossing are 2:00 pm and 2:00 am. This places northern hemisphere, mid-latitude over-flight times at approximately 1:30 pm and 2:30 am. The selected orbit has a 16 day repeat cycle, with a shorter five day period of approximate repeats over some mid-latitude areas. The HCMM orbit covered every area of the earth's surface between the latitudes of 85 degrees north and 85 degrees south at least once during the day and once during the night within the 16-day interval.

2. OBJECTIVES

2.1 Surface Temperature

The first objective of this research was to develop an accurate model for predicting land and water surface temperatures based on the Heat Capacity Mapping Mission (HCMM) sensed thermal infrared radiation. Although a model was supplied with the HCMM Users' Guide, the Project Scientist, John C. Price (NASA, 1980) noted that the preflight calibration was "not well understood". Lindenlaub and Davis (1978) point out that "...the relationship between radiant energy emitted... and temperature...is almost linear over small temperature ranges (for example, between 20 and 30 ^{o}C), thus allowing the use of a simple linear calibration function for the conversion of radiant energy measurements into temperature values". This statement prompted a decision to investigate the possibility of appylying a linear model to the data in hopes of obtaining an accurate linear correlation.

In addition to the development of this linear relationship, an evaluation of the HCMM supplied model was made. An appropriate offset was determined in order to obtain agreement between the model predicted temperature values and surface measured values. NASA (1980) reports that an offset of approximately + 5 ^{o}C has been applied by some other researchers.

In an effort to possibly locate any source of discrepancy between HCMM and ground measurements, as well as provide additional information on the model, the effects of various atmospheric parameters were also examined.

2.2 Water Quality

Another objective of this research was to establish and evaluate the relationship among HCMM sensed surface temperature and reflectivity on Utah Lake and water quality factors including algae concentrations, algae types, and nutrient and turbidity concentrations. The identification and development of measurable relationships would provide a means of employing satellite data to yield water quality information which otherwise would be collected by much less extensive and more costly methods.

The approach to the water quality study was to analyze and compare statistically the measurements made on Utah Lake by the HCMM Satellite with those made by in situ and laboratory testing. Previous studies have been conducted using infrared and near-infrared data to detect algae concentrations, wind influences on algae distribution, algae circulation patterns, and algae types (Bukata, et al, 1974, Tanis, 1978, Piech, et al, 1978, Matson and Berg, 1981, and Egan, 1980). These previous studies employed methods such as spectral analysis of algae specimens, multispectral aerial photographs, or positive film transparencies, and algae data sampling to try to evaluate the effectiveness of the remote-sensing techniques in identifying algae.

This study employed the HCMM discrete pixel intensity values along with field and laboratory measurements to evaluate the degree of accuracy with which the satellite data could identify algae concentrations and seasonal variations. Observations have been made for years on Utah Lake and studies have been carried out to determine the types of algae which grow each season.

Water quality parameters were compared with the HCMM day and night infrared and visible reflectivity measurements. Comparisons are on a one-to-one basis to determine what relationships exist and with what degrees of correlation. Conclusions have been made about the usefulness of the HCMM Satellite data for both directly and indirectly monitoring the water quality parameters.

2.3 Correlation Images

Both the day infrared and reflectance imagery give a good deal of information about the lake. However, the images separately were cumbersome to use. Therefore, another objective was to develop a composite image. These were called correlation images.

From the study of the day infrared and visible data it was anticipated that unique patterns would become clear in the correlation images. The combinations of infrared and reflectance intensities were evaluated in order to possibly identify different phenomena in various areas of the lake. The number of HCMM images available made it possible to also look for rough seasonal variations in the lake.

2.4 Evaporation

In the arid west evaporation accounts for a major loss of the water supply. Calculation of this evaporation is done with evaporation pans, windspeed functions, and computer models. The pan does not accurately model natural water bodies and so the data must be corrected by the use of coefficients. Simple windspeed functions use local data of humidity, temperatures, and wind to estimate evaporation. Most computer models seek to eliminate the need for external data by using latitude, daylight hours, altitude, solar radiation, etc., to estimate evaporation.

An objective of this study was to see if remote sensing offers the capability of using masses of accurate and comprehensive data in the calculation of evaporation. Would there be an increase in accuracy and a decrease in cost by reducing the extensive data collection programs? HCMM data was to be applied to empirical models in order to extend the capability of the models and enhance their accuracy. The satellite data were used to develop a Dalton evaporation relationship and study the effects of wind on temperature and hence evaporation.

Another objective of the research was to study the effects of algae on temperature and evaporation through the use of algae grown in evaporation pans. For years the effect of vegetation on evaporation has been studied with an emphasis on swamp vegetation varying from reeds to trees. Very little has been done to address the subject of algae and evaporation. In a remote sensing application the effect of algae on water is important to know.

The HCMM data were compared to other climatological data of 1978 and 1979. The purpose of these studies was to discover the extent to which HCMM data corresponded to hydrological data. Pan evaporation was compared to the HCMM day and night temperatures and the day/night temperature difference. The relationship of wind to evaporation and temperature was investigated. Also analyzed were the relationship of the HCMM temperatures to the minimum and maximum pan temperatures and the relationship of temperatures in different parts of the lake to each other.

2.5 Thermal Springs

Several studies have been conducted on the location of thermal springs in Utah Lake. Some of the springs around the periphery of the lake have been known for years. The late summer and fall HCMM data have been used in an attempt to locate areas within the lake where significant thermal sources exist. Both day and night thermal infrared data were studied with this objective in mind.

2.6 Groundwater

It has been suggested that shallow aquifers can affect soil surface temperatures. The final objective of this research was to examine the feasibility of using the HCMM sensed surface temperatures to locate areas of near surface groundwater. The depth of groundwater was defined as the depth at which standing water can be found in a shallow hole. The concept of thermal inertia would suggest that diurnal temperature differences would possibly correspond quite accurately to the location of near surface water bodies. However, the lack of corresponding day/night HCMM images constrained this research principally to investigation of absolute daytime surface temperatures. An attempt was made to establish the measurable existance of such a relationship, as well as determine its nature.

3. LITERATURE SURVEY

3.1 Temperature Calibration

The HCMM Users' Guide (NASA, 1980) indicates that there was an instrument calibration problem at launch and that all distributed data are susceptible to errors of the order of several degrees (Celsius). Evaluation of data from five satellite passes in May and June of 1978 prompted a decision to offset the pre-launch calibration values by -5.5 °Celsius in order to force agreement between the satellite and surface measurements. This offset was applied to all standard processed HCMM data.

The initial testing of the calibration of the HCMM thermal sensor was done on METSA III, a freshwater lake surface located near the White Sands Missile Range. The water surface testing target was chosen over two nearby ground surfaces, because of its more uniform physical characteristics (Barnes, 1980).

Further comparisons were carried out for data acquired in October and December of 1978, and February of 1979. The results of these comparisons suggested an offset of approximately + 5 °Celsius (in a direction opposite to the already applied correction). The more recent data would suggest that the prelaunch calibration should not have been modified.

According to Barnes (1980) the data taken during October of 1978 indicated that satellite observed temperatures were substantially cooler than surface truth, giving rise to roughly the same order of temperature differences as before the adjustment was carried out. During the period in question, the water surface in the reservoir used to test the accuracy of the calibrated sensor was lower. The surface temperatures, therefore, may not have been completely uniform. The surface truth measurements, in turn, may not have been truly representative of the large area covered by the HCMM pixel.

As HCMM data are examined in detail by the global scientific community, it is anticipated that this ambiguity will be resolved through a substantial number of satellite/ground truth comparisons (Barnes, 1980). It is also apparent that monitoring of additional parameters describing instrument performance should be considered during the development of future

missions of this type. Although there is no evidence that the radiometer performance changed over the period of time of the mission, this possibility cannot be ruled out based on the apparent change in performance at the time of satellite launch.

Studies are being made involving the calibration of the HCMM model to specific areas. Preliminary results by various researchers have shown that the equation is very sensitive to atmospheric effects, thereby requiring careful calibration to any specific area of study. Variations of several degrees have been encountered when comparing ground truth measurements with predictions from the uncalibrated equation.

3.2 Water Quality Applications

In the water resources engineering field, satellites have provided especially interesting and useful information. Landsat data have been used to observe and analyze biomass circulation, trophic states and some water quality parameters by Welby, et al, (1977) as well as to predict water quality according to water color by Chase and Reed (1973) and to detect algal blooms by Strong (1972). Satellite data have also been used by Egan (1980) to measure turbidity and energy absorption properties of water bodies. Gramms and Boyle (1971) have studied the feasibility of using selected wavelengths for differentiation between algae types. Their research also notes the effects of turbidity on reflectance measurements and an increase in algae distinguishability when phosphorus is removed from the system.

Advanced methods of statistical analysis of Landsat data as presented by Shih and Gervin (1980) in the Okeechobee Lake investigation make satellite data even more useful to the engineer. Successful comparisons by the International Society of Photogrammetry, 1980 Working Group 5 (Schott, et al, 1980) of aerial and surface measurements of several water quality parameters also led to the conclusion that large-scale satellite remote sensing operations can be very valuable when their application to these measurement techniques can be demonstrated.

A study done by Anderson and Horne (1975) on remote sensing of water quality in water bodies in semi-arid climates considered the reflectance caused by gas vacuoles produced by Aphanizomenon flos-aquae, the variations in spectral reflectance of blue-green algae as a function of cell activity, disruption and death, and the reflectance of sediment turbidity. This study,

together with additional analyses conducted and documented by Horne and Wrigley (1975), Wrigley, et al, (1975), Wrigley and Horne (1975), and Wrigley (1980) concerning lake eutrophication, detection of algae circulation patterns, and biomass measurements, all provided knowledgeable background.

Several studies have been made on the growth of algae in Utah Lake and the parameters which affect it. These include studies by Squires, et al, (1979) and Whiting, et al, (1978) on the competitive displacement factors and effects of nutrients and environment on algae growth. Hanson, et al, (1974), explain that ERTS-1 data were not very useful in detecting algae growth on Utah Lake. Research done by Ikeda and Adachi (1978) on the effects of nutrients on phytoplankton growth in Lake Biwa is also applicable to Utah Lake.

In the visible region the presence of algae increases the energy reflected in the green wavelengths and decreases those in the blue. The HCMM band width was large enough to make correction for this unnecessary. Previous studies have preliminarily determined that the presence of algae caused or occurred with increased water temperatures (Whiting, et al, 1978 and Squires, et al, 1979). Several authors have presented detailed lists of Utah Lake algae, the cycles of competitive displacement, and the environmental interactions of the algae (Whiting, et al, 1978 and Squires, et al, 1979).

3.3 Evaporation Studies

Evaporation is of such importance in the analysis of water resources that much research has been directed to this effort over the past decades. As the amount of data available has been historically small, great effort has been made to find suitable relationships that will minimize the need for extensive climatological data. One of the first equations developed was the so called Dalton Equation which involves an empirical windspeed function.

Variations of this equation have been developed (Rohwer, 1931) and many forms of the windspeed function relationship have been used in the derivation of yet other equations (Penman, 1948, Kohler, et al, 1955, Kohler, et al, 1967, and Morton, 1975). The unpublished notes of Dr. A. Woodruff Miller, Brigham Young University, contain many examples.

The Dalton type evaporation relationship was chosen for study because of its applicability to pan data and its simplicity. This relationship states that evaporation is a product of the windspeed function and the vapor pressure difference of the water surface and overlying air.

From published literature, there are several sources of error identified. On small bodies of water a change in windspeed has a significant effect upon evaporation (Morton, 1975, 1979, & 1980, Penman, 1948). The effect of wind on evaporation decreases with the increasing size of the lake (Kohler, 1955). It is expected that Utah Lake is of sufficient size to be free of the wind effects. Previous studies have given estimates of the pan coefficients.

Vapor pressure measurements can be affected by the vapor pressure blanket over the lake. The location at which vapor pressure measurements are taken with respect to that of the wind can induce a "size effect" into the equation. The measurement of vapor pressure should be upwind of the lake in air unaffected by the vapor blanket of the lake. The relationship between temperature and saturation vapor pressure is curvilinear and therefore the use of average daily temperatures and dewpoints bias the equation (Kohler, 1955 and 1967).

The evaporation model which was to be modified for remote sensed data was that of F. I. Morton (1975, 1979, and 1980). This model had been used in previous studies of Utah Lake and had been compared to other evaporation estimates by Miller, et al, (1980).

The growth of algae is such a common occurrence in bodies of water that it was thought that a search of available references would be particularly rewarding. Very few references on the effect of algae on evaporation were found. Rohwer (1931, 1933) suggests that the color of the algae is expected to have a noticeable effect on the amount of evaporation because of the change in color of the water.

There have been studies concerning transpiration and vegetation covered bodies (Idso, 1981 and Eisenlohr, 1966). The effect of swamps on evaporation has been covered in other studies (Rijks, 1969, Linacre, et al, 1970, Linacre, 1976, and Munro, 1979).

Size and location are important factors in describing the evaporation of a swamp. Evaporation from the perimeter of an extensive swamp or from a long narrow swamp is enhanced by the prevailing wind. The low humidity and

the additional energy from the warm winds will increase evaporation. It has been concluded by Rijks (1969) that the amount of evaporation in a swamp increases with an increase in windspeed although the relationship is complicated by canopy roughness. This is in accordance with the premise of the windspeed function.

3.4 Groundwater Studies

A review of available literature on the use of satellite data for determining groundwater depths through correlation with surface temperatures yielded very little. Much of the research dealing with HCMM data is currently being done and is therefore not yet published. The ability of remote sensing to detect groundwater, however, has been recognized for more than three decades (Reeves, 1975). On conventional aerial photographs, springs and seeps are located indirectly by identification of particular vegetation types, especially in arid regions.

In expanding the search to include related material, it was found that Rosema and Bijleveld (1978) had done an investigation using HCMM data to estimate the surface relative humidity of bare and scarcely vegetated soils. Their procedure involved estimating the moisture content of the top layers of soil. Their conclusion that vegetative cover and soil mineral composition both have a significant effect on HCMM values was considered relevant to this study.

Whiting (1976) noted that there is a direct relationship between the measured temperature of bare soil, as well as vegetated areas, and the amount of moisture in that soil. Furthermore, although airborne infrared scanners had frequently shown variations in soil moisture from a qualitative point of view, very little work of a quantitative nature had been documented. One of the primary reasons given for this was the lack of quantitative ground truth measurements for correlation with airborne data.

Le Shack, et al, (1975), using measurements from a number of agricultural fields, obtained a direct linear relationship between soil moisture (sampled 10 cm. below the ground surface) and the maximum daily surface temperature (Ts max). A sign discrepancy (compared to theory and other experimental data) was noted, however, and the overall range of surface

temperatures examined was only 3 °Celsius. Previously, Bartholic, et al, (1972) had claimed that Ts max of bare fields decreased as near surface soil moisture content increased.

Idso and Schmugge (1975) reported that remote sensing of surface soil temperature may provide a practical means of assessing soil water status in the uppermost few centimeters of bare soil. Also noted was the need to establish the feasibility of obtaining the required temperature measurements from satellite remote sensors and more precisely define the depth to which water contents could be inferred from surface temperature measurements.

Tunheim and Beutler (1980) reported an attempt to use thermal-infrared images to locate springs and wells through the location of near surface groundwater in South Dakota. Two principle conclusions from this study were: (1) Bare soil plots with different soil moisture differ in surface temperature during the diurnal cycle, and (2) A thick crop canopy destroys the apparent surface difference during nighttime hours. They indicated that due to a large number of variables (atmosphere, wind, humidity, etc.) the differences in surface measurements show much better correlation that absolute values. This was attributed to a partial cancellation effect when dealing with differences. Also, Tunheim and Beutler (1980) noted that the predawn data was most useful for identifying shallow aquifers. The need for a model relating subsurface soil moisture to surface temperature was emphasized in their report.

Another study by Bonn (1977) gave evidence that grass covered areas gave smaller temperature variations than those for bare ground. Ground truth measurements showed better correlation to remotely sensed data in vegetated areas if taken at approximately two-thirds of the canopy height above the ground surface. This would seem to indicate that ambient air temperatures have a significant effect on remotely sensed data in vegetated areas and need to be taken into account.

Myers (1970) examined the ability of thermal infrared data to detect the presence of shallow acquifers in an area covered by glacial drift. Thermal infrared data were obtained just before dawn during the month of August. It was felt that at this time of the year shallow aquifers would be cooler than their surroundings and the presence of cool areas in the imagery was expected to indicate the presence of shallow aquifers. The results of the statistical analysis indicated a significant correlation between the thermal

data and aquifer thickness, thermal diffusivity coefficient, and depth to bedrock. Apparently, the correlation with depth to water and depth to the top of the aquifer were not statistically significant.

4. STUDY AREA

4.1 Utah Lake

This HCMM hydrological study was carried out using Utah Lake (Figure 4.1) as the primary target. Utah Lake is located in central Utah, approximately 40 miles south of Salt Lake City and is the primary freshwater lake in the Jordan River drainage basin. The lake is one of the largest freshwater lakes west of the Mississippi River, covering approximately 385 km (95,000 acres) at "compromise level" (1368.35 m, 4489.34 ft.). The compromise elevation is the established level to which the lake is permitted to rise before free flow through the outlet works is allowed.

Although the lake covers over 25% of the valley floor, it has an average depth of only 2.4 m (Fuhriman, et al, 1974). Utah Lake is a shallow, unstratified, eutrophic, arid region lake with approximately 50 surface inflows and one surface outflow. The water is highly turbid with Secchi depth readings averaging 24 cm and ranging from 12 cm to 50 cm. The lake basin receives inflow from numerous mineral springs within and around the periphery of the lake and as a result the water has a high carbonate and sulfate content.

An accelerated eutrophication process has occurred in Utah Lake. When the Mormon pioneers first settled in this area the Utah Lake fish population was dominated by a species of cutthroat trout (Salmo clarki) which was adapted to the already slightly eutrophic conditions of the lake. Due to the use of Utah Lake and tributaries for irrigation and waste disposal and the introduction of other fish species into the lake, the trout have become extinct (Whiting, et al, 1978).

The growth of algae in Utah Lake has increased with the increase in nutrient loads caused by sewage disposal into the lake and the return flows from irrigated fields, pastures and corrals in the drainage basin. Algal blooms on the lake during late summer and early fall are common. The large algae concentrations in Utah Lake cloud and discolor the water and produce obnoxious odors and decomposing mats of organic matter on the surface and around the shoreline. Perhaps the most serious concern is the depletion of dissolved oxygen in the lake caused by the decaying algae. All of these

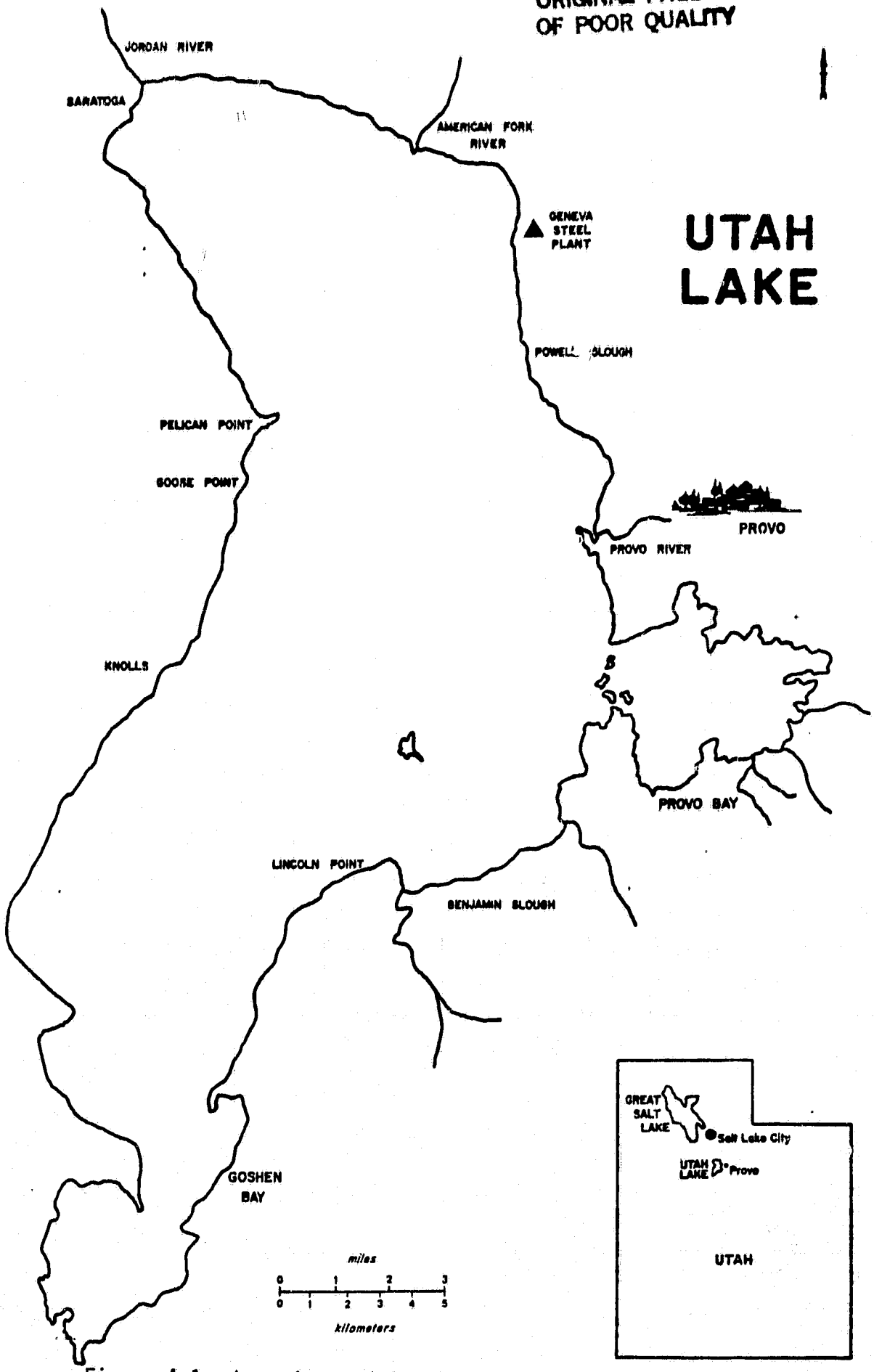

Figure 4.1 Location and Configuration of Utah Lake.

factors combine to reduce the attractiveness of the waters of Utah Lake for use as a domestic or industrial water supply and as a site for fishing, swimming or skiing.

The lake is considered an ideal size for the satellite imagery study, covering approximately 40 X 70 HCMM pixels. A large water body has several distinct advantages for a remote sensing hydrology study. Several of the more important advantages are homogenity, thermal stability, minimal relief, and size. Jackson (1980), in attempting to use HCMM imagery, indicated that it is extremely difficult to locate a nine pixel sized field.

Utah Lake is a vital part of the Central Utah Project being developed to fulfill the need for water in these valleys. Measurements of water quality parameters in Utah Lake have been made for several years, including 1978 and 1979. The existence of the large number of recorded measurements made Utah Lake the ideal location for analysis and comparisons of ground-truth measurements with the data returned by the HCMM Satellite.

4.2 Southeast Utah Valley

The area immediately to the southeast of Utah Lake was chosen to study the correspondence of HCMM intensities to near surface groundwater. This area is chiefly agricultural, but is broken by large tracts of land too poorly drained to be effectively farmed. These poorly drained, "high groundwater" areas are ideal for the groundwater portion of this study. Numerous areas cover several pixels spacially and due to their close proximity to Utah Lake, are relatively easy to locate. The actual area examined extends from the foot of West mountain, in an easternly direction, to the residential area of Springville, Payson and Spanish Fork. The southern boundary is roughly between Payson and the southernmost extremity of West mountain, while Utah Lake marks the northern limit. The study area is generally quite flat, largely between 5 and 20 feet above the surface of the lake.

5. HCMM DATA

5.1 Instrumentation

The HCMM satellite carries a single sensor, the Heat Capacity Mapping Radiometer (HCMR). It acquires high spacial resolution daytime reflected and thermal infrared data. The HCMR has a geometric instantaneous field of view (IFOV) of 0.83 milliradians, high radiometric accuracy, and a wide coverage swath on the ground. The instrument is a two channel scanning radiometer, one spectal channel covers the reflectance band from 0.5 to 1.1 micrometers, while the other channel views the thermal infrared band between 10.5 and 12.5 micrometers. The two channels thus provide measurements of reflected solar and emitted thermal energy, respectively. The overall measurement accuracy in the thermal channel is approximately 0.5 ^{o}C at 280 ^{o}K.

The spacial resolution of the infrared channel is approximately 600 by 600 meters at nadir. These values are masked by data processing, which generates registered data at a 481.5 meter pixel size. The swath of data coverage along the track is approximately 716 km wide. The scale of imagery is nominally 1: 4,000,000. The HCMM satellite officially terminated its mission in October of 1980, having provided reliable data chiefly during 1978 and 1979.

5.2 Data Products

For convenience master output tables were used which consisted of digitized raw counts from both channels 1 and 2 of 8-bit (0-255) indices. This yielded the result that a count value from any of the HCMR data tapes always represented the same value of radiance or temperature. These data were used to produce geometrically corrected images of day and night temperature and day radiance intensities.

HCMM Satellite data employed in this study were supplied by NASA as positive and negative prints of thermal and reflective intensities, represented by grey tones, together with computer compatible tapes. A total of 23 HCMM daytime images were available for the study area. Five HCMM night images were also available. Table 5.1 lists the dates of images used.

Table 5.1

Dates of HCMM Images Used

Type	Day	Month	Year	Type	Day	Month	Year
Day	13	May	1978	Day	24	March	1979
"	6	July	"	"	14	July	"
"	22	"	"	"	9	August	"
"	27	"	"	Night	9	"	"
"	2	August	"	Day	25	"	"
"	7	"	"	"	4	September	"
"	11	"	"	Night	4	"	"
"	17	"	"	Day	11	"	"
"	23	"	"	Night	11	"	"
Night	12	September	"	Day	16	"	"
Day	13	"	"	"	21	"	"
"	23	"	"	"	14	November	"
Night	23	"	"				
Day	9	October	"				
"	14	"	"				
"	25	"	"				

5.3 Utah Lake Location

The computer tapes were used to generate line printer maps on which Utah Lake was located in order to match particular pixels with measurements made on the lake itself at about the same time. The HCMM scene is about 700 km square. From this it was necessary to locate and extract the Utah Lake window. The starting row and column of this window within the full image were established. The distance was measured to the corner of the window on the NASA print. This was then used to calculate the number of rows and columns. The VAX computer system was used to locate and extract the Utah Lake windows.

HCMM digital thermal and reflective data were printed on a line printer as a two dimensional array in a Fortran I3 format. Locating the Utah Lake study area was rarely difficult, due to the characteristic difference between land surface and water surface radiation values (Figure 5.1). Differences were on the order of twenty to fifty intensity units (7 to 16 ^{o}C)

5.4 Sampling Stations Location

Location of corresponding township and range lines was necessary because most available surface data was referenced to the State Township and Range System. While the lake body was easily located, the scale was severely distorted due to the digitized format. It appeared as roughly a 3 horizontal (east-west) to 1 vertical (north-south) proportion as compared to actual ground distances. The daytime lake map was skewed approximately 11 degrees, apparently as a function of the flight path of the HCMM Satellite. The nighttime images exhibited a skew of approximately 15 in the opposite direction.

Township and range lines were located by using geometric triangulation and scaling ratios, employing several prominent features located around the lake as reference points (Figure 4.1). The east-west protrusions were much more prominent on the HCMM digital images than were north-south protrusions. Due to this amplified prominence, east-west protrusions were used wherever possible in the triangulation procedure.

Having established the most prominent triangulation points, alternating section lines, both north-south and east-west, were scaled vertically and horizontally across the study area. The scaling was done by using U.S. Geological Survey quadrangle maps. These section lines were then transferred to an overlay of the Utah Lake line printer maps, using the

```
148147144140136136136134134137136140145149145142145141113 86
147142140139138140138138139140139140145147145145143125 96 81
146144140140141142139141146145143146149151150152142109 86 82
144142141138137138141142144145144148149149154149125 91 83 82
141143144141138139142143146147147149148144140121 98 82 79 80
146145147147146145144144147148149153153135105 89 83 82 80 79
145146148148147147147146146148152138119 98 84 79 80 80 79 79
147149148148148148146149155154137104 87 82 80 79 79 78 78 80
150153154154151150150153143118 97 85 80 80 80 80 79 80 80 79
149152154159157153148135107 84 79 78 77 76 75 76 76 76 76 75
150154159160158152144113 88 79 79 80 79 78 77 77 76 76 77 78
153152155156152143118 86 79 79 77 77 76 77 76 77 77 76 75 77
161156161149142110 87 79 79 77 77 77 77 76 76 77 76 76 76 76
159157151144125 94 82 80 79 79 77 78 78 78 77 77 78 79 79 78
154149142115 90 79 77 76 75 75 74 74 76 75 76 75 75 76 76 77
151146128 97 81 78 79 77 76 75 74 75 76 75 75 75 75 76 76 76
147136110 88 80 79 78 76 76 76 76 76 77 77 76 76 77 76 77 77
147121 90 78 78 78 76 75 73 74 73 75 75 75 75 75 74 75 76 75
147121 89 80 79 78 76 76 74 77 76 76 76 76 77 77 77 78 77 78
143124 95 80 78 78 77 77 75 75 76 75 75 75 75 75 76 77 78 77
147134112 86 79 78 76 76 75 74 75 75 75 74 76 76 76 77 78 81
145143136109 85 76 76 76 74 74 74 75 74 74 75 75 77 77 81102
139138130123103 82 76 73 73 73 73 73 73 74 74 76 76 80 99132
141134118119118 92 76 77 76 75 75 75 74 76 75 77 79 97124148
141138119 99 95 85 76 75 75 75 74 74 73 75 75 78 93129148149
139142126 91 76 75 75 73 73 73 73 73 74 75 74 80106143150147
138141126 94 80 77 76 74 73 72 72 74 75 76 74 85114146147138
133140129101 80 76 75 73 73 72 71 74 75 75 77107139149142143
132139138115 91 77 75 75 73 74 74 73 74 78100138155149139127
132142141131111 85 79 77 77 76 76 76 81101132154156146135133
140148133137127102 84 79 78 76 77 77 88117143154152142133130
145145141138135119 95 79 77 76 76 78 82 95127149144135134133
146145142143141132115 91 80 74 74 75 75 73 93124124119121126
149145140138135135131108 85 79 78 80 82 97117126126124127131
148132133125122125129116 92 80 79 79 87124143132128128127131
146137127122116115123119 98 82 80 90111134138131128129130130
142127119112103 97101014 93 82 89115133143142137132133134131
142123111101 93 89 86 88 85 86104116119135146141134135136135
131115101 91 87 86 83 82 82 97114111113132148145141139137136
138121102 89 84 81 81 80 83102117114114130140146145139136136
143126104 93 92 87 82 81 91110117111110120134154151140138139
147131112108113110107108116119113109107114126150153146140144
135126120122126131126125122112105106109115114127145151144146
139132131129131136133128122115112107107116117114124146148146
135131133132133131132132129124117104101107110104105132146145
138138137133129130132130124114106103102103105104104119140145
```

Figure 5.1. HCMM Sensed Land Surface Emissivity vs. Water Surface Emissivity (Goshen Bay Area)

distance ratios as determined from the quadrangle maps. The non-scaled section lines were then drawn exactly between the scaled lines. This method proved to yield sufficiently accurate overlays of the study area.

Overlays of Utah Lake were prepared for each format and the sampling points identified on them. These overlays were then placed on the HCMM data printouts to identify the pixel intensity values which corresponded with the local sampling stations for any particular day. Tables containing the pixel intensities together with the other measurements made at the sampling sites for each day when data were available were made.

6. GROUND TRUTH DATA

6.1 Sampling Stations

During the period when the HCMM was collecting data, several studies of Utah Lake were also carried out. These studies, sponsored by the U.S. Bureau of Reclamation, produced the data with which the HCMM information was evaluated. The Water Quality, Hydrology and Aquatic Biology (WHAB) study was conducted by the Eyring Research Institute, of Provo, Utah and consisted of an extensive sampling and evaluation of Utah Lake waters at 15 stations throughout the lake. The locations of these sampling stations are indicated on Figure 6.1. The prefixes indicate the area of the sample stations, i.e., UL-Main body of Utah Lake, GB-Goshen Bay at the southern end of Utah Lake and PB-Provo Bay on the eastern side of the lake.

Transect sampling was done on September 28 and November 21, 1978 and April 25 and 27 and July 16 and 17 of 1979. These transects were established in separate parts of the lake in order to determine whether the biota at a point in time were homogenous throughout the lake or showed local variations. Samples were taken quarterly so that seasonal variations in the biota could also be determined. Figure 6.2 shows the locations of these transects and sampling points. Information on the WHAB studies included herein is from Rushforth, et al, (1980 and 1981).

6.2 Temperature Measurements

Water temperature, being a relatively important water quality parameter, was routinely included in the water quality data. Examination of this data revealed that fourteen stations had data pertinent to this study. These stations are chiefly in the central parts of the lake, thus reducing the possibility of the shoreline influencing the radiation measured by the HCMM sensor. Data from the stations that were in closer proximity to the shore, primarily the Provo Bay and southernmost Goshen Bay locations, were analyzed carefully to insure that no land surface overlapped the pixel boundary. WHAB data are tabulated in Merritt, et al, (1981).

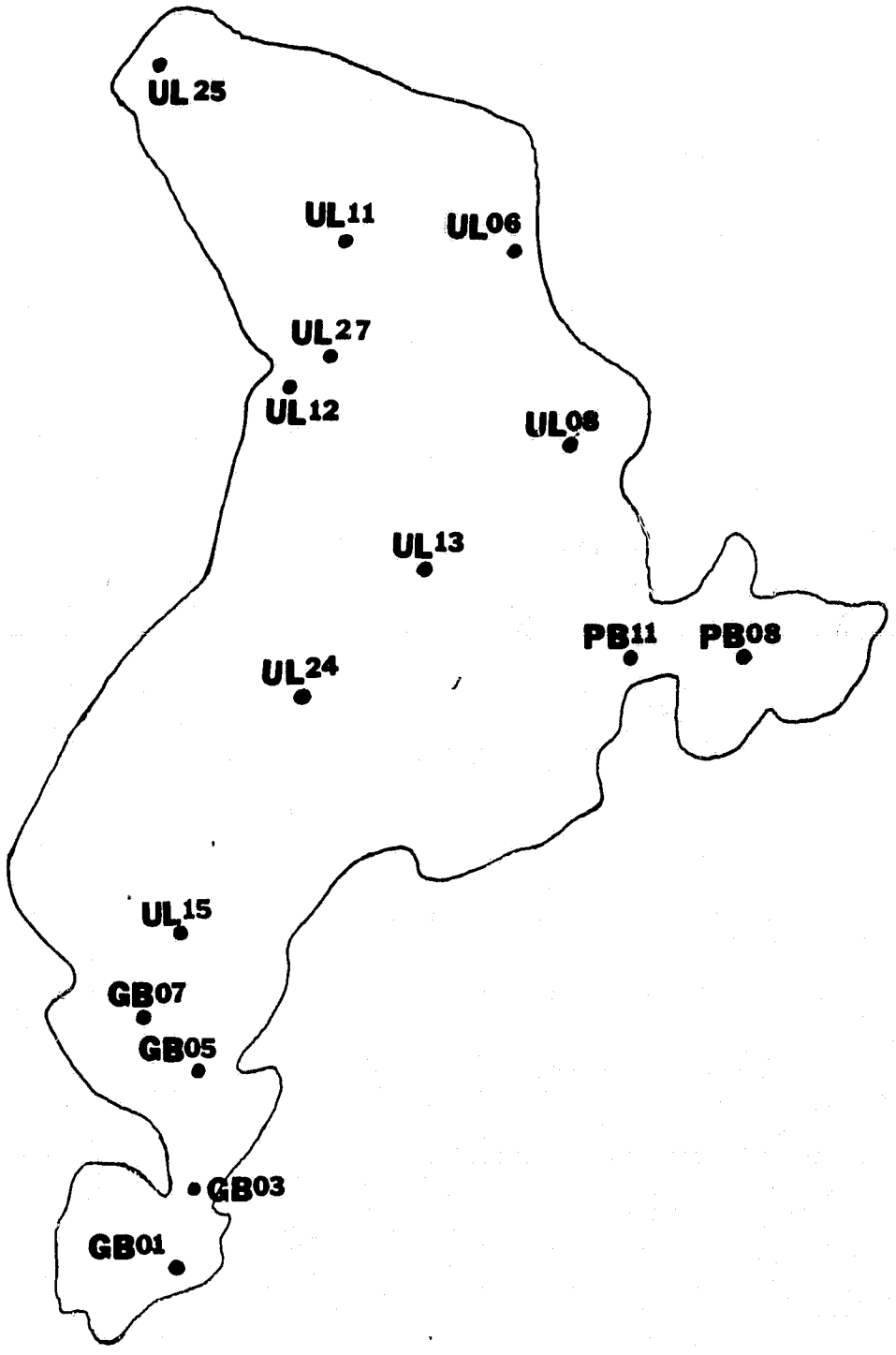

Figure 6.1. Map of Utah Lake showing locations of sampling stations established in the lake.

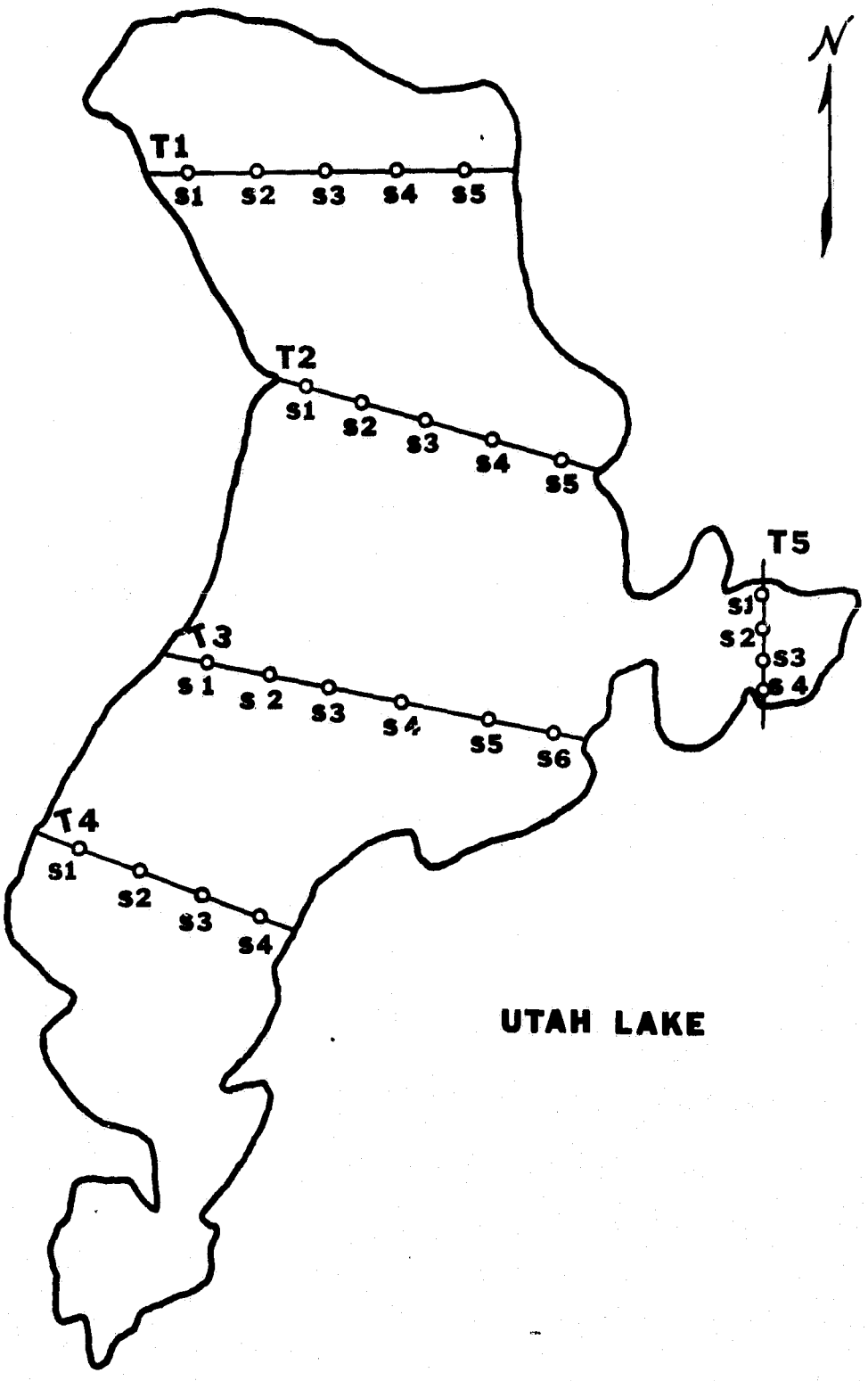

Figure 6.2. Map of Utah Lake showing the position of transects and collecting stations established in the lake.

The other important source of temperature calibration data was a study done by the Utah State Division of Wildlife Resources. This project involved the capture of fish samples for research dealing with the aquatic biology of the lake ecosystem.

Water temperature and location were routinely tabulated, along with other data, for each sample taken. The majority of this data were taken from a small boat, but due to the objectives of the project, were generally quite close to shore. Because of this, extreme care was taken to minimize the probability of including land surface effects in the HCMM values. In cases where it was felt that significant land surface was included in the pixel, the intensity value from the adjoining (lake side) pixel was used. In cases where the location appeared to fall between pixels, the arithmetic mean of the surrounding pixels was used.

While it was felt that the surface measurements were of relatively similar accuracy, one other factor needed to be taken into account. The HCMM Satellite was designed to pass overhead at the warmest part of the day, approximately 1:30 p.m. The surface data, on the other hand, was generally collected throughout the course of the day. For this reason, it was determined that a certain degree of fluctuation should be expected in the data, simply to account for the daytime surface temperature fluctuation of the study area.

Examination of all available day/night HCMM images with a 12 hour interval of separation showed that characteristic lake areas had roughly a 3 ^{o}C (9.2 HCMM intensity units) diurnal temperature variation. It was also determined that this value was most likely slightly low. This determination was based on two facts. First, the nighttime temperature was sensed by HCMM at approximately 2:30 a.m. The coolest portion of the night, on the other hand, occurs slightly before dawn. Therefore, the nighttime HCMM reading was felt to be higher than the true "nighttime low" temperature. Second, all available day/night corresponding images were during the months of August and September. Since calibration data was used for periods from March through November, it was felt that the seasonal fluctuation in diurnal differences was not truly represented. The August-September period in fact, had the smallest diurnal fluctuation of the study period. Based upon the above observations and calculations, it was determined therefore, that the measured data would likely have a fluctuation of around 2 ^{o}C.

6.3 Algae Measurements

Phytoplankton samples were collected in one of two ways. If the water contained large numbers of algae, lake water was collected directly by immersing a 15 liter bucket beneath the surface of the water and lifting it to the surface. A subsample was then removed from the bucket and placed in a Nalgene container. These containers were returned directly to the laboratory for analysis. Samples collected in this manner were designated total plankton samples.

When the algal concentration in the water column was too low for direct water analysis, known quantities of water were passed through a plankton net and the algae were collected in attached 30 ml vials. These samples were designated as net plankton samples. When these samples were collected corresponding nannoplankton samples were usually taken by catching a portion of the water that was passed through the net in a Nalgene jar. These were returned to the laboratory for analysis.

Standing crop measurements were made by counting algae using Palmer Cell counting chambers. These chambers were placed on the microscope and the algae present in the field of vision were counted under 400x magnification. The slide was then moved to the adjacent field and the algae in that field counted. In this manner the slide was moved from end to end and the number of algae counted in this transect was recorded. The number of organisms present in the water of the lake was then calculated by multiplying the counted quantities by determined factors.

Several statistical analyses of the data were performed, including, analysis of diversity using the method of Shannon and Weaver (1963). Calculation of importance values (Ross and Rushforth, 1980) was also performed as well as several other tests.

6.4 Climatological Measurements

Climatological data needed were readily available. Humidity data was collected and tabulated during the study by the Bureau of Reclamation. Humidity data was taken on the east side of the lake. This is on the downwind side with respect to the prevailing winds and as such may induce some bias.

Evaporation is measured at two sites along the lake, the Bureau of Reclamation (USBR) pan at the Provo Airport and the Utah Lake Lehi weather station. Both sites have wind data and Lehi has pan and air temperature data. Both pans are close to the edge of the lake. Wind data from Provo is at both

a height of 11.5 m and at pan height. Lehi wind is at pan height. The velocity of wind over water changes relative to that on land and increases depending upon the fetch. As both sites are on the downwind side of the lake, wind velocity measurements correspond closely to that of wind over water.

Evaluation of the HCMM temperature and evaporation data yielded fourteen days of HCMM day infrared data and five day/night infrared pairs that could be used in the analysis. HCMM temperatures were used to calculate the saturation vapor pressures of the surface of the lake. Maximum air temperatures from the Lehi station were used in calculating the prevailing vapor pressure.

6.5 Groundwater Measurements

An extensive search through Federal, State, County and local sources revealed little reliable quantitative near-surface groundwater data. The Bureau of Reclamation study included extensive groundwater sampling, but was primarily concerned with deeper aquifers and provided no useable data. Similar situations were encountered with the U.S. Geological Survey, the Utah State Geological Survey, and the Utah State Engineers office. The only quantitative data available was from Utah County Watermaster records of percolation testing. County authorities felt that some of the data was quite reliable. Part of the records, however, were from tests not supervised by county officials and such tests were marked accordingly. The lack of reliability of these unsupervised tests caused the requirement for official supervision to be instituted in 1979. Nevertheless, all data, whether from supervised or unsupervised tests, were tabulated and used in the development of the quantitative groundwater relationship. The possible differences between predictions based on supervised and unsupervised tests were investigated.

After failing to find a reliable and extensive source of depth to groundwater data, a program of field interviewing was instituted. Local residents, farmers and ranchers chiefly, were interviewed in an effort to recreate the groundwater history of the area throughout the study period. This method met with limited success for several reasons. Individuals were generally able to furnish information concerning only their own fields, or fields that they worked. There was an extremely high number of

contradictions, some with differences of up to several feet, in neighboring and similar areas. Feeling that this procedure was not yielding useable data, it was discontinued.

Because of the limited data base from which to develop a statistically significant quantitative relationship, it was decided to also explore the possibilities of proving the existance of such a relationship from a qualitative point of view. The search for quantitative data had produced a number of sources of data capable of being used in a broader and less precise study. The most valuable was a "wet season water table" map developed by Ben Everitt (1981), formerly of the Utah State Geological and Mineral Survey. This map was based on existing data obtained from reports and files, both published and unpublished, as well as interviews with various government agencies and consulting firms. With the exception of a Bureau of Reclamation study, most of the data were one time readings of water levels in temporary shallow bore holes or trenches. Measurements were generally from the 1960's and 1970's.

The Bureau of Reclamation study consisted of a detailed drainage investigation in Southern Utah Valley and Goshen Valley. This investigation was done as part of the planning phase of the Bonneville unit of the Central Utah Project. More than one hundred shallow water table observation holes were monitored over the fifteen year period from 1953 to 1967.

Care was taken to use only data from the shallowest boreholes and excavations available. This was done in order that the influence of the piezometric heads of the deeper, confined aquifers upon the water table could be minimized. Toward the center of the valley, artesian pressures at very shallow depth have been reported, in two cases within ten feet of the surface (Everitt, 1981).

Another significant source of regional data was the "Soil Suitability for Septic Tank" study done by the U.S. Soil Conservation Service (SCS). This study provided detailed maps of locations in the county that experienced seasonal water table depths of four feet or less. Another map, developed by the SCS in conjunction with Utah County, showed poorly drained areas, as well as those subject to periodic flooding.

The above sources, combined with interviews with many local residents, water board members, and county officials having first hand knowlege of specific areas, were used to develop overlays showing areas that experienced

seasonal variation in groundwater depth. Special attention was focused on nonhomogeneous location; e.g., a deep water table area surrounded by shallow water table areas, and vice versa.

7. ANALYSIS METHODS

7.1 Sum of Squares of Residuals

One of the primary statistical concepts used for the determination of the comparative correlation of predicted data to actual ground truth was the "sum of squares of residuals" (SSR). This value is determined by subtracting the predicted temperatures from the measured ground temperatures, squaring the individual differences, and obtaining the sum of these squared terms. The model yielding the smallest SSR is chosen as the model best predicting the actual data. This is a widely accepted and commonly used method of comparing the relative "fit" of different models to actual values (Walpole and Myers, 1978). One important stipulation, however, is that the two models must each contain the same number of predicted values, and these in turn must have a one to one correspondence with measured or "true" values.

The effect of squaring the differences before summation possibly warrants further explanation. The terms are squared chiefly for the purpose of making all summed values positive. If this were not done, positive and negative values would cancel, and the comparative value of the respective sums would be lost.

One other effect of using the SSR as the chief indicator of fit is the exaggerated significance given to points lying significantly off of the predicting line. Since the difference is squared, a single "outlying" point can have a significant impact on the SSR. For this reason, data used to compute the SSR should be examined very closely for possible points that could unduely influence the results.

Possibly the most important tool for determining the goodness of fit of a specific statistical model is the analysis of residuals. The residual is the difference between actual and predicted values. Once the "best fit" model has been determined through use of the SSR, the residual values are plotted as dependent variables. Residuals can be plotted against parameters such as data location or time of acquisition. Any pattern emerging from a residual plot warrants close examination.

Although the SSR value can give a good indication of the best fitting model, it is not sufficient to determine if one model is statistically better than another, unless one model is a special case of the other. As this was not the situation with the models being compared, another test was needed. The available data was randomly divided into two portions. One set of data was used to determine the best linear model and then this same data was used as the test data base for the NASA model. The other set of data was used to determine the calibration coefficients for the NASA model, then used as the test data base for the linear model. This rather awkward arrangement was determined necessary in order to meet the mathematical requirements for a valid statistical test.

Each model was then applied to its respective data base, and the individual SSR values were determined. Each SSR was then divided by the number of data points used in its generation. The ratio of the two values obtained in this manner then met the requirements stipulated to follow a statistical F distribution. By forming an appropriate set of hypotheses and comparing the value obtained (the ratio) against tabulated values of the F distribution, the superiority of one model over another can be either proven or disproven (from a statistical point of view). Again, it was not the intent of this study to develop a better model, but rather to determine the feasibility of developing a computationally simpler model without sacraficing accuracy.

7.2 Linear Regression

The best linear model was determined through the use of simple linear regression. This is based on determining the line with the smallest SSR. The regression analysis, as well as most all data handling and manipulation, was done with the aid of Minitab II, a statistical software package developed by Professor Thomas A. Ryan Jr., of the Statistics Department at Pennsylvania State University (Ryan, et al, 1976).

Minitab II is a general purpose statistical computing system. It is easy to use, very flexible, and fairly powerful. It is designed primarily for small to moderate sized data sets, which can be stored in main memory. Minitab has been found especially useful in exploring data in the early phases of analysis, for plotting, and for regressions.

7.3 Correlations

In order to evaluate the relationships that exist between the various measurements used in this study, several assumptions were made. These include the relative independence of each of the measurements, a similar degree of accuracy of each of the measurements and a normal distribution of each of the data sets.

The assumption of independence implies only that no relationship was assumed until it could be proven; for example, was water temperature dependent on the algae concentration or was algae concentration dependent on the water temperature? In every case the correlation of the data sets as an independent bivariate function f(x,y) was established before performance of any linear regression analyses which require the assumption of dependence of one variable on the other. The determination of the degree of correlation of the data sets, together with information gathered from literature on previous research concerning the measurements in question, provided a key to the dependent relationships that existed.

The assumption of a similar degree of accuracy of the measurements allowed the use of one-to-one correlation of the data sets. In the cases where this assumption appeared to be unjustified or questionable, either adjustments were made and recorded as part of the evaluation procedure, or no correlation was established because of the incompleteness of some data sets. One principle adjustment which was made was the use of the log of the plankton counts, rather than the counts themselves, in order to evaluate data sets of similar magnitude and to increase the linearity of the sets.

The assumption of a normal distribution of the measurements in the data sets was necessary due to the often limited number of common points (less than 30) in the sets. This type of assumption is common to statistical analysis since it makes possible the substituting for a very difficult equation for evaluating the degree of correlation with a much simpler equation using the t-distribution. Since the t-distribution is similar to the normal distribution in that they both are symmetric about a mean of zero and are bell-shaped, there is no inconsistency in the simplification. Also, since the t-distribution is more variable, owing to the fact that the t values depend on the fluctuation of two quantities (the sample mean and variance), the accuracy

of the normal approximation is increased by the simplifying procedure. As the sample size increases to infinity the standard normal distribution and the t-distribution approach equality.

The correlation procedure used in this study assumed that both the X and Y sets in each comparison were random variables and the measurements were observations from a joint density function f(x,y). According to Walpole and Myers (1978) it is often assumed that the conditional distribution $f(x|y)$ of Y, for fixed values of X, is normal with mean $\mu(Y|x) = \alpha + \beta x$ and variance $\sigma^2 (Y|x) = \sigma x^2$ and that X is likewise normally distributed with mean $\mu(x)$ and variance $\sigma^2 (x)$.

It was important to understand the physical interpretation of the correlation coefficient and the distinction between correlation and regression. The straight line given by $\mu(Y|x) = \alpha + \beta X$ is the regression line. Since $r^2 = \beta^2 \sigma x^2 / \sigma y^2$ (Walpole and Myers, 1978), the value of the correlation coefficient r is zero when $\beta = 0$, which results when there is essentially no linear regression; that is, the regression line is horizontal. A value of r equal to +1 implies a perfect linear relationship with a positive slope, while a value of r equal to -1 results from a perfect linear relationship with a negative slope.

7.4 Color Graphics

One of the most valuable methods used in this study to interpret the HCMM Satellite data was the preparation of color representations of the pixel intensities on Utah Lake. These color pictures were made on the Tektronix 4027 color terminal in the BYU Civil Engineering Graphics Laboratory. The HCMM data tapes were read and stored on the DEC-10 computer and an interface was used to read these files into the Tektronix 4027. The range of pixel intensities on the lake was divided into seven smaller ranges and each of these had a color assigned. All pixel intensities higher or lower than those assigned were represented as black. Because of the normal difference between the water and land pixel intensities of 20 to 50 units the ranges could be selected so that the lake appeared in color on a black background. The colors were assigned so that they ranged from dark blue to red as the intensity measurements increased from the lower ranges to the higher.

These color pictures were especially useful in locating the extent and relative concentrations of algae in the lake waters and in identifying blooms within the algae fields. They also proved to be very valuable in identifying regions in the lake where some additional thermal energy appears to be present. When insufficient data were available to do reliable statistical analyses of the measurements, the color pictures sometimes provided the only means to evaluate data. In almost every case where statistical analyses could be compared with the color pictures, the pictures were found to be truly representative of the concentrations or other measurements in question.

In order to generate the infrared/reflectance correlation images a two dimensional graphics program developed in the BYU Civil Engineering Department was modified and used. The amount of color that could be displayed was limited and therefore the degree of refinement to be applied to the combination of the images was reduced. The pixel values of the day infrared and visible data were read into the program which split each data set into three ranges; high, middle, and low. The upper and lower limits of these ranges for the lake were established by inspection of the lake image printout in order to exclude edge effects at the shoreline.

The program compared each pixel intensity of the infrared image to the range limits and determined if the pixel value was in the top, middle, or bottom third of the lake image intensities. Each pixel value for the visible image was also read and assigned to the top, middle, or bottom third of the day visual intensity range. The infrared and day visible images were then compared as shown in Table 7.1. From this comparison a new image was formed in which the pixel values were the numbers assigned (columns 3, Table 7.1) from the comparison. The image was then read by the graphics program, displayed on the screen, and a picture was taken of the image.

Table 7.1. Numbers and Colors Assigned in the Comparison of Day Infrared and Visible Images to Produce the Correlation Pictures.

Day Infrared	Day Visible	Number Assigned	Color Assigned
H	H	7	red
M	L	6	pink
M	H	5	yellow
M	M	4	green
H	L	3	lt. blue
L	H	2	blue
L	L	1	dk. blue
H	M	0	black
L	M	0	black

8. TEMPERATURE CALIBRATION

8.1 Theory

The dominant energy fluxes controlling the earth's surface temperature are insolation, during daylight hours, and radiative and convective cooling, which occur throughout the 24 hour period. Solar input is concentrated in a wavelength interval centered at 0.5 micrometers, while radiative cooling to space occurs in a broad, longer wavelength spectral interval of from 6 to 30 micrometers. Alternation of the two fluxes causes a diurnal cycle of surface temperatures. The HCMM is designed to sense surface infrared radiation values at the peak of the cycle (1:30 pm local time) and near the early morning minimum (2:30 am local time).

An important concept in the use of thermal infrared imagery is the differentiation between reflectivity and emissivity. The range of daily surface temperatures is a function of a physical property of a material to absorb and re-emit the suns energy. Since this energy is conducted to a depth of two to five centimeters, the measurement of surface temperature variation provides information on a finite thickness layer of material being observed, and the sensed energy is a function of the type or state of material. This contrasts with measurements of reflected energy, which only provide information about the surface of the observed material.

Interpretation of surface temperature measurements obtained by HCMM are complicated by many factors, most of which are associated with the earth's atmosphere. Several of the more important factors are; cloudcover, surface winds, evaporation, water vapor, surface emissivity, directional characteristics of reflecting materials, the prior temperature history of the observed material, topography, and surface variability within the area of a HCMM pixel. In a general sense the complete energy and moisture budget at the earth's surface must be considered. The effects of some of these parameters were examined.

A spaceborne sensor must be able to "see" through the atmosphere to the ground without attenuation. Radiation may be lost in its passage through the atmosphere as a result of scattering from and absorbtion by suspended particles. The atmosphere's minor constituents, such as water vapor, carbon dioxide, and ozone create the major absorption bands.

The relative importance of the different absorbing molecules depends on the radiation path. A satellite located sensor receives radiation that has had to pass through the entire atmosphere. The HCMM thermal sensor waveband of 10.5 to 12.5 m corresponds to a rather pronounced window in the far infrared region.

8.2 Offset Calculations

8.2.1 Preliminary Analysis

The available measured temperature data were tabulated, along with corresponding dates, atmospheric parameters and HCMM radiation intensities. Also tabulated was a code identifying the region of the lake from which the data had been obtained. The lake was divided into four general regions, respectively (1) North Lake, (2) Middle Lake, (3) Provo Bay and (4) Goshen Bay. Although a large amount of data was tabulated for Provo Bay, much of it was during the late summer period. At this time, a large percentage of the Bay is essentially marsh, with significant expanses of water plants covering, shadowing or otherwise concealing the water surface. Feeling that the vegetative cover could possibly have a detrimental effect on the calibration, this area was carefully examined and much questionable data was eliminated from the tabulation. The tabulated data were then entered into Minitab for manipulation and analysis.

The first operation performed was to plot the surface measured temperatures over the curve predicted by the HCMM model. As can be seen in Figure 8.1, the HCMM curve seemed to fall somewhat below the majority of the ground truth data. In order to further clarify this, a plot was made of the surface measured temperatures against the HCMM predicted temperatures (from Users' Guide equation) in Figure 8.2. If the two were in reasonable agreement, the data would then be expected to fall generally on a 45° line, starting at the origin and bisecting the two axes. As can be seen from Figure 8.2, this was not the case. The data fell generally to the left of the line, indicating that the HCMM equation was predicting the surface temperatures to

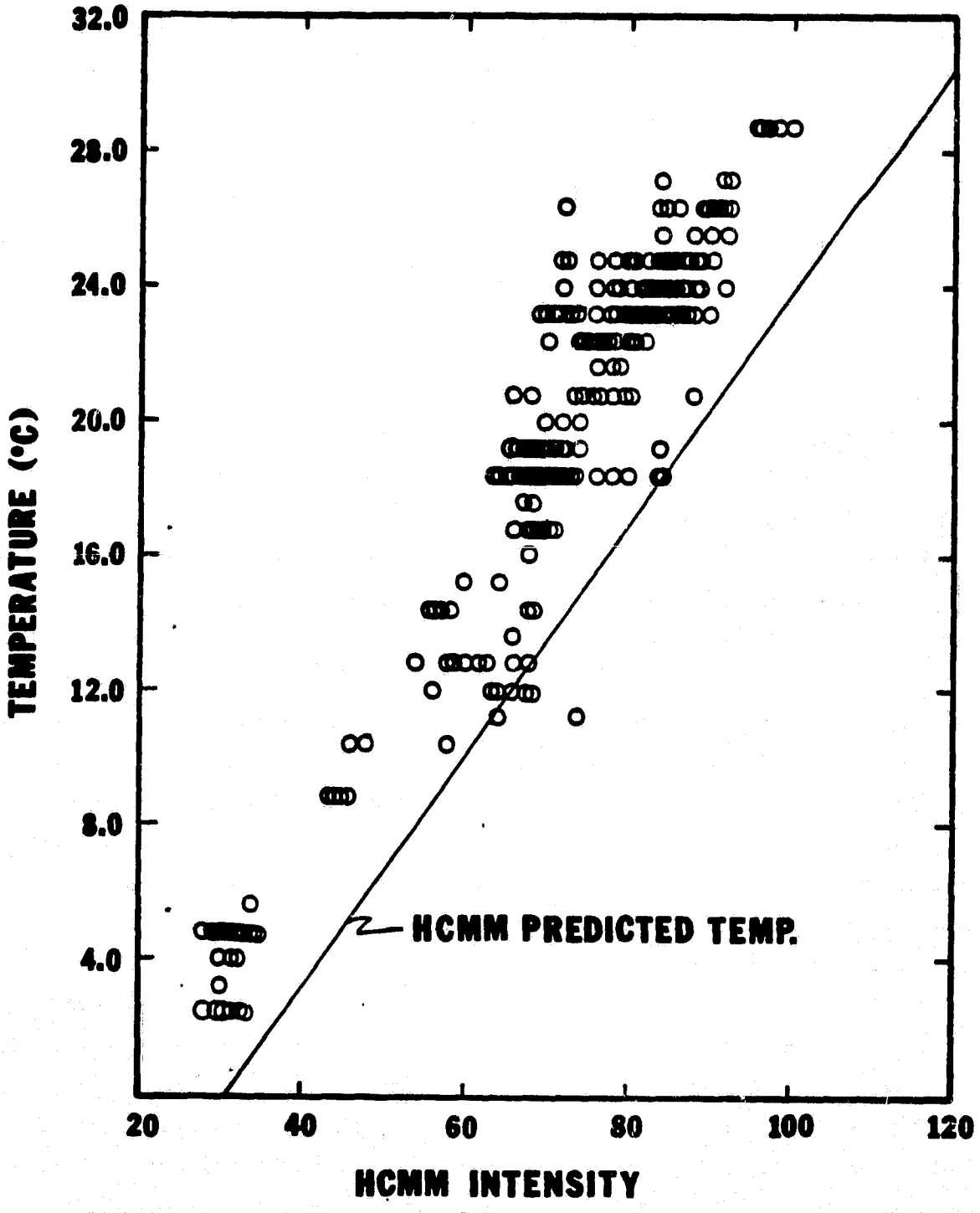

Figure 8.1. Measured Surface Temperatures vs. HCMM Model

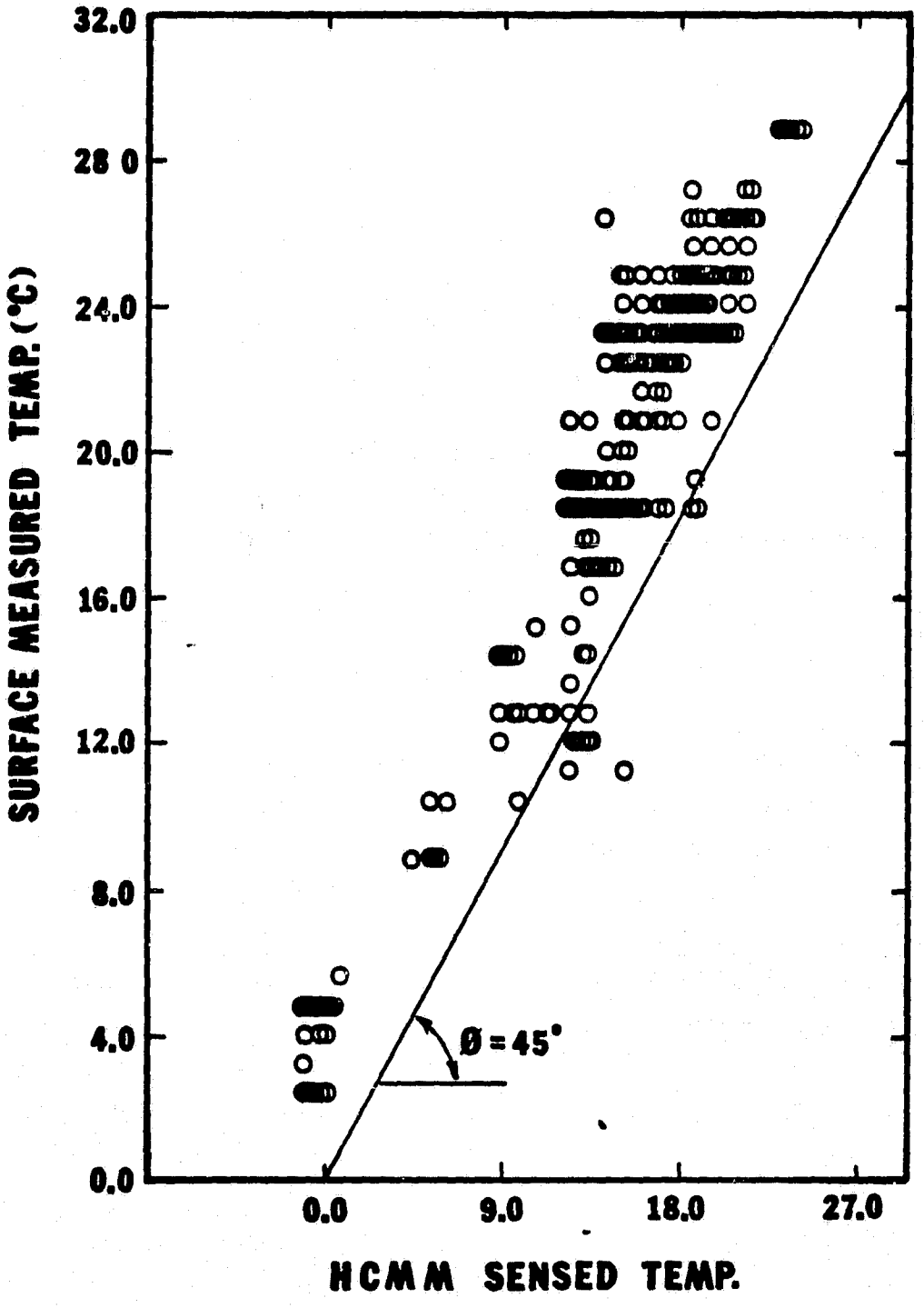

Figure 8.2. Measured Surface Temperatures vs. HCMM Sensed Surface Temperatures.

be lower than they actually were. This appears to agree with the conclusion of Jackson (1980) that temperature data obtained from the HCMM were consistently lower than temperatures measured with a low altitude thermal scanner.

Offsets were then added to the HCMM predicted values and the SSR was calculated for each of the applied offsets. Figure 8.3 is a plot of the SSR value verses the applied offset. As can be seen, the required offset to yield the smallest SSR, and thus the best fit, was about 4.6 ^{o}C. Figure 8.4 shows a plot of ground measured temperature against the HCMM predicted temperature with the 4.6 ^{o}C offset, along with a $\pm$ 2 ^{o}C envelope. As can be seen, a significant number of the data points lie outside the envelope.

In an effort to determine the possible causes of these deviations, several plots were made. A plot of the residuals verses lake location yielded no noticeable pattern. The plots of residual verses ground temperatures (Figure 8.5) and residuals verses months of the year (Figure 8.6) did yield usable results. Examination of Figure 8.5 showed that a group of data in the 10 to 20 ^{o}C temperature range had negative residuals. Examination of Figure 8.6 showed that data collected in the month of May, (5 month) also had negative residuals. However, plots of the residuals versus location, month, and ground temperature (Figures 8.7, 8.8 and 8.9, respectively) for only "same-day" data (with a presumed 5 ^{o}C offset) did not show the deviant points. This indicated that the data in question was collected on a day other than the day of the HCMM overflight.

In order to further isolate the data in question, the WHAB data was separated from the Fish and Wildlife data, and these sets further subdivided into delta day categories. Delta day categories are groups of ground surface data taken a specified number of days apart from the HCMM overflight. Figure 8.10 indicates that two groups of the WHAB data fall noticeably below the expected 45^{o} line (offset of + 5 ^{o}C added to HCMM temperatures). One group corresponds to a delta day of four days, the other group to a one day difference.

Upon detailed examination of the data, it was found that the Fish and Wildlife data collected during May 1978 were all in the 10 to 15 ^{o}C range, and all had large negative residuals. The first three plots, therefore, were all implicating the same data. An investigation of the time intervals further substantiated these implications. The HCMM overflight corresponding to this

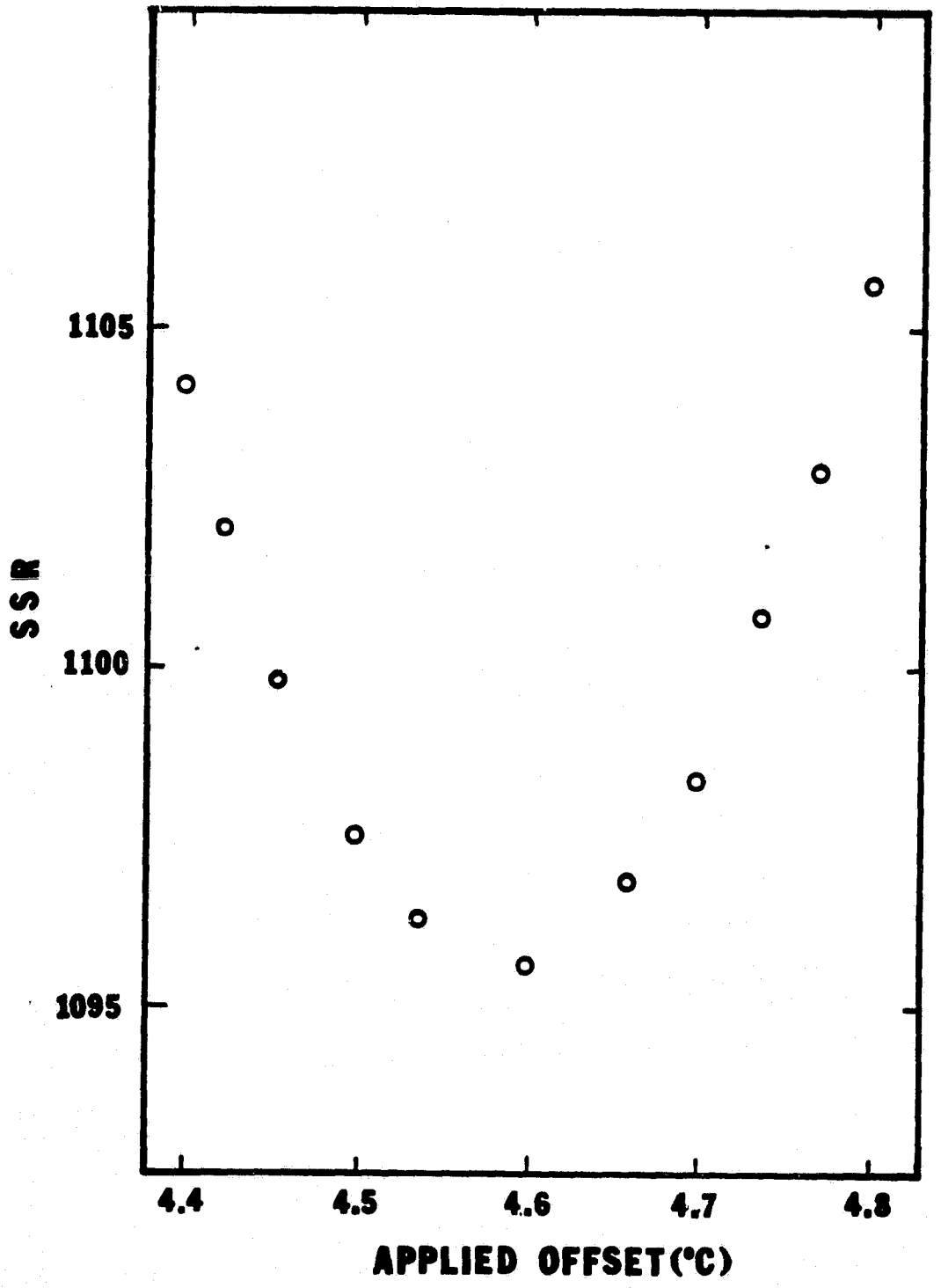

Figure 8.3. SSR vs. Applied Offset: All Tabulated Data

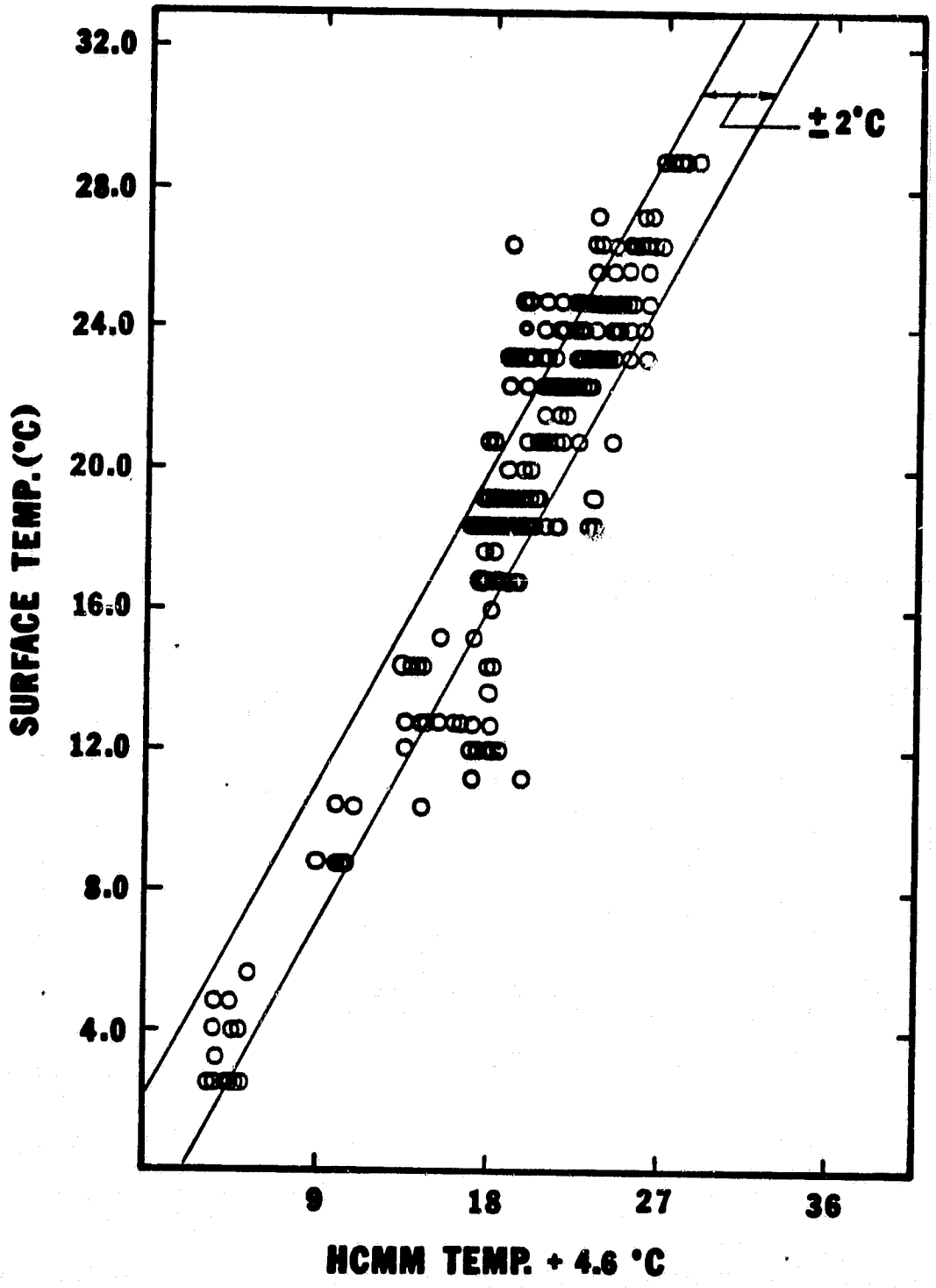

Figure 8.4. Measured Surface Temperatures vs. HCMM + 4.6 °C

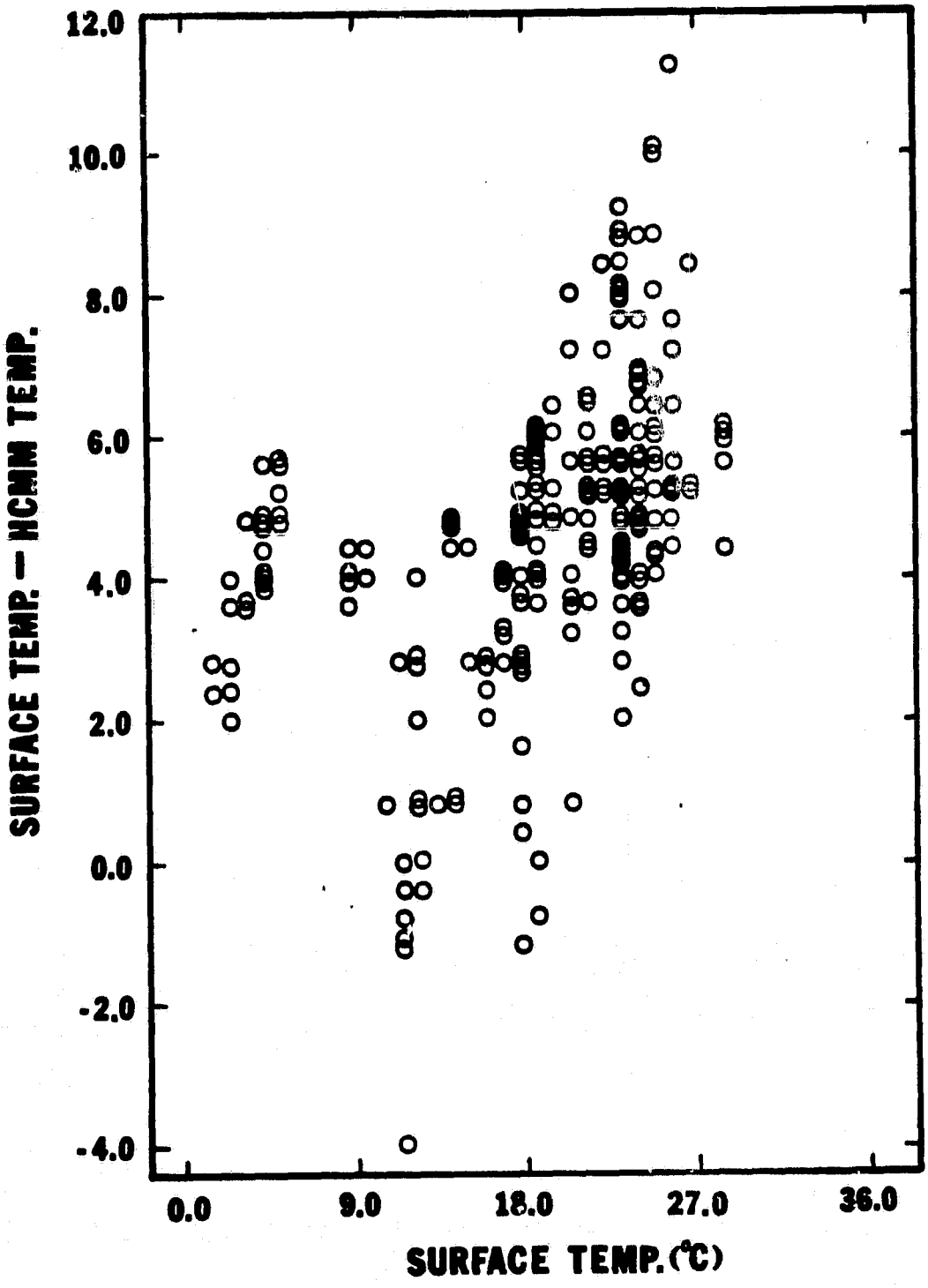

Figure 8.5. Residual vs. Measured Surface Temperature: All Data

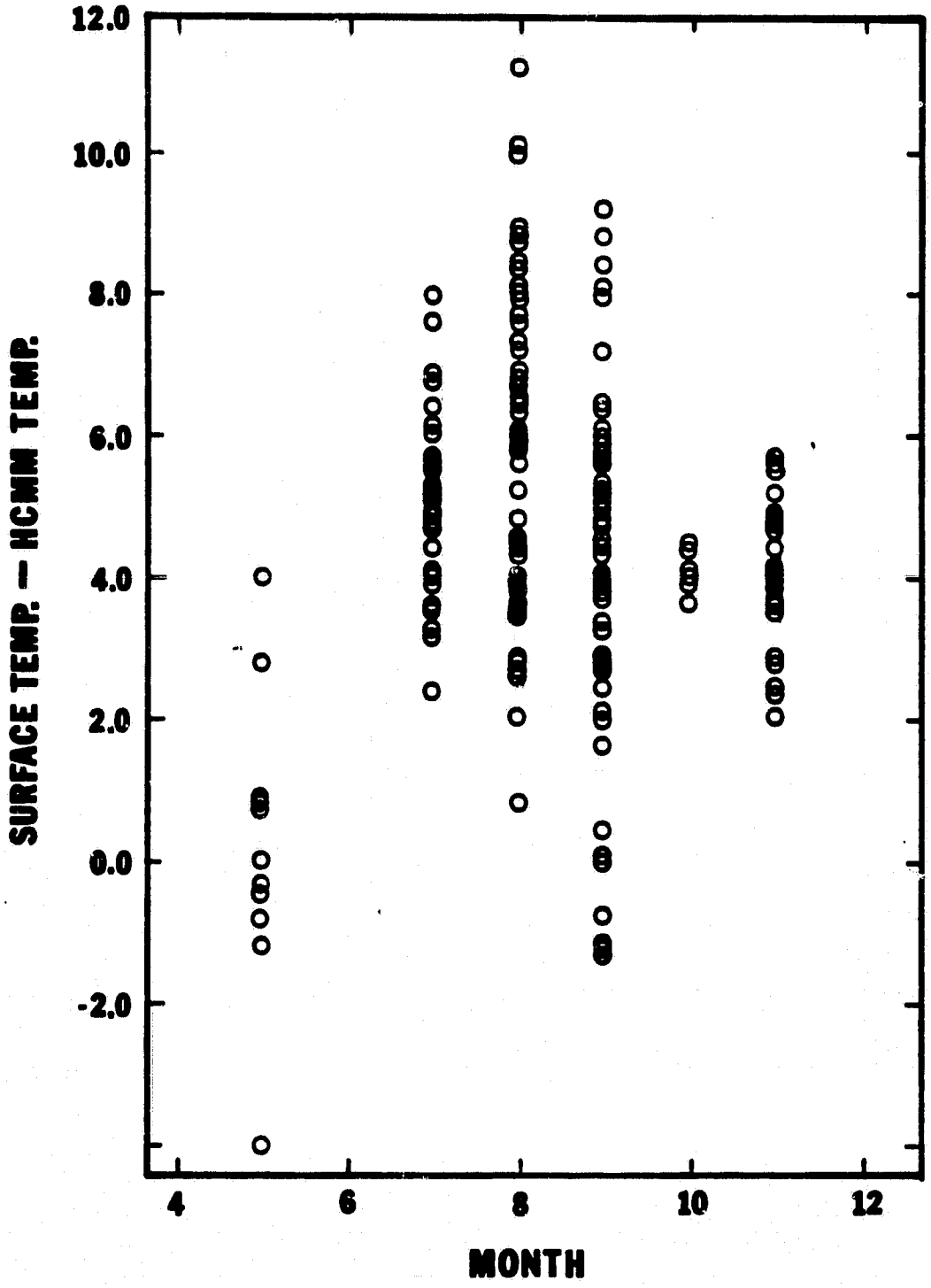

Figure 8.6. Residual vs. Month: All Data

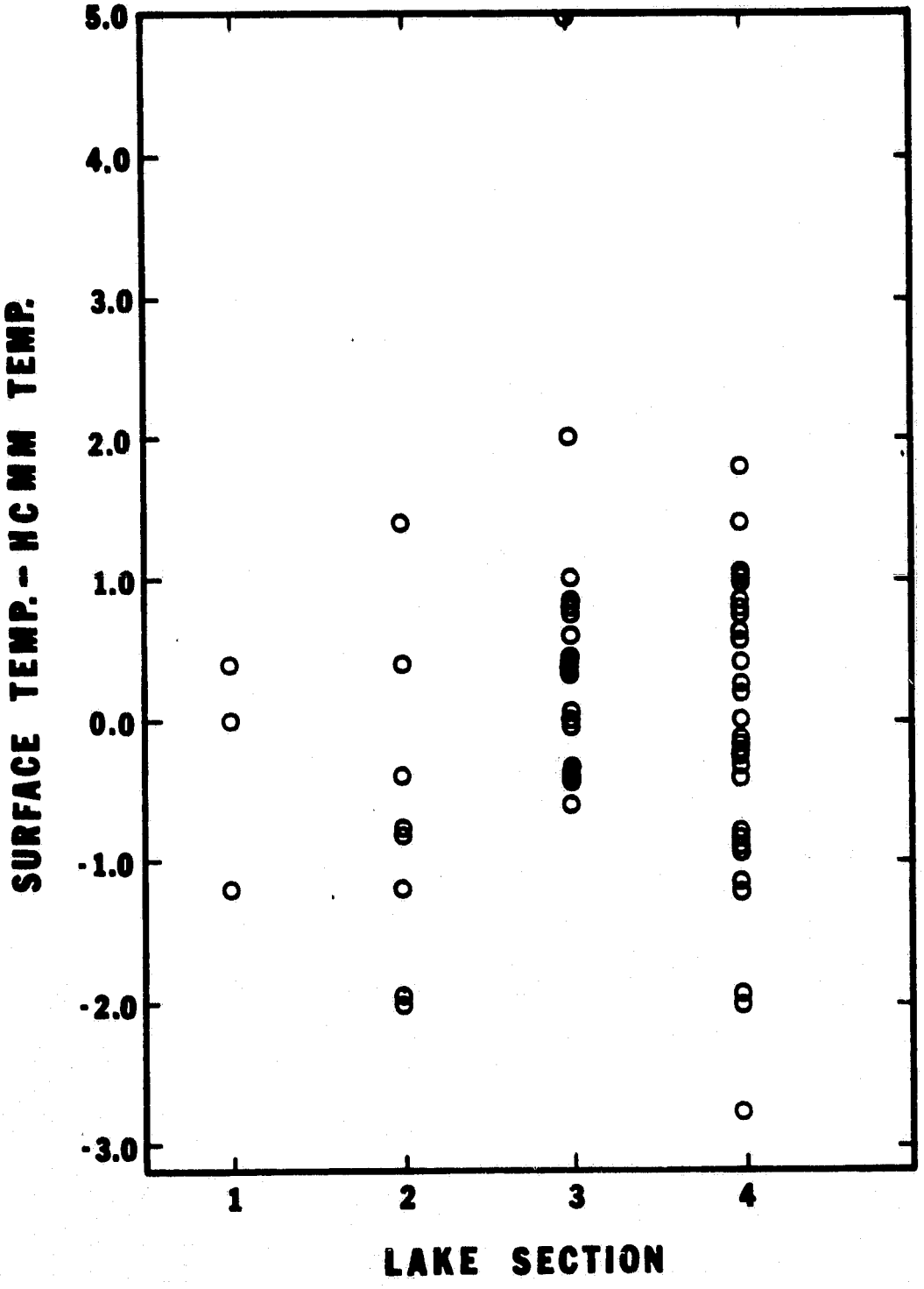

Figure 8.7. Residual vs. Lake Section: Same Day Data with 5 °C Offset

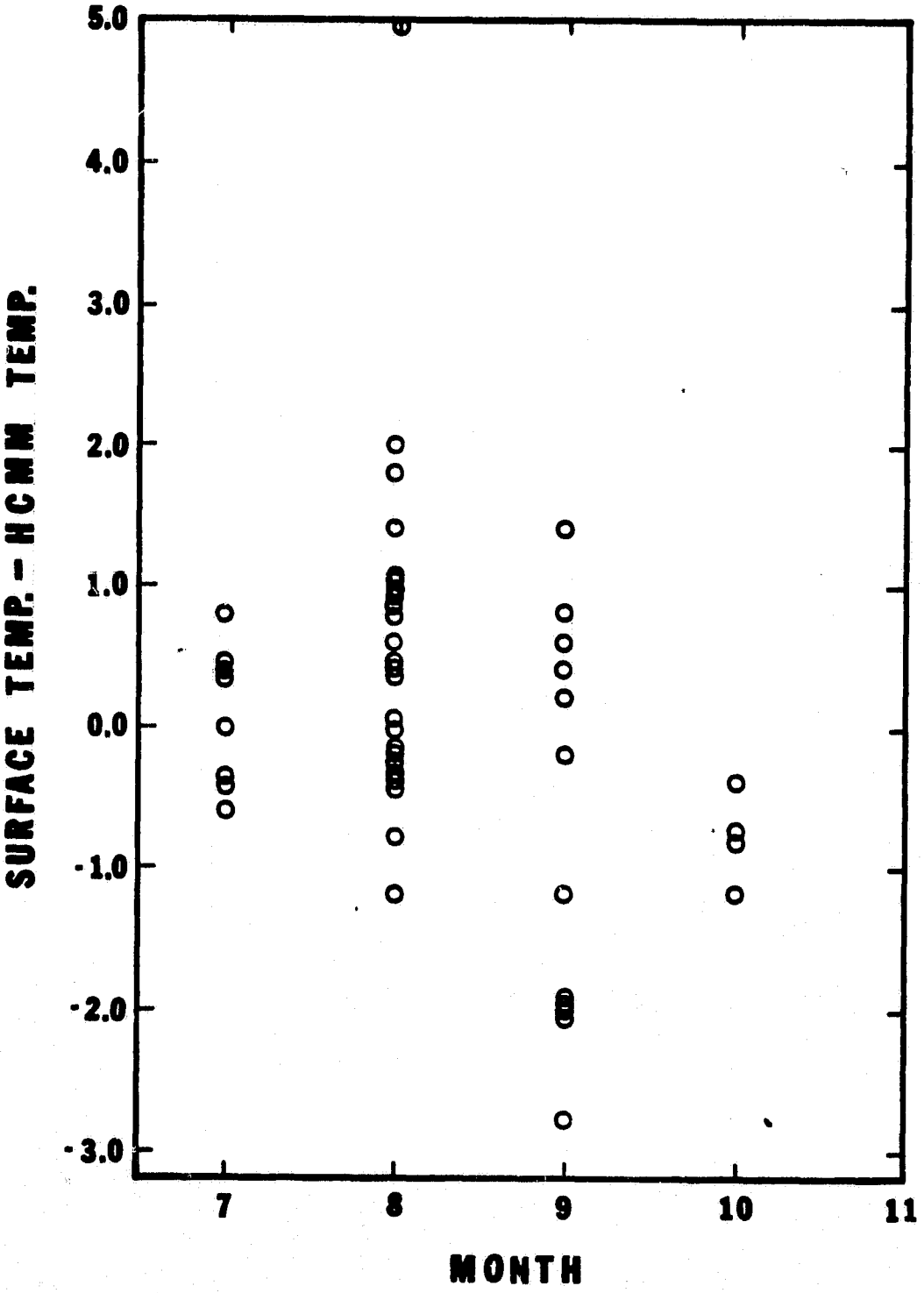

Figure 8.8. Residual vs. Month: Same Day Data with 5 °C Offset

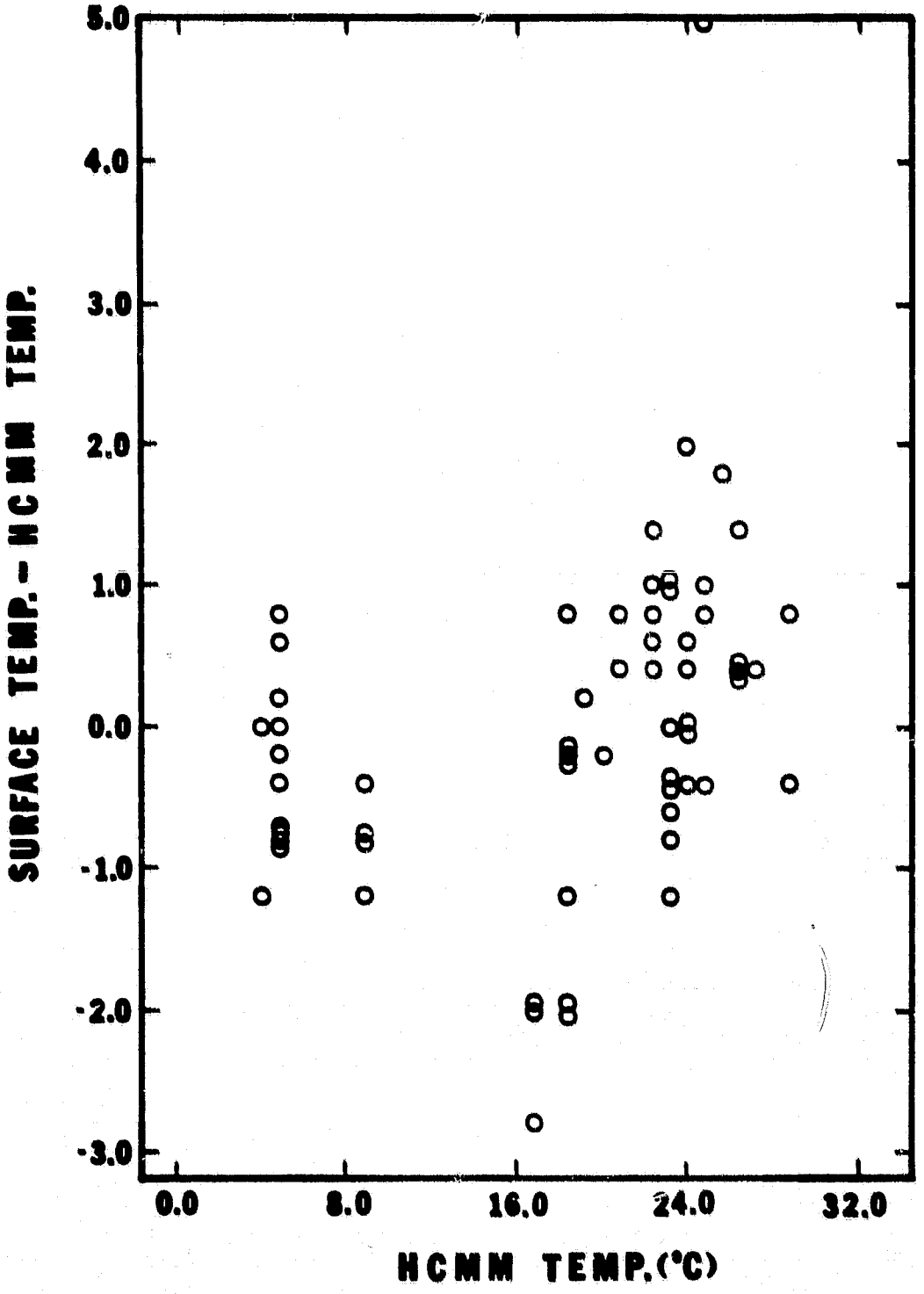

Figure 8.9. Residual vs. HCMM Temperature: Same Day Data with 5 °C Offset

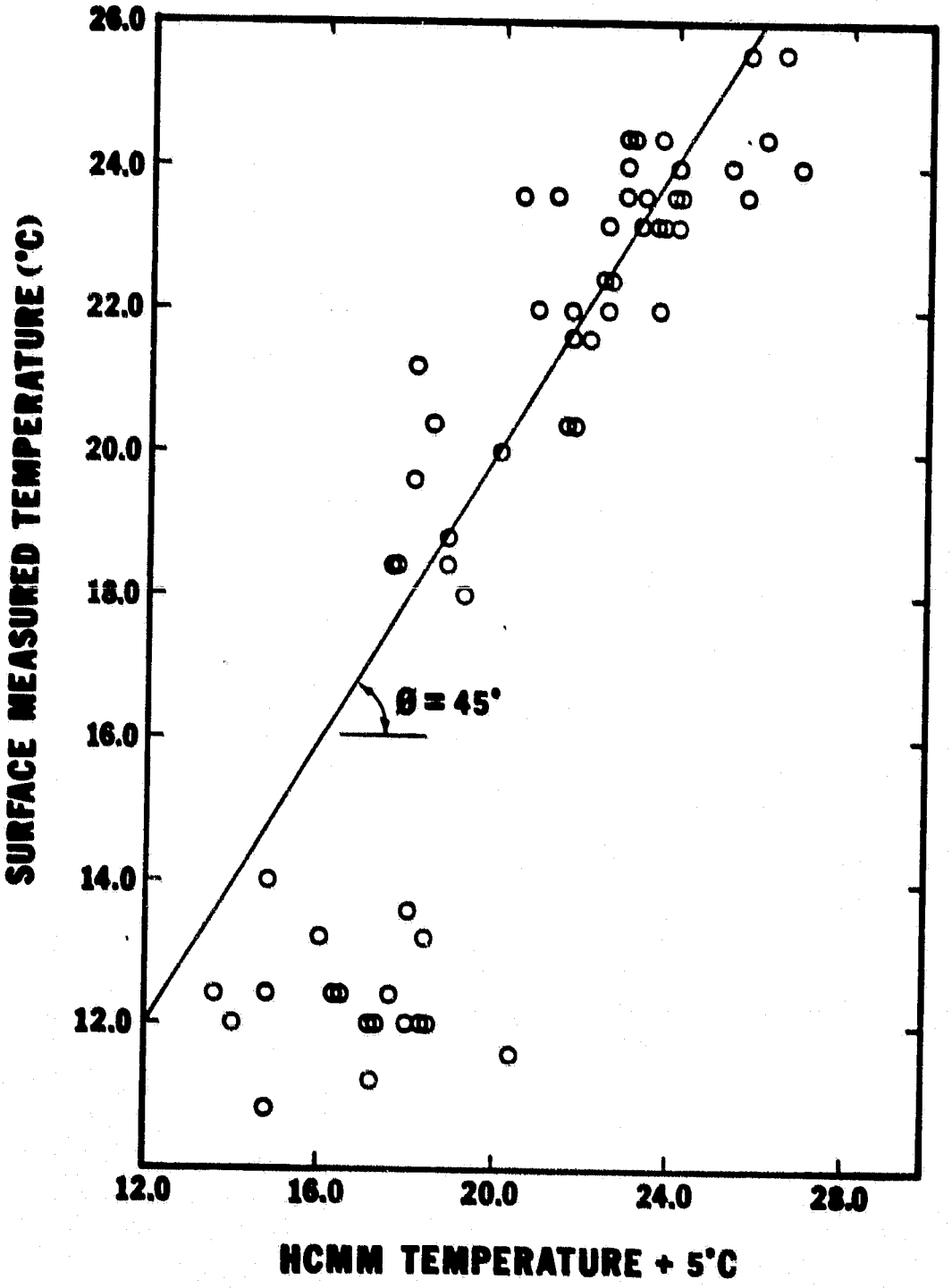

Figure 8.10. Surface Temperature vs. HCMM Temperature + 5 °C Offset

data occurred on the 13th day of May, while the ground surface data had been collected on both the 9th and 12th, the delta day values being 4 and 1, respectively.

An examination of various atmospheric parameters corresponding to this time period yielded some significant observations. The average air temperature for this period had risen 14.5 ^{o}F, while the recorded high pan temperature had risen 21 ^{o}F from the 8th to the 10th, dropped 6 ^{o}F on the 11th and risen another 7 ^{o}F by the 13th. Based on this data, it was determined that there had been a significant warming trend during this period, and that this trend would probably have been sufficient to have a marked influence on the lake surface temperature. A rigorous examination of the data that was collected on days other than HCMM overflight days was made in order to insure that circumstances such as this did not influence the calibration of the HCMM equation.

8.2.2 Detailed Analysis

A plot was made of the yearly record of several atmospheric parameters that were felt to be indicators of conditions on the lake surface. Table 8.1 is a list of the parameters used, as well as the sources of the data. Care was taken to select climatological data from stations felt to be representative of the study area, but in some cases the best data obtainable were still subject to question. The source of the climatological data was taken into account whenever use was made of it.

Data deemed questionable for reasons dealing with changing atmospheric conditions were not representative of conditions when the HCMM overpass occurred, and therefore, inappropriate for use in the calibration procedure. Such data were not totally discarded, however. Although not acceptable for the calibration procedure, this data was in some cases used in other phases, once the calibration had been completed.

The determination of which periods of time were in need of attention was made. It had previously been determined that a plus or minus two degree variation in the ground data should probably be expected, due to the methods used in its collection. In order to further refine this estimate, an examination was made of the variation of the residuals for the data taken on the same day as one of the HCMM overflights. A plot was made of the magnitude

Table 8.1

Atmospheric Parameters Examined

Parameter	Source of Data
Humidity	Provo Airport, U.S. Bureau of Reclamation Weather Station
Wind	Utah Lake, Lehi NOAA Weather Station
Sol-a-meter (sunlight intensity and duration)	Provo Airport, U.S. Bureau of Reclamation Weather Station
Evaporation	Utah Lake, Lehi NOAA Weather Station
Lake Stage*	U.S. Bureau of Reclamation Record at BYU Boathouse
Air Temperature	Utah Lake, Lehi NOAA Weather Station
High	
Low	
Average	
Water (evaporation pan) temperature	Utah Lake, Lehi NOAA Weather Station
High	
Low	
Average	
Cloud Cover (minutes of sunshine)	Salt Lake City, Utah, National Weather Service Forecast Office

*Lake Stage measurements were obtained by performing a linear interpolation between end of month readings.

of the residual for data collected on such days (delta day = 0). From this plot it was determined that the total spread is approximately 2.2 ^{o}C, somewhat smaller than what was initially expected.

The average residual for each day of data collection was then calculated, and these residuals compared to the spread of same-day collected data. Any days with average residuals falling outside the spread of the same day data were then closely examined for possible reasons for the deviation. In most cases, atmospheric changes corresponding to the dates in question provided sufficient reason for the deletion of the data. It should be emphasized, however, that no data was deleted unless sufficient evidence was found to justify the deletion. One notable example of this, occurred on the 4th and 5th of September, 1979. This period had one of the largest deviations found, yet an extensive search of all records showed that it corresponded to a time of atmospheric stability. No rational whatsoever was found for its deletion. Consequently, it was left in the data base used for the calibration process. Figure 8.11 gives the respective spreads in residuals for all data eventually deemed acceptable for use in the calibration procedure.

8.2.3 SSR Results

Figure 8.12 shows the SSR verses offset curve for all data not previously eliminated due to unstable atmospheric trends. As shown, the offset required based on this data is approximately + 4.7 ^{o}C. This is in close agreement with the offset determined by several other researcher as noted in NASA (1980).

Required offset vs. SSR curves were constructed for various subsets of the same data used in Figure 8.12. Figures 8.13 through 8.16 depict these curves for data obtained at the various time differences from the HCMM overflights (delta day = 0, +1, -1, and the combined -4 and -5, respectively). Table 8.2 summarizes all the results with September 4 and 5 data (discussed above) deleted. A summary of the results obtained for only same day data is found in Table 8.3.

Upon examination and comparison of these two tables, it is evident that all required offsets are within the previously established spread of $\pm$ 2

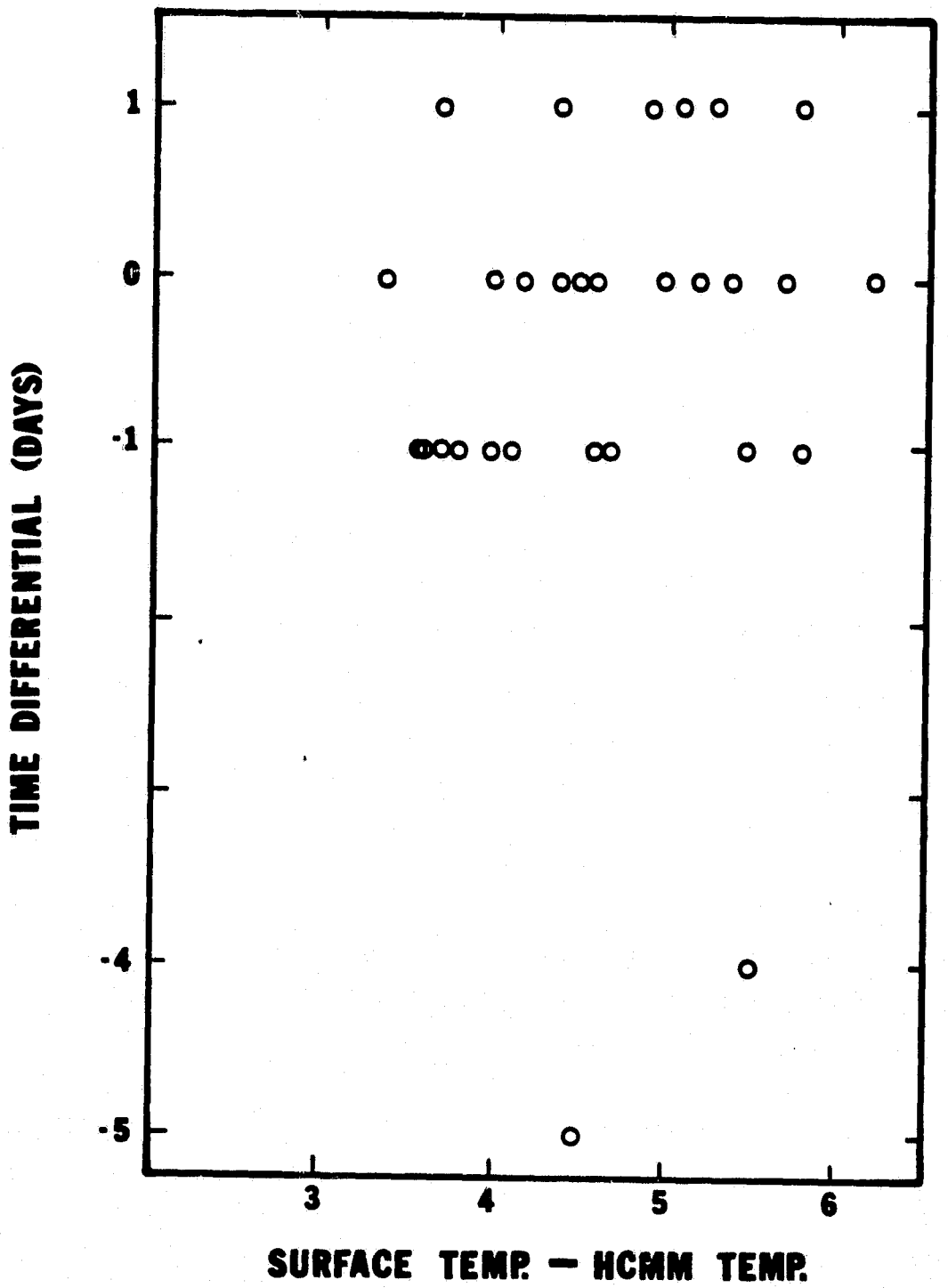

Figure 8.11. Total Spread Encountered in Average Residuals

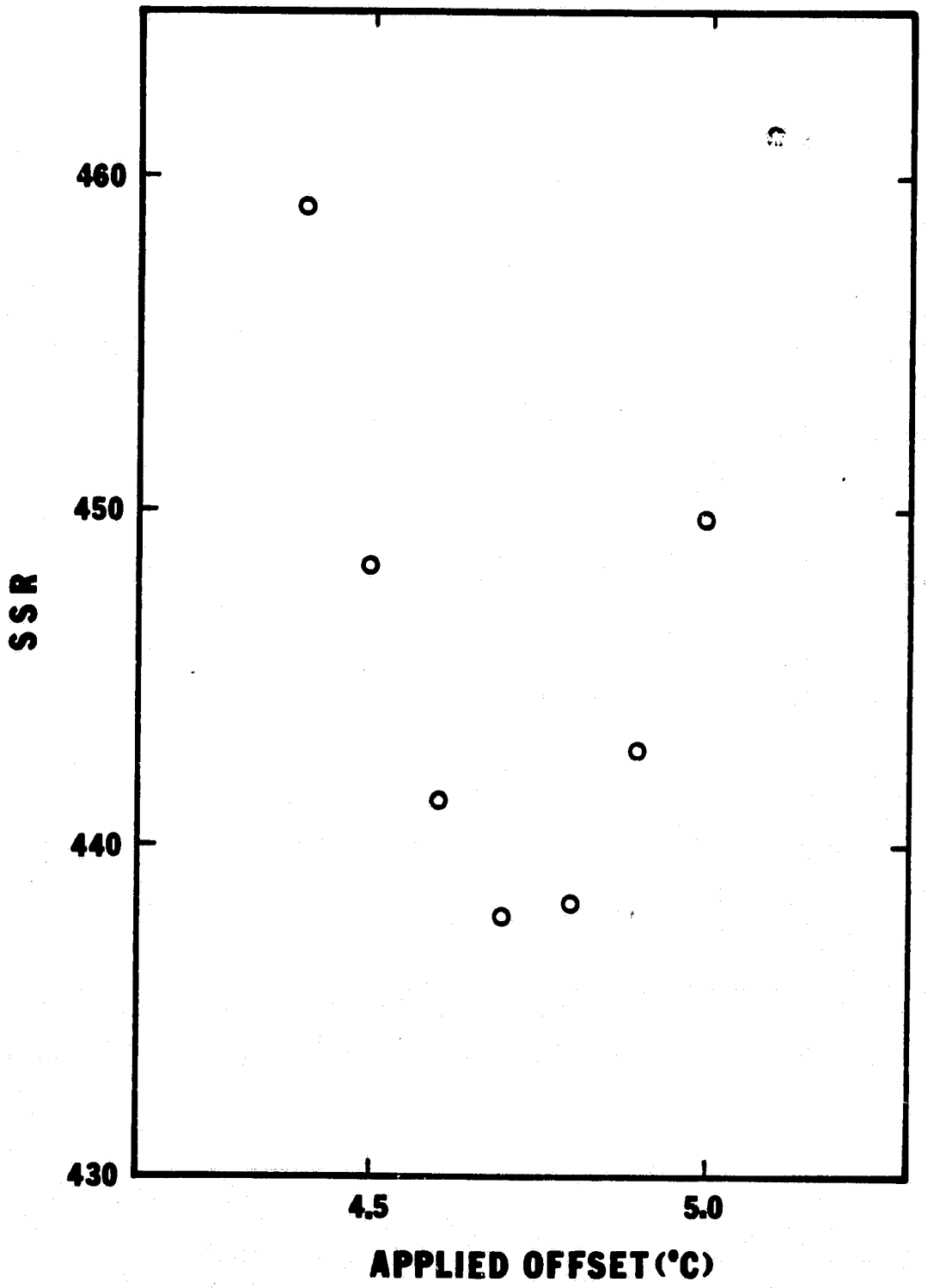

Figure 8.12. SSR vs. Applied Offset: Atmospherically Stable Data

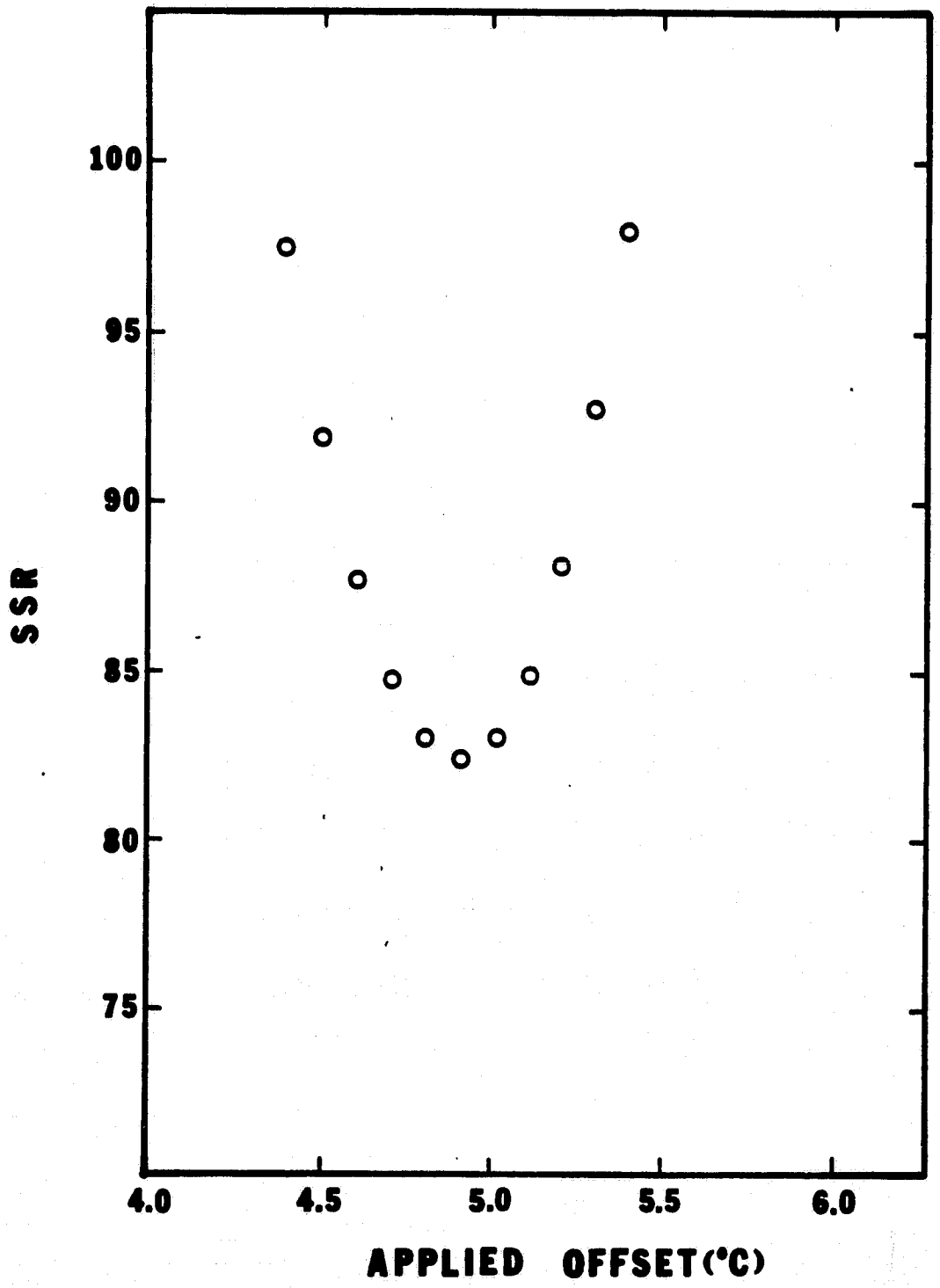

Figure 8.13. SSR vs. Applied Offset: Day 0

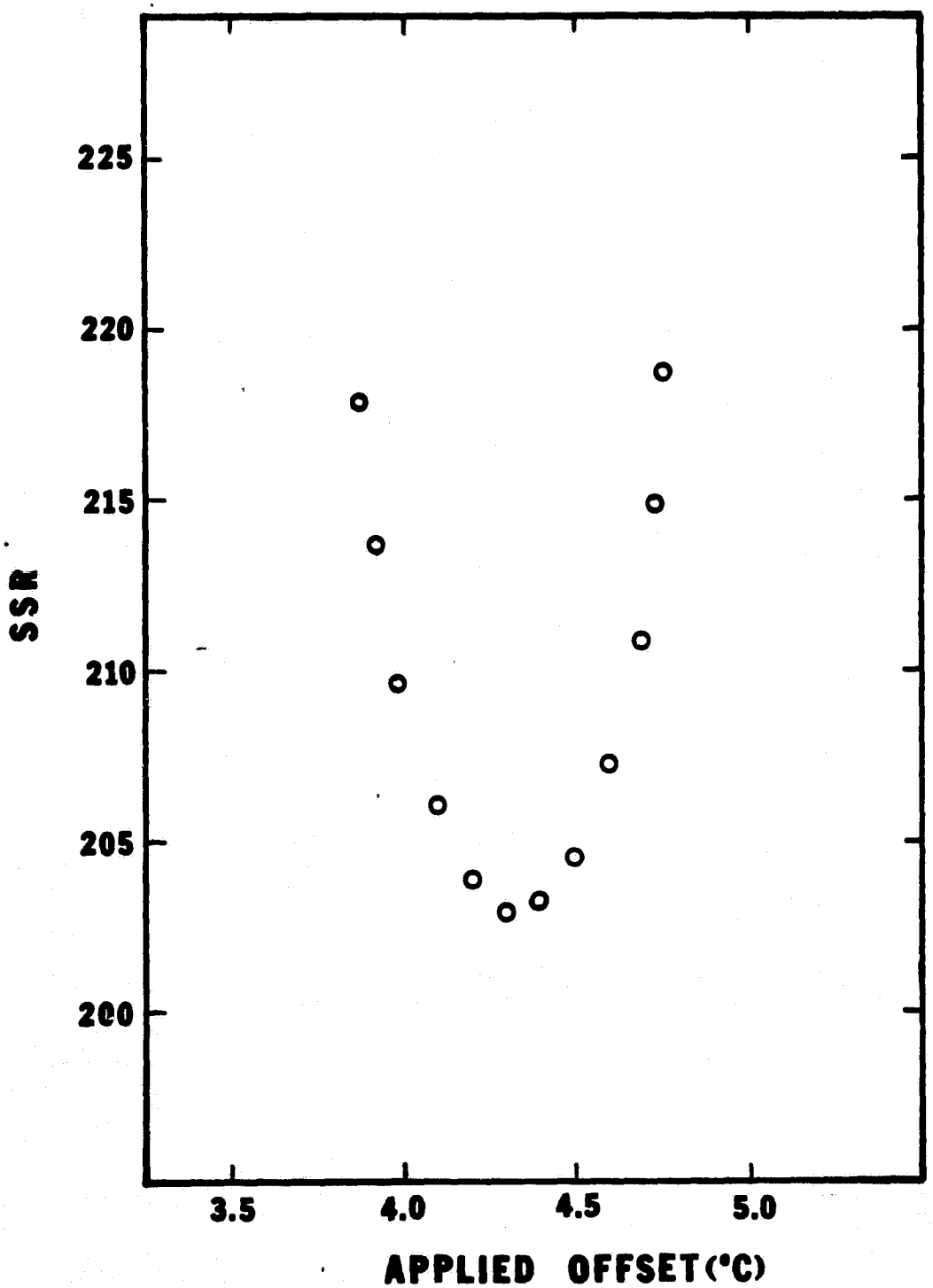

Figure 8.14. SSR vs. Applied Offset: Day + 1

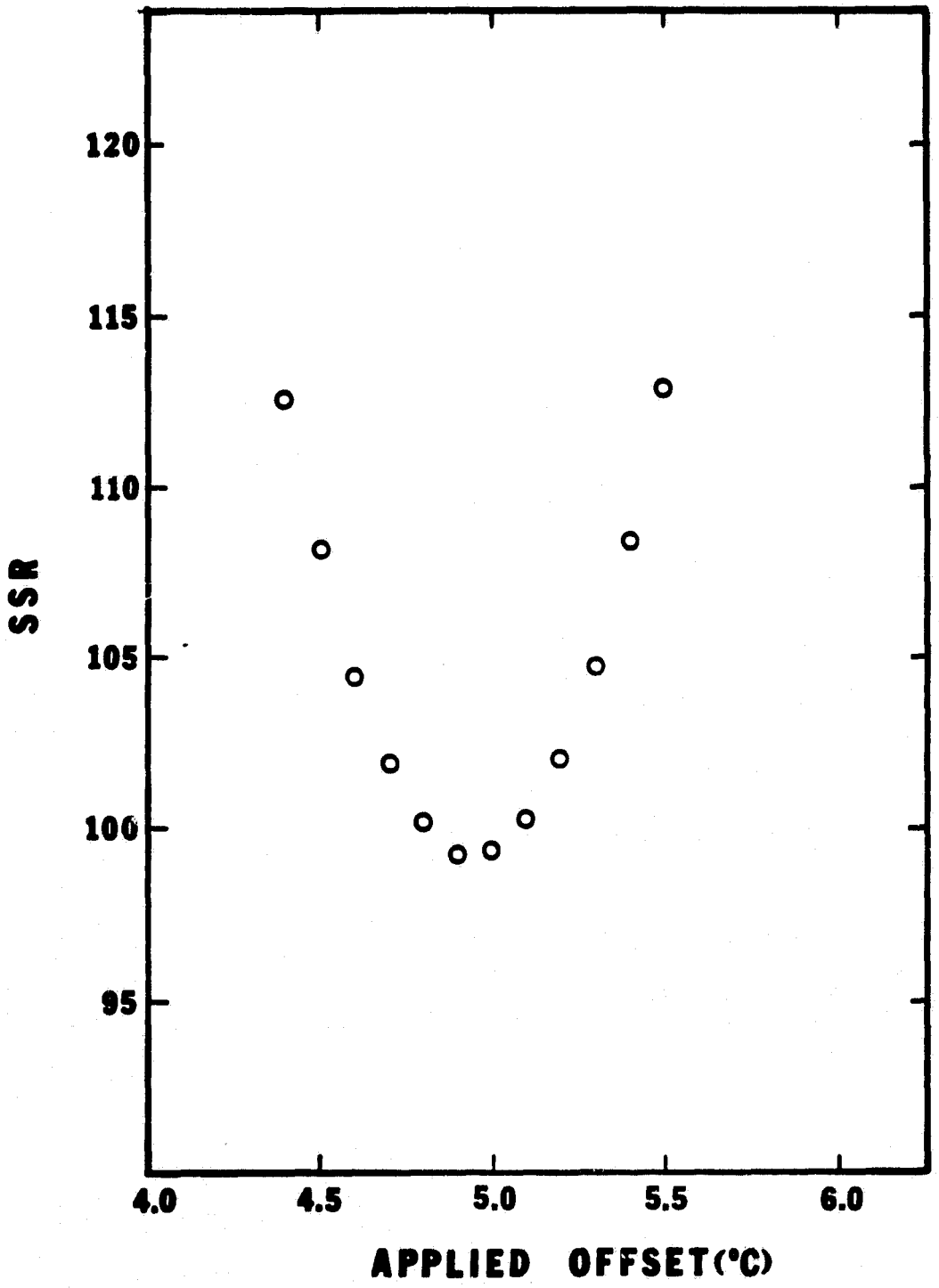

Figure 8.15. SSR vs. Applied Offset: Day -1

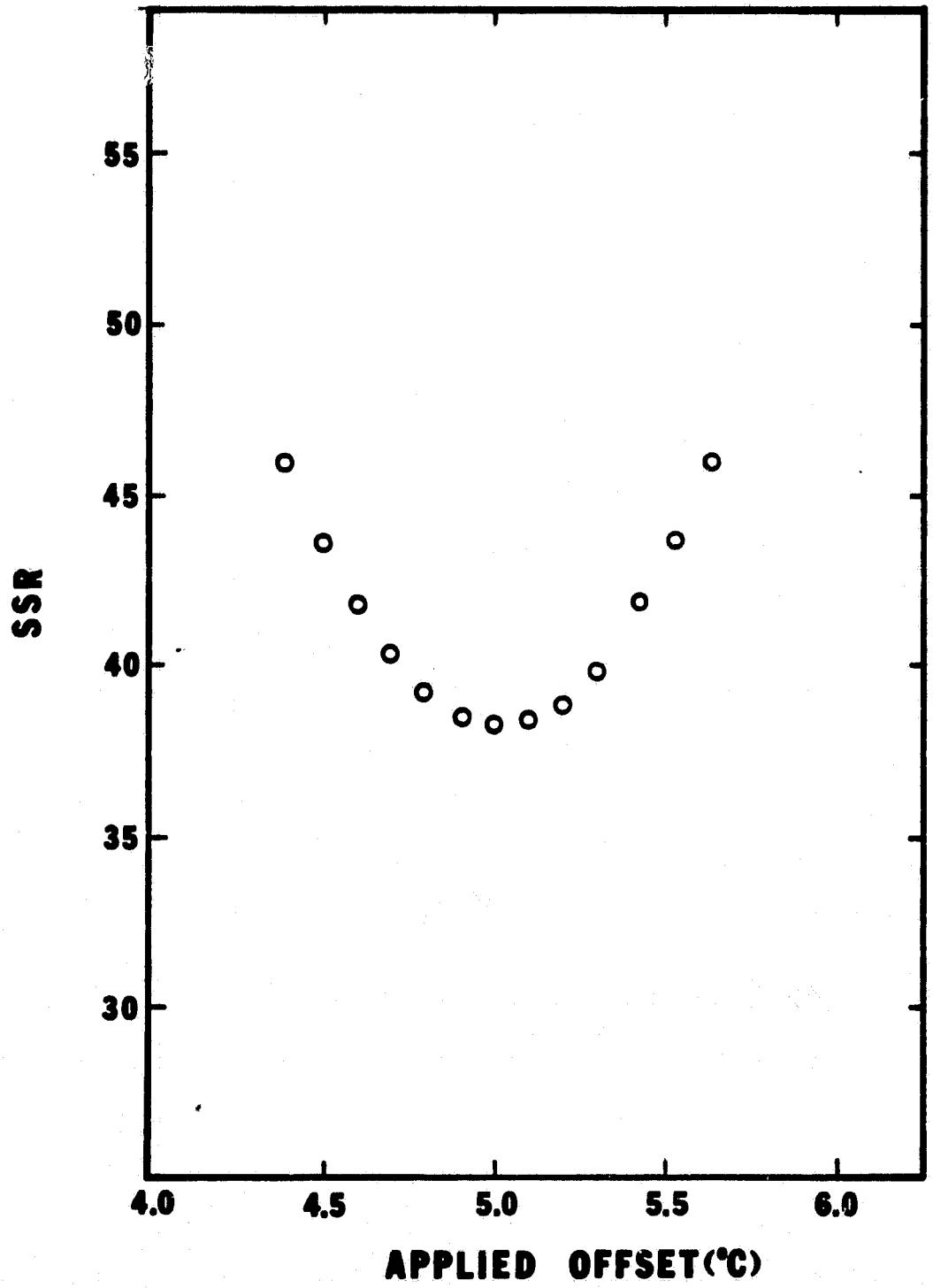

Figure 8.16. SSR vs. Applied Offset: Day -4 and -5

Table 8.2

Summary of Required Offsets with Early September Data Deleted

Subset	Offset	Number of Data Points Involved
All Data	4.89	179
North Lake	5.16	26
Central Lake	4.06	24
Provo Bay	4.76	48
Goshen Bay	5.13	81
July	5.07	30
August	5.05	70
September	5.02	49
October	4.06	6
November	4.16	24
Same Day	4.90	61
+ 1 Days	4.80	53
- 1 Days	4.95	45
- 4 Days	5.47	11
- 5 Days	4.47	9
Fish & Wildlife	4.81	137
USBR	5.17	42

Table 8.3

Summary of Offsets Using Only Same Day Data

Subset	Offset	Number of Data Points Involved
All Data	4.90	61
North Lake	4.61	3
Central Lake	4.17	8
Provo Bay	5.44	19
Goshen Bay	4.77	31
July	4.95	8
August	5.50	25
September	4.16	12
October	4.04	4
November	4.63	12

°C. In fact, assuming 4.7 to be the average offset and calculating to the nearest tenth of a degree, all data fall within ± 1 °C of the average. For this reason it was felt that the results obtained from this analysis were highly reliable, being based upon such a large amount of data with such a small relative variation. Table 8.4 summarizes the previous tables including the September data (all data) and also gives standard deviations.

Based upon the above procedure and information, it was determined that the proper offset to apply to the HCMM model is 4.9 °C. Although the SSR plot for all data used indicates an offset of 4.7 °C, it was felt that the 4th and 5th of September data was having a significant impact, and although insufficient evidence could be found to delete it from the data base, it differed from all other data sufficiently to warrant exclusion from the actual calibration procedure.

8.3 Atmospheric Effects

In order to evaluate the effect of various atmospheric parameters on the calibration, the value of the atmospheric factor being examined required to force agreement between surface measured and satellite measured temperatures was determined. Only same day data were analyzed. Table 8.5 summarizes the correlation coefficients between the values of each individual atmospheric parameter examined and the offset required. None of the parameters have a statistically significant effect on the HCMM calibration.

However, the presence of a single point in the low air temperature range was all that prevented a high degree of correlation (0.740). Since this trend did not entirely disappear in either the average or high air temperature plots (both being considered better indicators than the low air temperature), it was determined that a more extensive examination should be made.

In an attempt to attain a better understanding of the air temperature effect all available data was analyzed, as opposed to only data collected the same day. The result of the addition of the supplementary data was to destroy the trends noticed when using the same day data only. There was not, however, a significant increase in the amount of low temperature data. While it is possible that the addition of the "off day" data is masking trends, it appears that air temperature, as well as other parameters evaluated, does not have a measurable effect on the calibration of the HCMM equation over the range of temperatures examined.

Table 8.4

Summary of Offsets with Additional Statistical Information

Data Set	Required Off et	Number of Points	Standard Deviation
All Data	4.74	185	1.54
All Data Less Early September Data	4.89	179	1.31
Same Day Data Only	4.90	61	1.17

Table 8.5

Correlation Coefficients of Atmospheric Parameters and Required HCMM Offsets

Parameter	Correlation Coefficient
Humidity	-0.203
Wind	0.051
Sol-a-meter	-0.247
Evaporation	0.074
Lake Stage	0.233
Air Temperature	
High	0.386
Low	0.486
Average	0.442
Pan Temperature	
High	0.240
Low	0.457
Average	0.339
Cloud Cover	-0.288

8.4 Linear Model

The development of a simple relationship between the available thermal intensity and desired surface temperature values was considered. It was determined that a more accurate model (equation) could not be found, due to the theoretical backing of the HCMM model as opposed to the empirical nature of any other developed relationship. It was felt, however, that a computationally simpler model with similar accuracy could be developed. The relationship between temperature and emitted thermal infrared radiation is very nearly linear over small temperature ranges. A linear model for use over the anticipated range of surface temperatures could realize a significant savings in conversion and computation time. It should be emphasized that the linear model is based on empirically determined constants and has no theoretical justification. The model would only be useful if it were shown to be equally accurate as the HCMM supplied theoretical model.

The procedure consisted of randomly dividing the data into two groups, group A and group B. Group A was then used to re-calibrate the HCMM equation, while group B was used to determine the coefficients for the linear model. The re-calibration of the HCMM equation was done in essentially the same manner as the initial calibration, while the linear model was developed through the use of the Minitab statistical package which uses standard simple linear regression techniques.

The re-calibrated HCMM equation was then applied to the data of group B and the SSR between actual surface and model predicted temperatures was determined. The linear model was then applied to group A data and the corresponding SSR value determined.

With the SSR values determined through the above procedure, the ratio of the two values follow a statistical F-distribution, which allows the two models to be tested for equality of accuracy. The linear model developed using all available data is:

$$T = -7.172 + 0.37494\ I$$

where T = temperature ^{o}C $(0 < T < 30)$
and I = HCMM thermal infrared intensity

Figure 8.17 shows the correlation between the linear model and the HCMM model in the range from 1 ^{o}C to 27 ^{o}C. The correlation coefficient of the above equation is 0.982. It is suggested that the above equation can be used in cases where the utilization of a simpler model is justified.

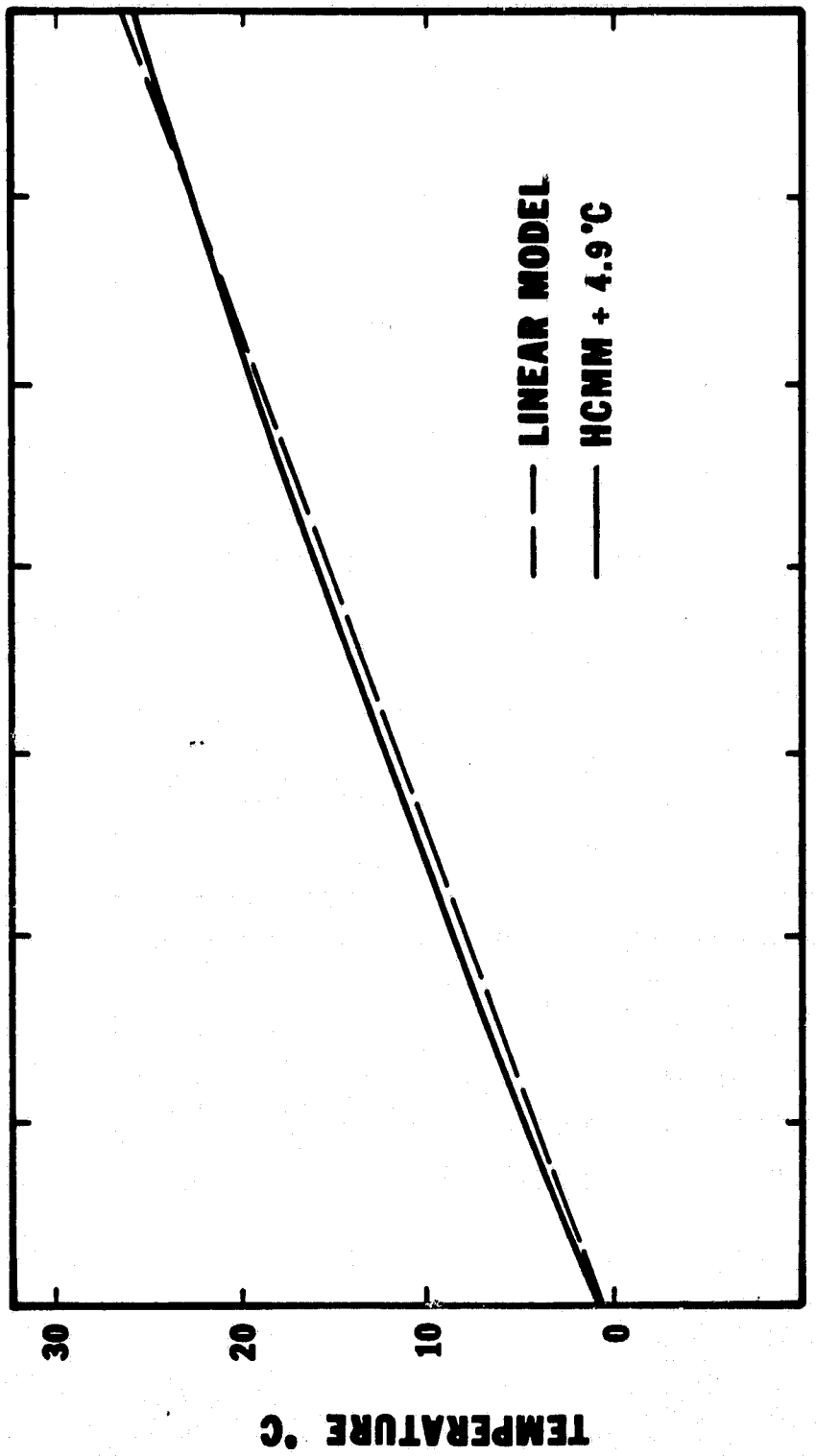

Figure 8.17. Linear Model vs. HCMM Model + 4.9 °C

9. WATER QUALITY

9.1 Methodology

The one-to-one correlations presented in this section were developed with the HCMM data and water quality parameters according to the methods explained in Section 7. Correlation coefficients and graphs of the regression lines representing several data sets are included. In each case the regression analysis shown was performed on a data set which represented the typical correlation of that particular comparison. A description of each of the parameters correlated in this analysis has been included.

9.2 Day-Infrared Correlations

The day infrared (DIR) intensity nearest each lake sampling station was identified and tabulated for this correlation analysis. The net plankton measurements taken on Utah Lake have been used to represent the algae concentrations present in 1978. The major reason for this is that more complete records were kept in 1978 of the net plankton counts on the lake than of the total or nanno plankton counts. Since the accuracy of this investigation increases with an increase in the number of correlations made, the net plankton counts were chosen. These counts were assumed to be representative of the total plankton population in Utah Lake. They are hereafter referred to as plankton counts or plankton concentrations. Correlation of the total plankton counts was used for measurements made in 1979.

The correlation during the summer months of the log total plankton (algae) concentration in Utah Lake and the emitted heat (DIR) from the water surface is very high for a naturally occurring system. Correlation coefficients are given in Table 9.1. The level of significance α for each correlation is also given. If the level of significance of the correlation between the algae concentrations in the lake and the DIR were 0.05 this would mean that all but 5% of the distribution of the correlation could be interpreted as being significant in the substantiation of this relationship. If the significance of the correlation were greater than 0.05 the correlation was considered "not significant" and was designated by n/s.

Table 9.1

Correlation Coefficient of DIR and log Total Plankton
1978

Date	07/28	08/03	08/10	08/17	08/23	09/13	10/14	10/25
Corr.	0.841	0.749	0.640	0.977	0.783	0.605	0.758	0.479
Sig.(α)	0.005	0.01	0.025	0.005	0.005	0.05	0.005	n/s

Table 9.2

Correlation Coefficients of DIR and log of
Ceratium Hirundinella Concentration
1978

Date	07/28	08/03	08/10	08/17	08/23	09/13
Corr.	0.754	-0.224	0.220	0.533	-0.176	0.705
Sig.(α)	0.01	n/s	n/s	n/s	n/s	0.025

As the algae concentration in the water increases it appears more like a land mass on the DIR printouts; i.e., collecting more heat during the daytime hours so that it appears warmer and then losing heat more rapidly than the clearer waters during the nighttime. This phenomenon can be observed very easily by comparing the day and night infrared data as displayed by the color graphics. The color pictures of the DIR and NIR (night infrared) data clearly show the same areas in Utah Lake being respectively warmer and cooler.

The description of the waters concentrated with algae being similar to land bodies is valid since the same phenomenon is responsible for the behavior of each with respect to temperature. The addition of the algae to a mass of water has the effect of lowering the specific heat of the mass from the specific heat of clear water (1.00 cal/gm-^{o}C). Since the specific heat of land is also lower than 1.0, both the land and the algae concentrated water acquire and lose heat more rapidly than clear water. This makes possible the detection of algae concentrations in water bodies such as Utah Lake by monitoring the heat from the lake during the day and night. Figure 9.1 is a graphical representation of the linear regression of the DIR and log total plankton as measured on Utah Lake, July 28, 1978. The regression equation and the value of r are included.

Ceratium hirundinella (Figure 9.2) is a solitary, unicellular plant. Its cells are generally narrowly fusiform with one apical horn and 2 or 3 stouter and shorter basal horns. The cells are 30 to 72 μm wide and 100 to 400 μm long. Although rare in early June on Utah Lake, this algae was one of the dominant plankton throughout the rest of the summer. It was often abundant enough to color the water muddy-brown and plug plankton nets (Rushforth, et al, 1980). Correlation and significance levels for CH are given in Table 9.2.

No real, continuous relationship could be established between the Ceratium hirundinella population in Utah Lake and the emitted heat (DIR) from the water surface. The most probable reason for this is that the Ceratium do not form clumps or clusters which would increase their density in the water and thereby increase both heat conductivity and storage. Another important observation is that while Ceratium is the second most dominant algae in the lake it constitutes less than 10% of the total algae count in the later summer months. This results in the Ceratium not having much effect on the observable heat emittance compared to the entire plankton mass.

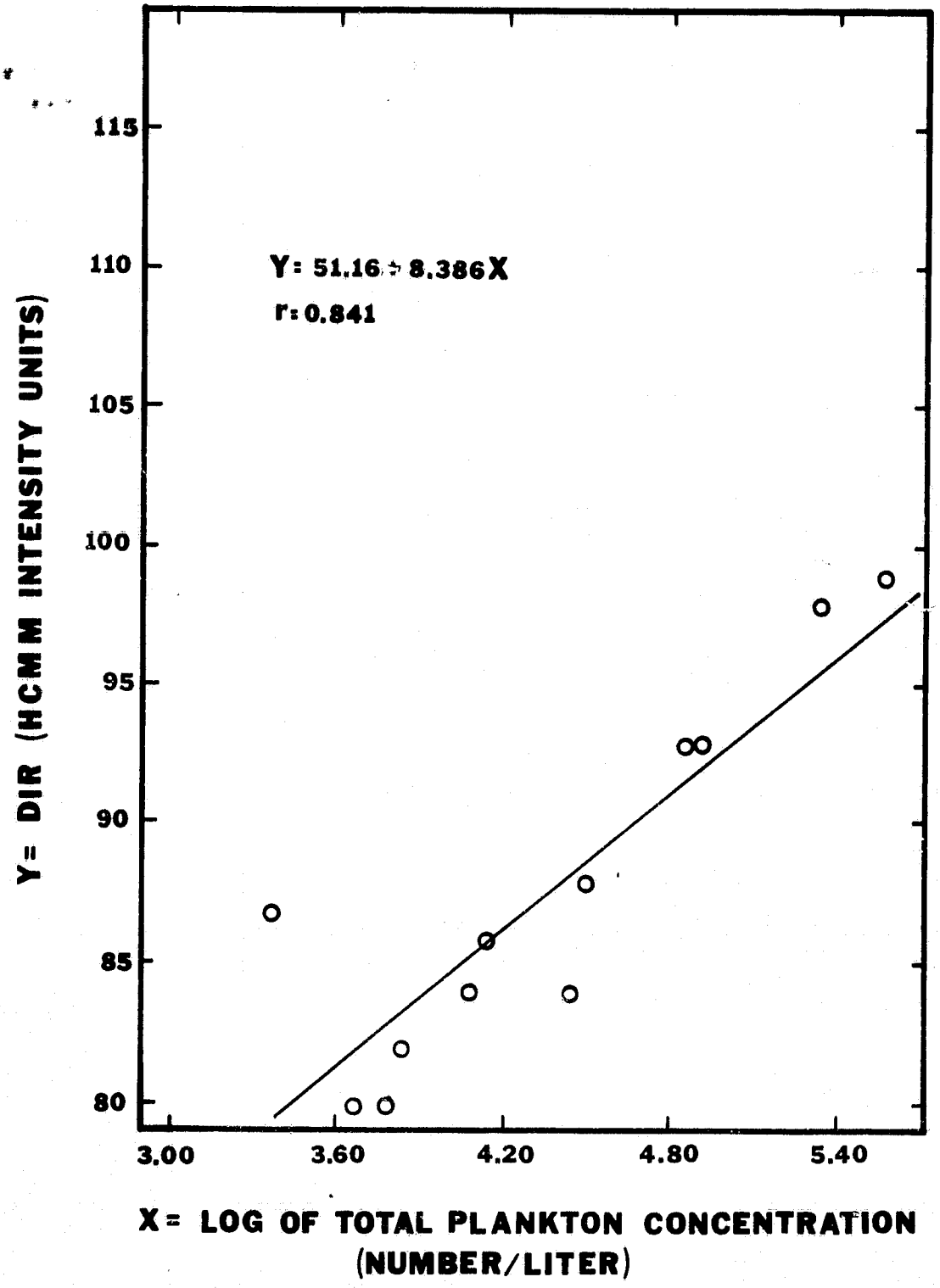

Figure 9.1. Plot of DIR and log of Total Plankton Concentrations on Utah Lake, July 28, 1978.

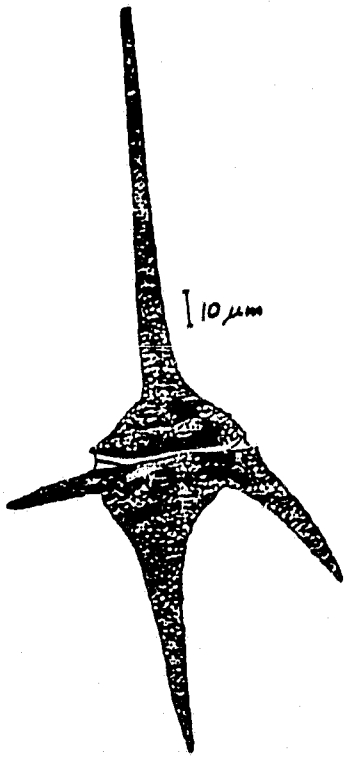

Figure 9.2. Ceratium hirundinella.

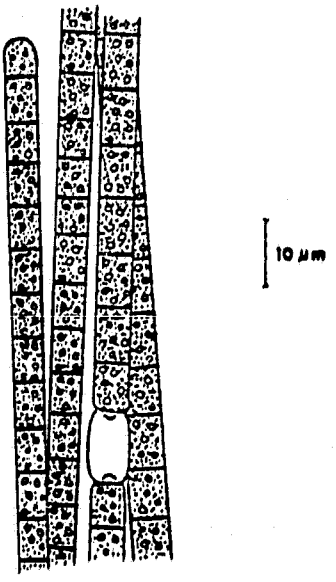

Figure 9.3. Aphanizomenon flos-aquae.

Aphanizomenon flos-aquae (Figure 9.3) is a parallel trichomes algae, united in bundles or flakes to form macroscopic aggregates. Its apices are broadly rounded with cells 5 to 6 μm in diameter and 6 to 8 μm long. Aphanizomenon contains numerous pseudovacuoles and oblong or cylindrical heterocysts. This blue-green algae was usually the most abundant and conspicuous summer plankton in Utah Lake. Table 9.3 shows correlations and significance levels for DIR and AFA.

Figure 9.4 shows an obvious relationship exists between Utah Lake DIR in the summer and the Aphanizomenon concentration in the lake. These correlations closely parallel those of total plankton which was expected since nearly 90% of the plankton count in Utah Lake in the late summer is Aphanizomenon. This study did not attempt to explain the reasons for the change during the summer season from a large diversity of species of plankton to essentially only two by late summer. However, this phenomenon has been substantiated by the similarity of the Aphanizomenon and total plankton correlations with the DIR measurements.

9.3 Reflectance Correlations

The HCMM visual reflectivity measurements (VR) were made by the satellite sensor and tabulated for this comparison. The VR intensity nearest each station where lake measurements were made was recorded. Table 9.4 gives the correlations and significance of VR and total plankton relationships.

During the early summer and on through the middle of August a very high negative correlation exists between the algae concentration in the lake waters and the reflectivity of the lake surface. This negative correlation indicates that as the concentration of the algae increases in the Utah Lake waters the reflectiveness of the water surface decreases or appears darker. Figure 9.5 is a representation of the regression of the VR and log Total Plankton on August 17, 1978.

In late August this inverse relationship between VR and total plankton concentration decreases and by October there is essentially no relationship. The reason for the breakdown of this relationship appears to be the occurrence of blooms of algae on the lake surface. These whitish, floating matts of algae and air bubbles are very reflective. Development of

Table 9.3

Correlation Coefficients of DIR and log
Aphanizomenon Flos-Aquae Concentration
1978

Date	07/28	08/03	08/10	08/17	08/23	09/13	10/14	10/25
Corr.	0.993	0.728	0.628	0.987	0.783	0.599	0.767	0.503
Sig.(α)	0.005	0.01	0.025	0.005	0.005	0.05	0.005	n/s

Table 9.4

Correlation Coefficients of VR and log
Total Plankton Concentration
1978

Data	07/28	08/03	08/10	08/17	08/23	09/13	10/14	10/25
Corr.	-0.960	-0.946	-0.972	-0.979	-0.652	-0.740	-0.190	0.005
Sig.(α)	0.005	0.005	0.005	0.005	0.025	0.025	n/s	n/s

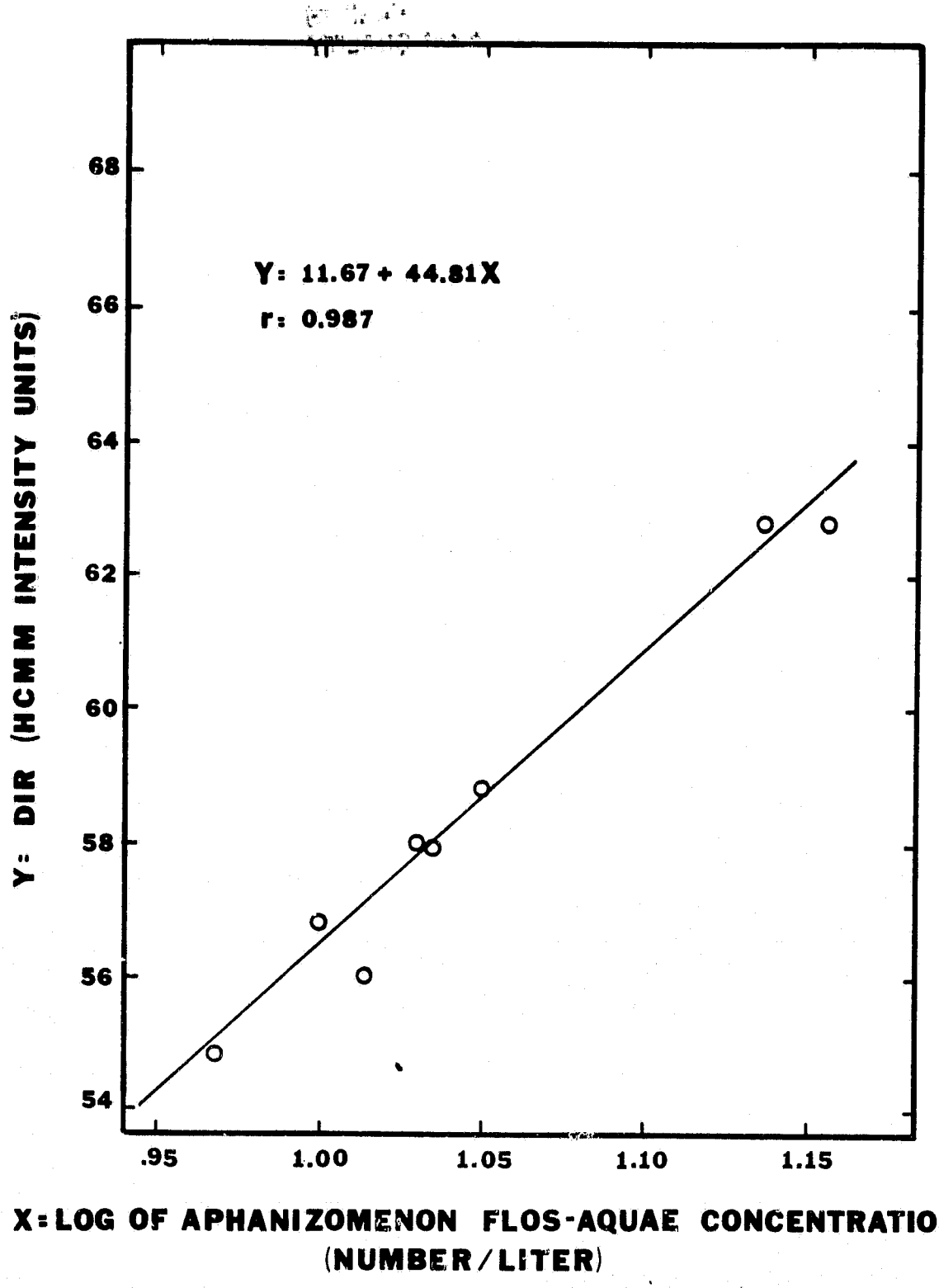

Figure 9.4. Plot of DIR and log of Aphanizomenon flos-aquae Concentrations in Utah Lake, August 17, 1978.

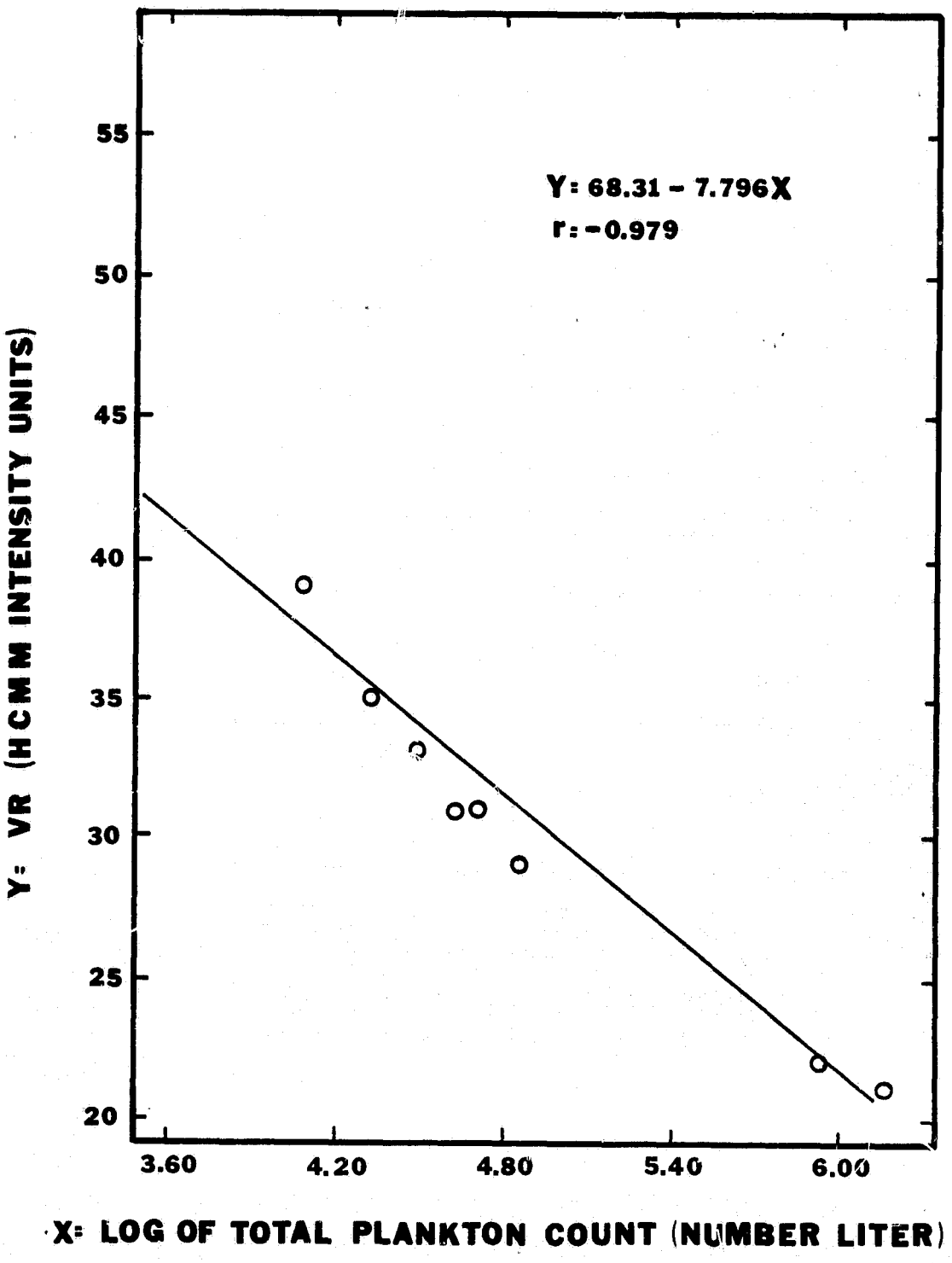

Figure 9.5. Plot of VR and log of Total Plankton Concentration on Utah Lake, August 17, 1978.

these reflective blooms over the area of highest algae concentration which had previously been the least reflective areas on the lake effectively reduces the inverse correlation between the HCMM VR and the algae concentrations.

While some correlations between the VR and log of net Ceratium hirundinella count are quite significant, no continuous relationship could be established. The probable reasons for this are the same as those for which no continuous relationship could be established between Ceratium and DIR; i.e., the Ceratium cells do not join together to form larger bodies in the water and the proportion of the total plankton concentration made up by Ceratium is relatively small. This lack of correlation and significance are shown in Table 9.5.

Because the correlation analysis for VR and Aphanizomenon shown in Table 9.6 doesn't give a different pattern of results than that given for VR and total plankton, a conclusion could not be reached about the reflective properties of Aphanizomenon as compared with the total phytoplankton in Utah Lake. The decline in the inverse correlation beginning in late August is caused by the same phenomenon, algal blooms, which is responsible for the decline in the relationship between VR and the total plankton concentration. Figure 9.6 shows a graph of the linear regression of VR and the log of Aphanizomenon flos-aquae concentrations in Utah Lake, August 10, 1978.

9.4 Nutrients

Analyses were made on samples of Utah Lake waters taken at the lake measuring stations to determine the amount of phosphorus present in the sample. These analyses were made in the Brigham Young University Water Research Laboratory. The measurements of phosphorus concentration which coincide with the algae and HCMM measurements made on Utah Lake have been compiled by date of sampling. Table 9.7 gives the correlations and significance of the phosphorus and plankton concentrations.

These correlations indicate that at least in the first half of the year the plankton concentration in Utah Lake is dependent on the concentration of phosphorus present. This was to be expected since phosphorus is a basic nutrient of nearly all blue-green algae. There were only two dates on which data was available to analyze the correlation between the phosphorus concentrations and Aphanizomenon concentrations in Utah Lake. Therefore, it is difficult to determine any meaningful relationship from these results.

Table 9.5

Correlation Coefficients of VR and log
of Ceratium Hirundinella
1978

Date	07/28	08/03	08/10	08/17	08/23	09/13
Corr.	-0.883	-0.362	-0.467	-0.571	-0.313	-0.585
Sig.(α)	0.005	n/s	n/s	n/s	n/s	0.05

Table 9.6

Correlation Coefficients of VR and
log Aphanizomenon Concentration
1978

Date	07/28	08/03	08/10	08/17	08/23	09/13	10/14	10/25
Corr.	-0.945	-0.836	-0.949	-0.994	-0.645	-0.731	-0.214	-0.005
Sig.(α)	0.005	0.005	0.005	0.005	0.025	0.025	n/s	n/s

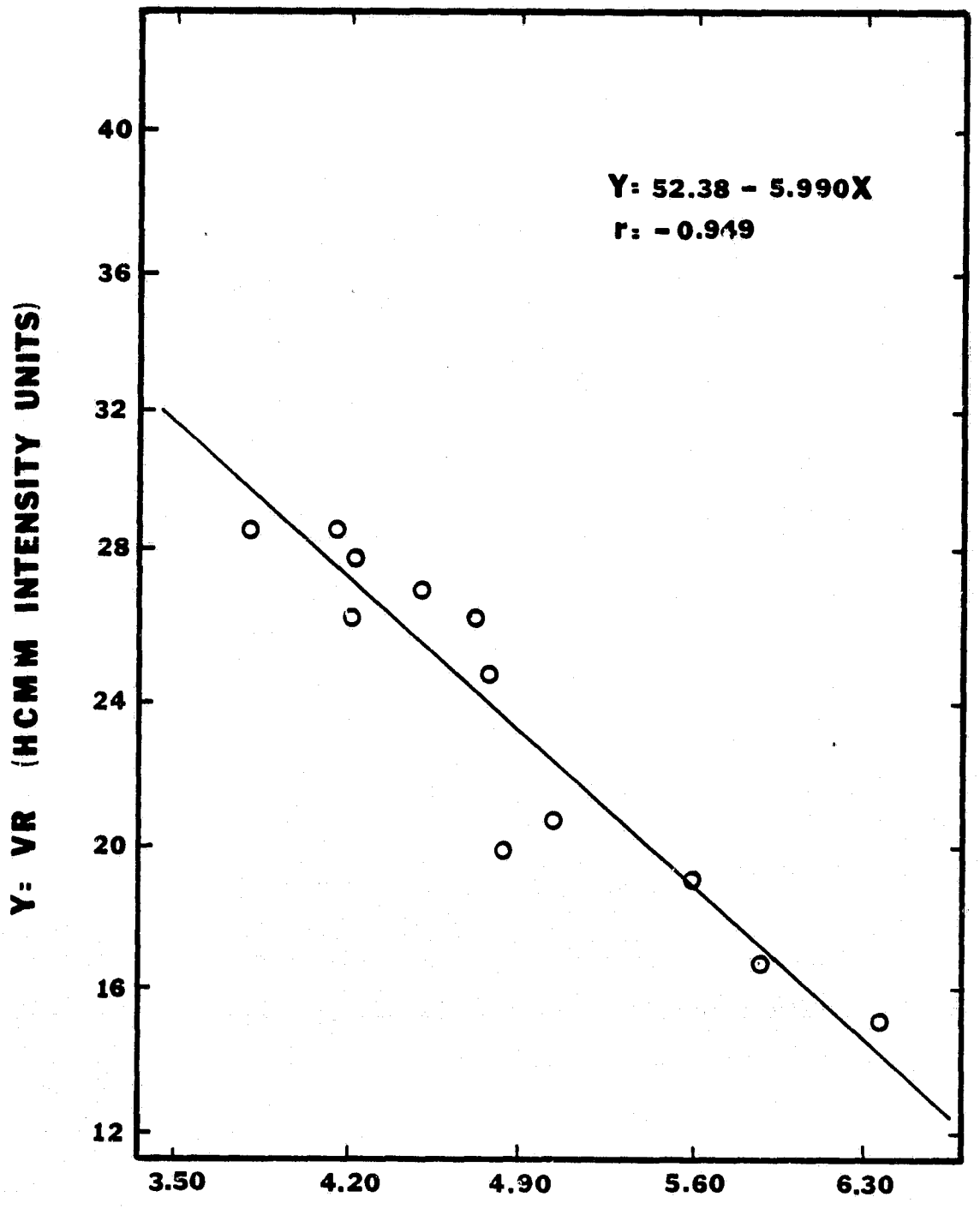

Figure 9.6. Plot of VR and log of Aphanizomenon flos-aquae Concentrations on Utah Lake, August 10, 1978.

Table 9.7

Correlation Coefficients of Phosphorus and log of the Total Plankton Concentrations

	DIR and log Total Plankton			DIR and log Afanizomenon	
Date	07/28/78	03/10/79	05/12/79	07/28/78	05/12/79
Corr.	0.488	0.566	0.725	0.864	0.384
Sig.(α)	n/s	0.05	0.01	0.005	n/s

Table 9.8

Correlation Coefficients of Nitrogen and the log of the Total Plankton Concentrations

Date	07/28/78	03/10/79	05/12/79
Corr.	0.688	0.556	-0.066
Sig.(α)	0.025	0.05	n/s

Analyses were performed in the Brigham Young University Water Research Laboratory on water samples taken at testing stations on Utah Lake in order to also determine the concentration of nitrogen in the samples. The nitrogen present was classified as ammonia, nitrite or nitrate. The total of the nitrogen measurements which coincide with algae and HCMM measurements made on Utah Lake have been compiled by date of sampling. Correlations of these measurements are shown in Table 9.8.

Nitrogen is a nutrient necessary for algae growth; however, the results of this correlation analysis are inconclusive. This is because there were only a few days on which measurements were made of both nitrogen and algae concentrations.

9.5 Turbidity

Turbidity is the measure of opacity or light scattering properties of the water sample. Turbidity measurements of several Utah Lake water samples have been made with a Model 2100A Turbidimeter in the Brigham Young University Water Research Laboratory. This meter measures in Nephelometric Turbidity Units (NTU) which are a measure of the intensity of the light scattered in the sample at an angle of 90° from the direction of the incident light source. The readings which coincide with the algae and HCMM measurements made on Utah Lake have been compiled by date of sampling. Correlations of these measurements presented in Table 9.9.

There does not appear to be any significant correlation between the turbidity of the water samples and the concentration of the plankton in them. This may be explained by several factors. First, Utah Lake is a very shallow lake so winds cause complete turnover in the lake waters and stir up into suspension the bottom sediments. These suspended sediments may be principally responsible for the turbidity measured in the water samples. Secondly, the algae present in the water column are not so likely to scatter incident light as suspended solids because they are relatively transparent when not clustered together and allow more light to be passed or refracted than diffracted.

Correlations from Table 9.10 show that the more turbid waters of Utah Lake do not appear to emit any more heat (DIR) than the other waters of the lake. This is consistent with the result that there was no significant correlation between algae concentrations and turbidity.

Table 9.9

Correlation Coefficients of Turbidity and the log of the Total Plankton Concentration

Date	07/28/78	03/10/79
Corr.	-0.121	0.520
Sig.(α)	n/s	n/s

Table 9.10

Correlation Coefficients of DIR and Turbidity

Date	07/28/78	07/10/79	08/24/79	09/22/79
Corr.	0.158	-0.150	0.240	-0.456
Sig.(α)	n/s	n/s	n/s	n/s

Table 9.11

Correlation Coefficients of VR and Turbidity

Date	07/28/78	08/31/78	07/10/79	08/24/79	09/22/79
Corr.	0.137	-0.189	0.604	0.090	0.857
Sig.(α)	n/s	n/s	0.025	n/s	n/s

As Table 9.11 shows, there does not appear to be any significant continuous relationship between the reflectivity of Utah Lake and the turbidity of the water. Again, this confirms the results of the correlation between plankton concentrations and turbidity; i.e., that there was no significant relationship between them.

9.6 Day Infrared and Reflectance Correlations

The relationships of Table 9.12 show a certain level of negative correlation which was expected in this analysis since the DIR had a strong positive correlation with algae concentrations while VR had an even stronger negative correlation with the same. These results are simply a statistical expression of the fact that algae may be presumed to be present in the waters of Utah Lake wherever VR intensities are relatively low.

From early summer until late fall the DIR and VR color graphics were very useful in identifying areas within the lake of higher algae concentrations. The high negative correlation between the HCMM VR data on Utah Lake and the plankton concentrations justifies the use of the VR color prints to locate algae concentrations. Areas which appear to be warmer on the DIR color prints and darker on the VR prints are areas of higher algae concentrations in the lake. Either the DIR prints or the VR prints could be used individually to predict the location of plankton concentrations in the lake, but the use of the two measurements together increases the probability that the areas on the lake where both indicate algae are in fact locations of higher algae concentrations.

Figures 9.7 and 9.8 illustrate this application of DIR and VR color pictures of the HCMM data. The DIR (Figure 9.7) and VR (Figure 9.8) sensed from Utah Lake on July 6, 1978 indicate a particularly high concentration of plankton in Provo Bay and a significant concentration in the middle of the lake. Reference to the tabulated measurement of plankton concentrations for July 6, 1978 substantiates the prediction of higher concentrations of algae in the areas indicated. The highest recorded concentrations for the entire lake on this date were in Provo Bay. The stations along the eastern side of the lake near the main body also indicated higher concentrations.

Table 9.12

Correlation Coefficients of DIR and VR

Date	07/28/78	08/31/78	07/10/79	08/24/79	09/22/79
Corr.	-0.837	-0.796	-0.628	-0.535	-0.547
Sig.(α)	0.005	0.005	0.025	0.05	0.05

Table 9.13

Correlation Coefficients of NIR and log of the Total Plankton Concentration

Date	08/31/78	09/13/78
Corr.	-0.918	-0.727
Sig.(α)	0.005	0.025

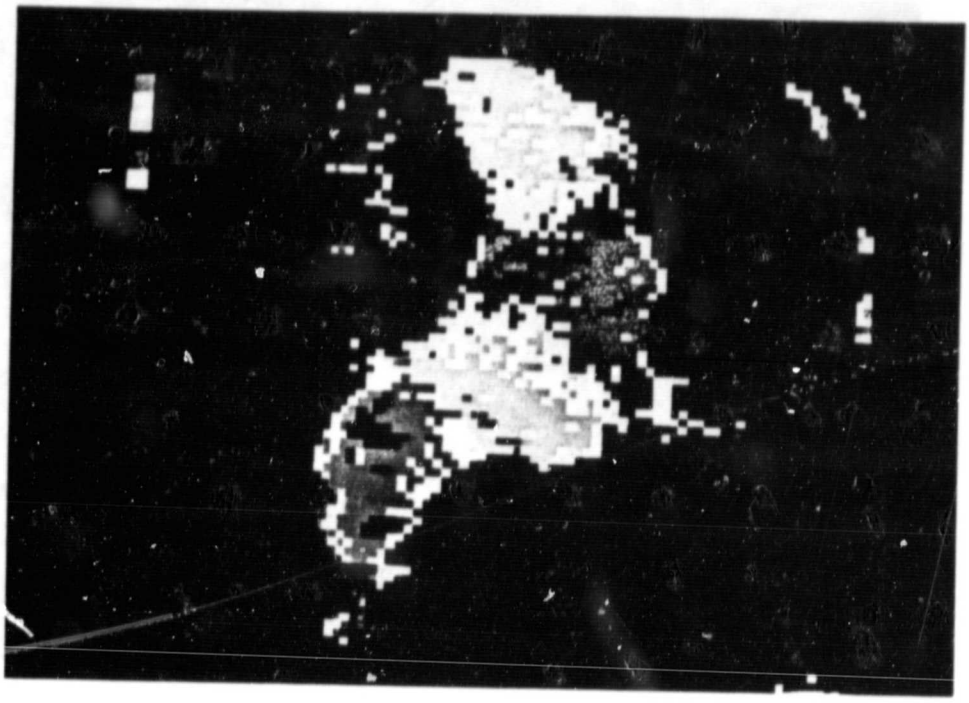

Figure 9.7. DIR on Utah Lake, July 6, 1978.

Figure 9.8. VR on Utah Lake, July 6, 1978.

9.7 Night Infrared Correlations

The HCMM Night Infrared (NIR) measurements were made by the satellite and tabulated for this comparison. The NIR intensity nearest each station where lake measurements were made was recorded. Table 9.13 gives the correlations and significance level of the NIR and plankton data.

Due to the fact that only a small amount of NIR data was available for this study, only two dates on which NIR and total plankton measurements were made could be used. Data from a few other days were acquired but were unusable because of clouds which made the intensity readings inaccurate. The two correlations which were performed however indicate a strong negative relationship between the emitted heat from Utah Lake at night (NIR) and algae concentrations in the lake waters. This result agrees with the observation made with respect to the correlation of DIR and plankton concentrations, that waters with significant suspended algae mass behave in a similar manner to the surrounding land. They heat up more quickly than the clear waters in the daytime and cool more quickly at night. Figure 9.9 shows a plot of the linear regression of the NIR and the log of total plankton count of Utah Lake, August 31, 1978.

Locating areas on the day and night IR color graphics scenes which are respectively warmer and cooler is a method of identifying areas within the lake with a relatively high algae concentration. Figures 9.10 and 9.11, the color representations of the HCMM DIR and NIR intensities measured on Utah Lake September 23, 1978, illustrate this relationship. The lake's northwest corner is the warmest area during the day (Figure 9.10) and one of the coolest during the night (Figure 9.11), indicating the presence of higher concentrations of algae.

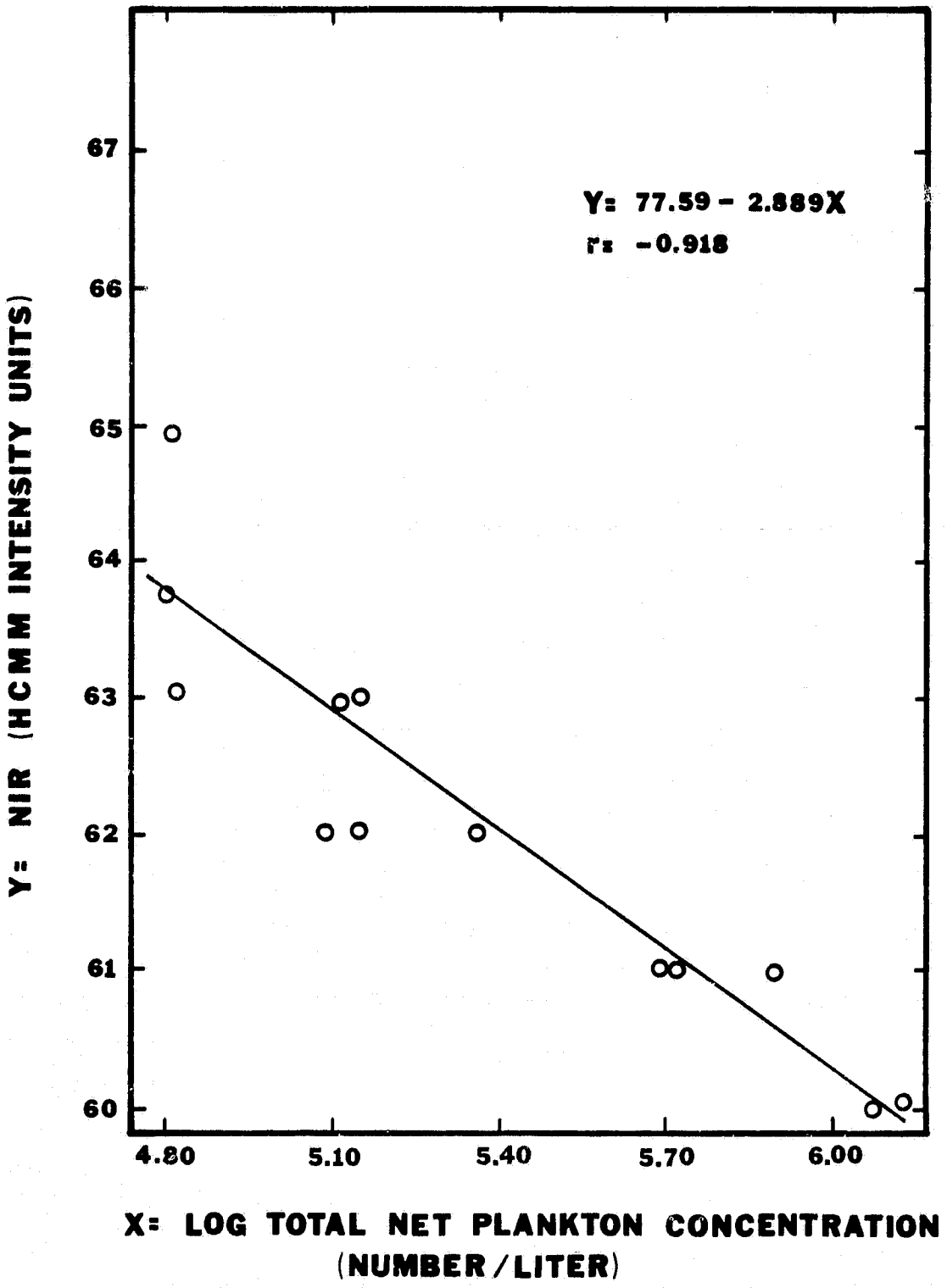

Figure 9.9. Plot of NIR and log of Total Plankton Concentrations on Utah Lake, August 31, 1978.

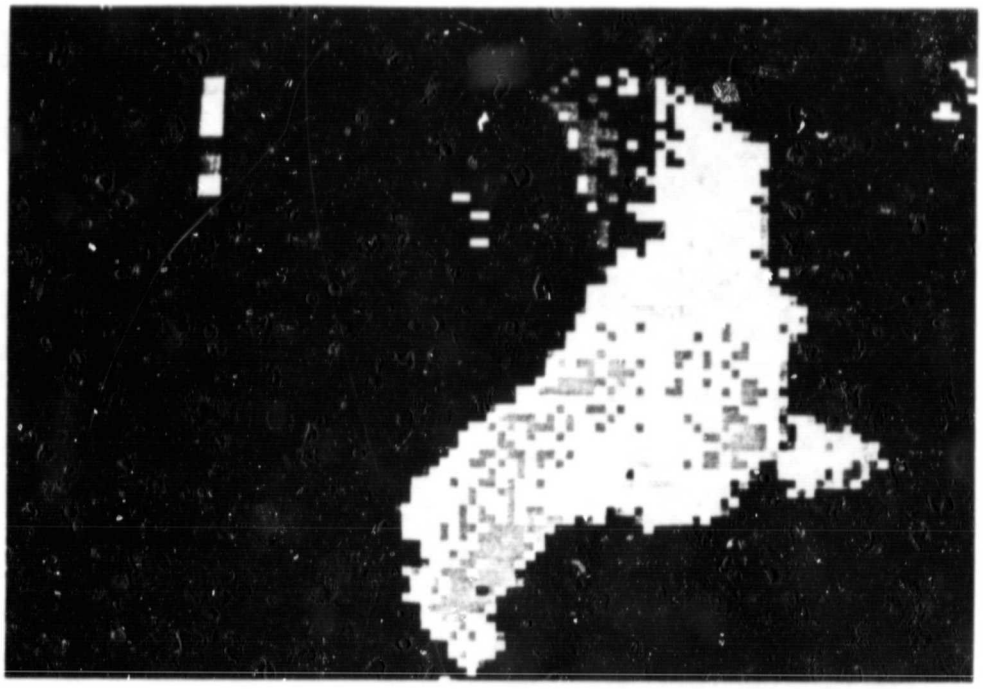

Figure 9.10. DIR on Utah Lake, September 23, 1978

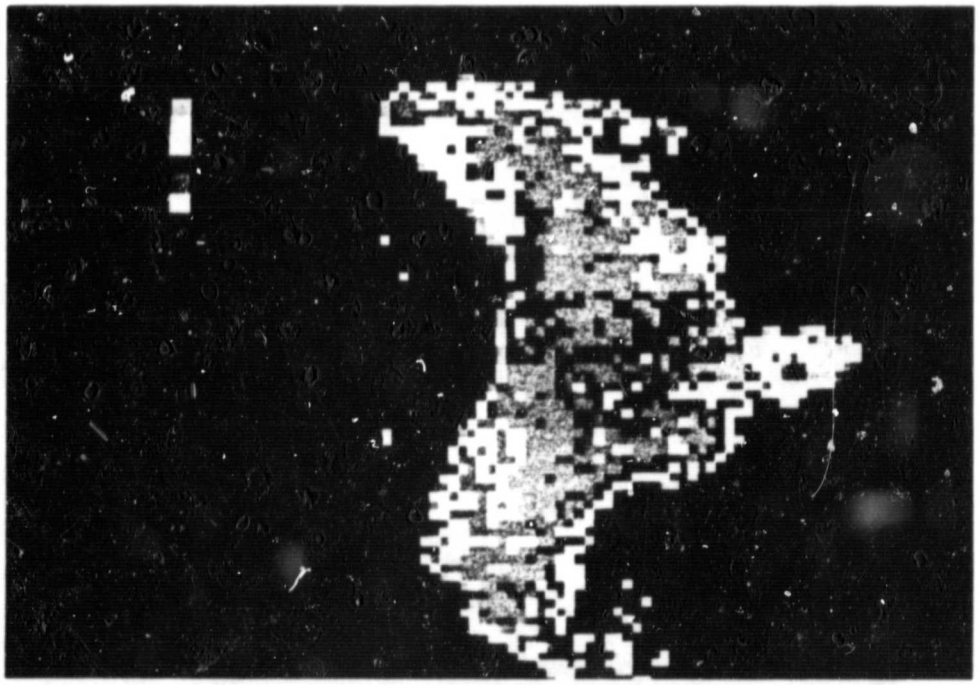

Figure 9.11. NIR on Utah Lake, September 23, 1978

10. CORRELATION IMAGES

10.1 Background

The day infrared and visible (reflectance) imagery both show the effects of algae blooms and other phenomena. Warmer areas of the lake show in the infrared. The reflectance data show the turbid areas. The images separately however, give only a limited overall picture of the lake from which conclusions could be made. Therefore, a composite or correlation image was formed for each date.

The study of the images showed that the algae blooms have high infrared and high reflectance values. Other combinations of infrared, and reflectance intensities were evaluated in order to identify different unique features in various areas and throughout seasonal variations in the lake. No statistical studies were undertaken to relate the ground truth to the correlation image beyond the identification of seasonal patterns.

HCMM coverage for 1978 and 1979 was sufficient to indicate definite patterns in the lake. Each part of the lake was analyzed separately throughout the entire year. Conclusions are given as to the cause of the patterns in the lake. The names of the months are abbreviated to the first or the first two letters except May is MY, March is MR, July is JL and September is S or SE. The number that starts the file name is the day of the month.

10.2 Goshen Bay

Early summer and middle summer correlation images are from March through July, as shown in Figure 10.1. The southwest side of Goshen Bay shows a low infrared and a high visible reading (L-H) (refer to Section 7.4, Table 7.1). This persists into the end of July. The 22 July picture (22 JL.COR) shows part of the Bay interspersed with black, which because of its position with respect to the other colors is low infrared and medium day visual (L-M), and dark blue (L-L). The persistence of this pattern for several months would seem to overrule algae or diatom blooms as the cause. It is surmised that

C-2

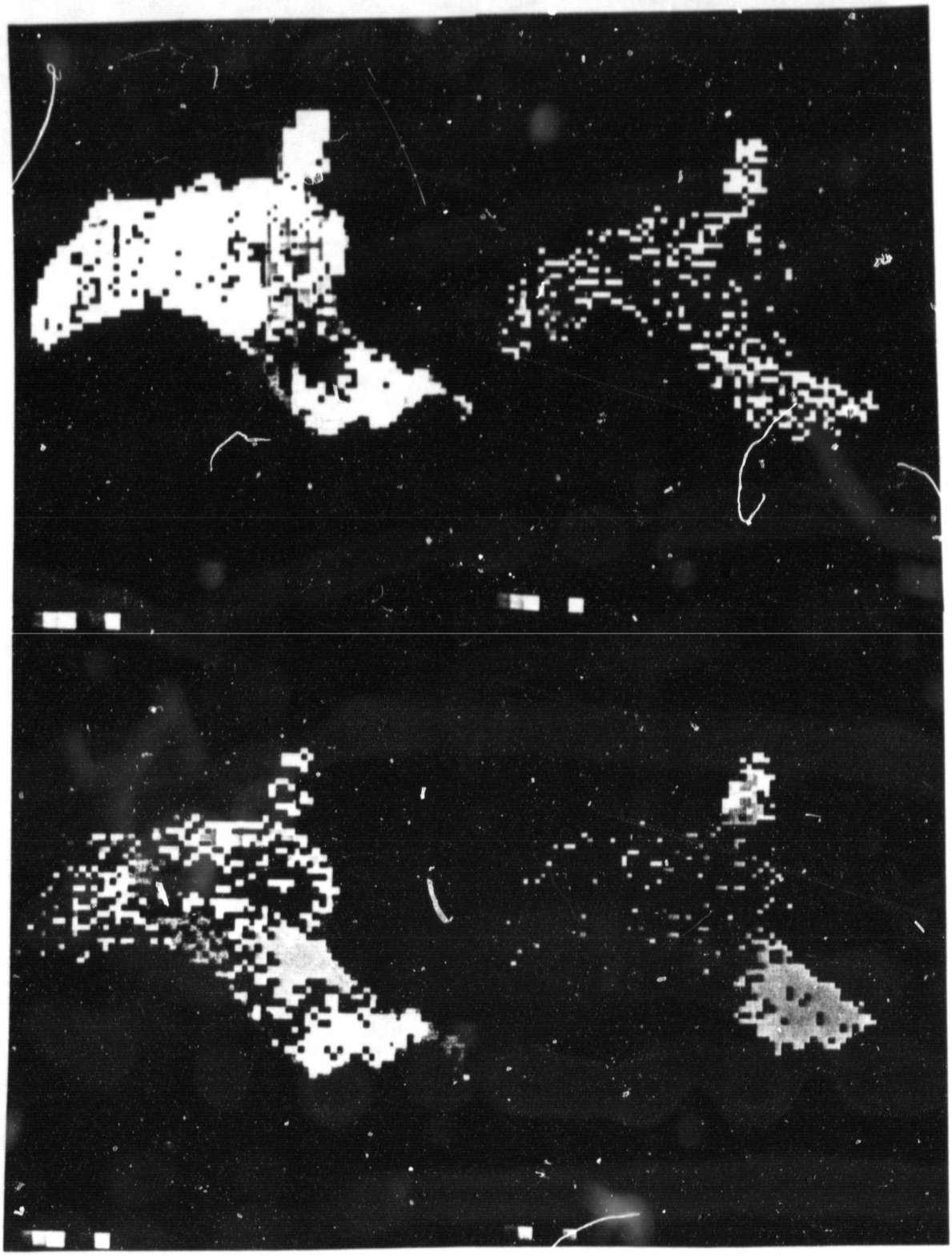

Figure 10.1 Spring Infrared - Visible Correlation Images.

this is the result of suspended sediments or turbidity caused by the wind. The south area of Goshen Bay is very shallow and requires little wind action to cause turbulence.

The northern end of Goshen Bay shows much more variation. During March it is L-L and L-M. In May the boundary of Goshen Bay and the Center Lake area is M-H, which is yellow. This seems to indicate a mixing between the Center Lake (M-M) and the north of the Bay (L-H) to produce this M-H intensity. The July images indicate a return to the L-L and L-M intensities that are normally associated with this part of the lake.

The late summer sequence in Figure 10.2 follows the same pattern as that of spring and summer. From the southwest to the northeast the change is from L-H to a mixture of L-M and L-L. The image of 11 August shows a disturbance in the southern part of the Bay. The reason is unknown and the lake returns to the normal pattern. The September, late summer, images confirm that the usual pattern in Goshen Bay is disrupted and re-established throughout the summer (Figure 10.3). The variation in range of the 11 September picture causes the masking of detail in the Central Lake as well as Goshen Bay.

The fall images in Figure 10.4 show much more variation in Goshen Bay. In dividing the infrared and visual images into three intensity ranges, some detail may be lost because the large variation in the summer temperature and reflectivity ranges mask subtle differences. This contention is not substantiated by the spring pictures however, which are of a cold lake and show no masking of data due to variation in the image. The final blooms and the death of the algae in October(Figure 10.4), probably account for this variation in intensities along with some effect from the increasingly uniform temperature of the lake.

After the 9 October image the familiar pattern in the Bay disappears and is replaced by a patchwork that is of medium and high infrared with the entire range of visible reflectivity high to low. The breakup of the algae has been indicated as a probable cause. In the 14 October image there is a possibility that this is caused in some areas by groundwater from thermal springs. The northwest side of Goshen Bay is known to have a large number of springs. The temperature and amount of inflow may be so small that they do not effect the temperature of the water enough to be seen until late autumn and winter when the lake has a cold and fairly uniform temperature.

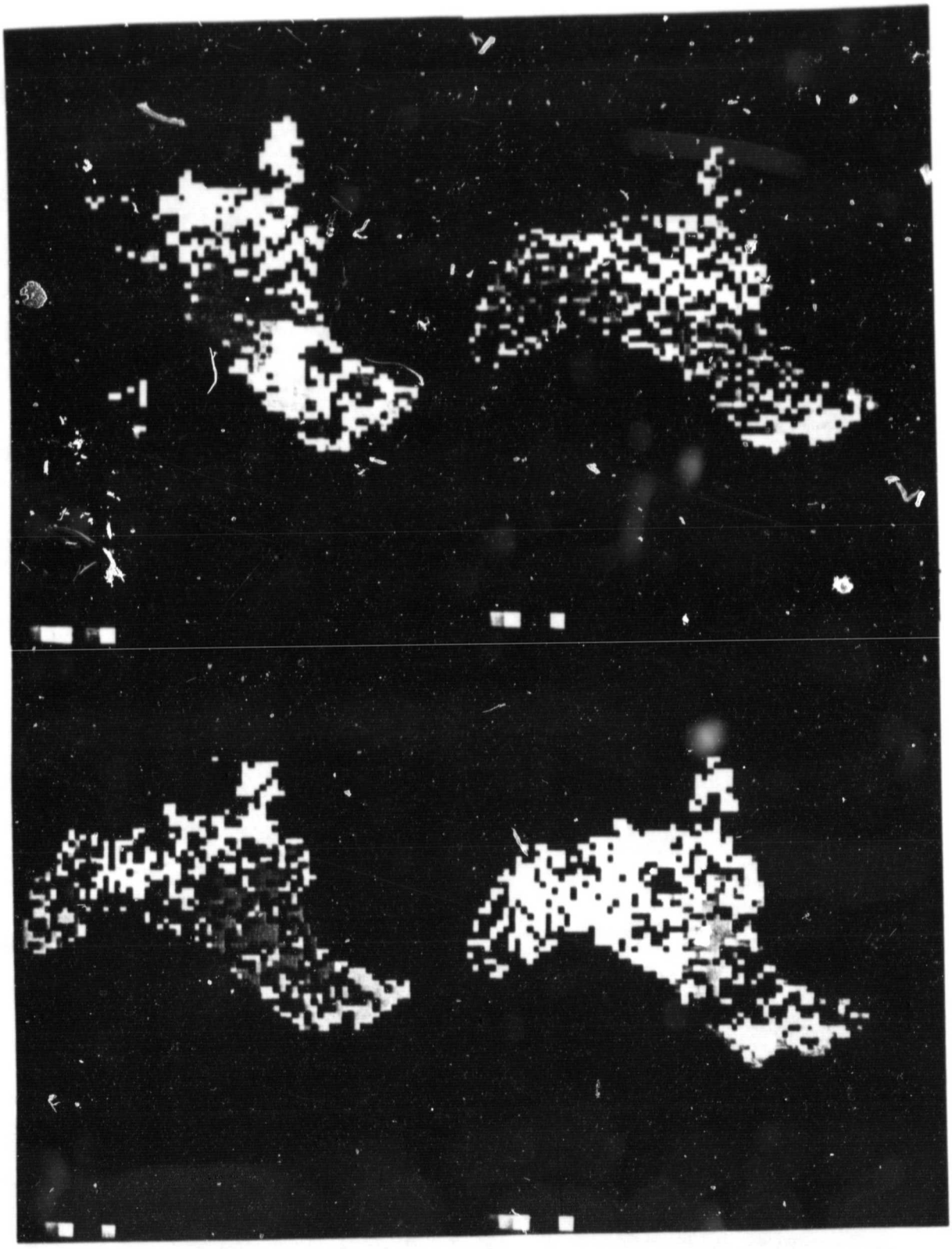

Figure 10.2 Summer Infrared - Visible Correlation Images.

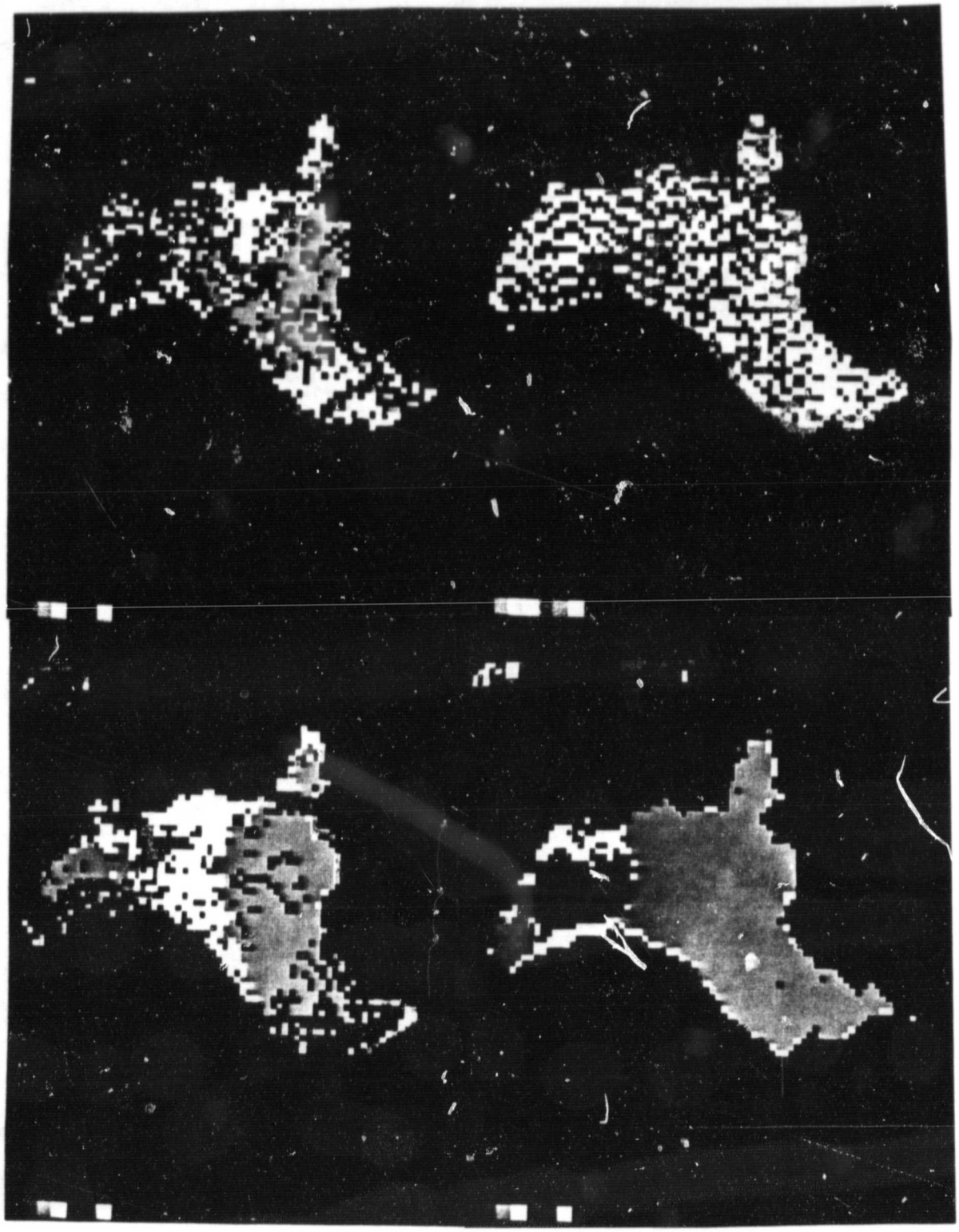

Figure 10.3 Late Summer Infrared - Visible Correlation Images.

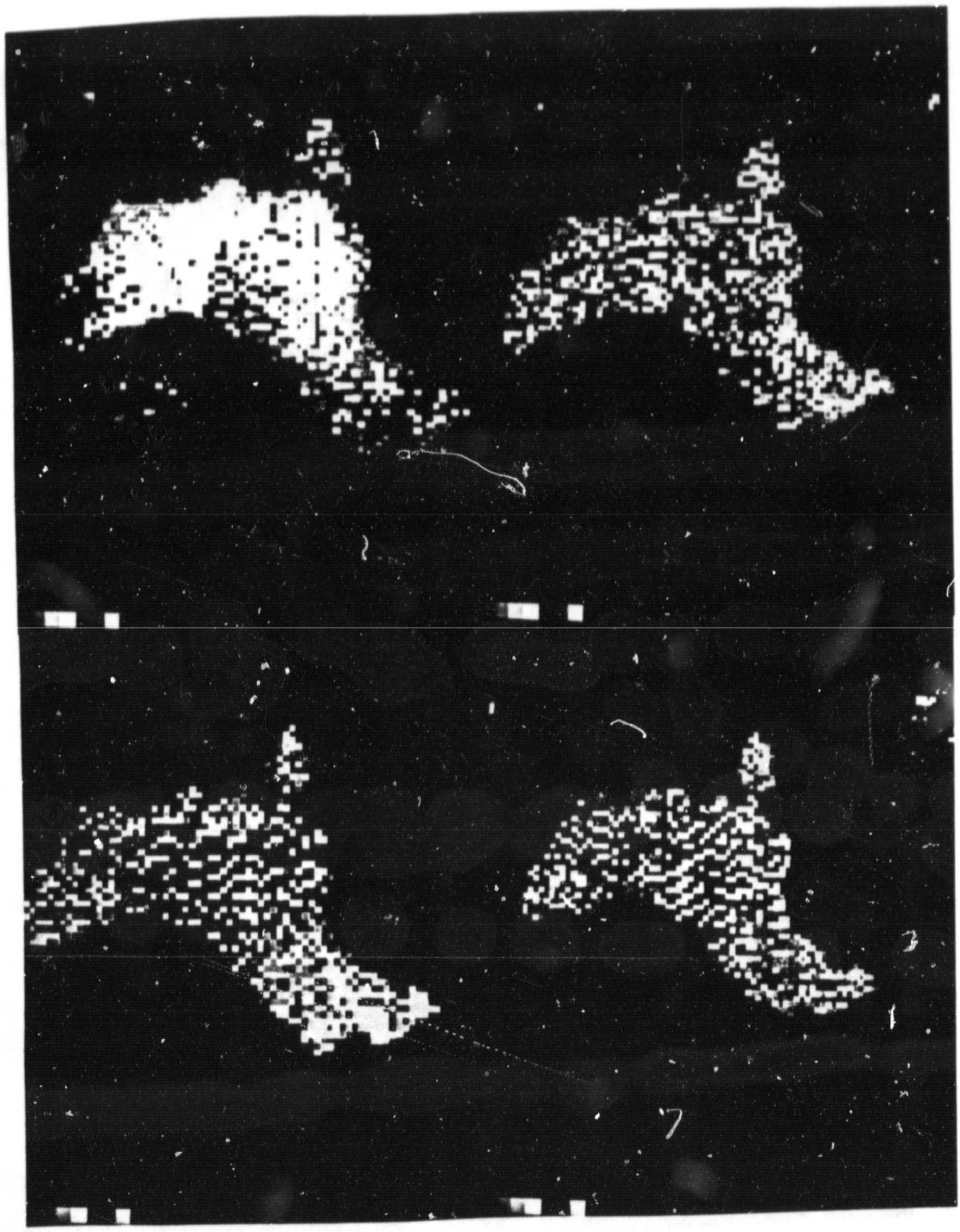

Figure 10.4 Fall Infrared - Visible Correlation Images.

10.3 Provo Bay

The summer sequence, Figure 10.2, shows Provo Bay initially with the infrared varying from middle to high and the visible from middle to low. By the end of July this has changed to H-L and this is maintained through the middle of August. By the 23 of August the homogeniety of Provo Bay is gone. It is largely a patchwork of M-M, M-L, L-L. With some disturbances and with varying contribution of different combinations, this pattern holds through the middle of October with the addition of some areas of M-H.

The 25 October image is primarily L-M and L-H, which carries through to the 14 November image, Figure 10.4. Provo Bay is shallow and surrounded by swamps and reed beds. Combined with a constant fresh water inflow, this causes Provo Bay to have a different environment. The decrease in water elevation would add to the increase in reflectance.

10.4 North Lake

The north lake is commonly thought of as the area which has the greatest biological activity. Because of this the comparison of infrared and visible was expected to change radically and often. An inspection of the images throughout the year contradicts this assumption. The lake appears to return or attempt to return to an equilibrium condition. This equilibrium condition is one of a low infrared and the full range of reflectance, from L to H. The north lake area seems to be where the disturbances in the lake migrate and not where they begin. It has been established that these disturbances as seen in the satellite imagery are caused by biological activity. This has been confirmed in the study of algae.

The winds affect the floating algae, Aphanizomenon, and cause it to concentrate and to move. The monthly average of the wind direction at the Salt Lake City Airport is from 160 to 190 degrees. Thus, any floating material is be pushed into the north end of the lake. Inspection of the images indicates that the disturbances start in the central part of the lake and migrate to the north. Conditions in the central lake and the prevailing winds seem to be the answers to questions of the conditions in the North of the lake.

10.5 Center Lake

On the 24 March image the center of the lake is predominantly M-M with large areas of M-H and M-L. This pattern fills all of the central portion of the lake from the east side to the west side. Throughout the season this same pattern forms in the central lake, migrates north or south, and then dissipates and reforms again in the center of the lake. This happens about once every month during the summer and the fall (Figures 10.1-10.4). The major inflow to the lake occurs on the south east side of the central section. This flow then goes north to the outlet. Most of the nutrients added to the lake would enter along the east side of the center of the lake.

10.6 Algae Bloom Cycle

There is one sequence of color graphics that is of particular interest. Figures 10.5, 10.6, 10.7 and 10.8 show an algae bloom cycle which occurred during September 1979. They outline the changes that take place in the life cycle of an algae bloom. On each figure the top picture is day infrared, the middle is the day visible and the bottom is the infrared-visible correlation. In the north central section of the first image for 4 September 1979 (Figure 10.5), there is a small patch which displays medium infrared (green, top picture), high reflectance (red and black, middle picture), and M-H correlation (yellow, bottom picture). This is surrounded by areas of M-M and M-L. This patch is the first indication that alge is concentrating.

The 11 September image (Figure 10.6) shows the bloom in full growth. At this time the processes involved in the transformation are not know. Many other images of the lake show areas of the same M-H relationship and yet did not develop further into major blooms. The central part of the algae bloom is a region of H-H. North and south of the center are areas of M-H and to the sides of this, M-M. The east-west edges of the bloom are of M-L intensities. From this it is presumed that the greatest concentration is in the red (H-H) region with a decrease in concentration to the yellow (M-H) and green (M-M) regions.

The 16 September image (Figure 10.7) shows the lake returning to the normal pattern. The warm area of 11 September has dissipated and the central lake area is now the warmest. The temperature difference of the north lake between the 11 September and 16 September images is about 2 ^{o}C. On 16 September the north end of the lake exhibits a reflectance that is only half

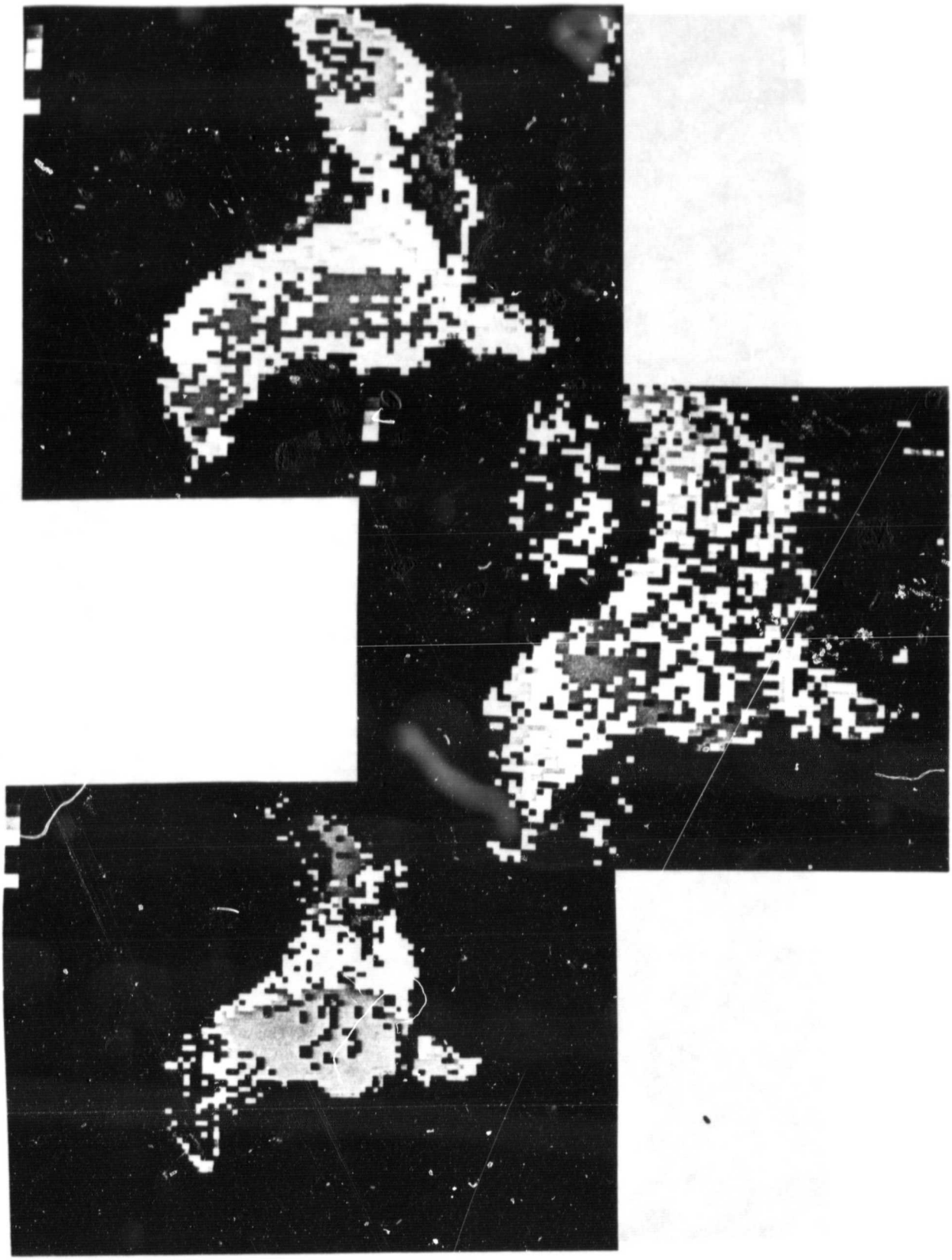

Figure 10.5 Day Infrared, Day Visible and Correlation Images, 4 September 1979.

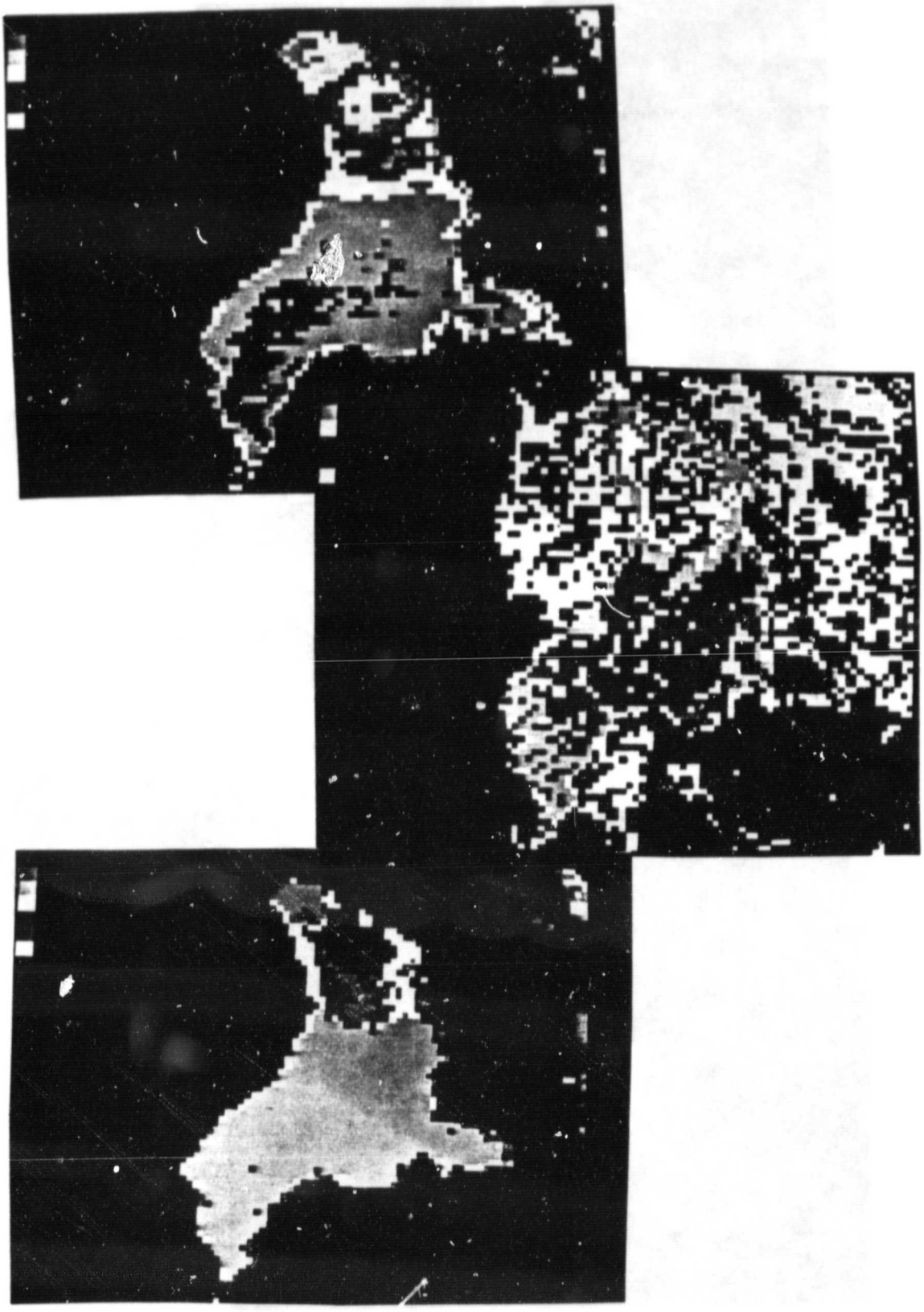

Figure 10.6 Day Infrared, Day Visible and Correlation Images, 11 September 1979.

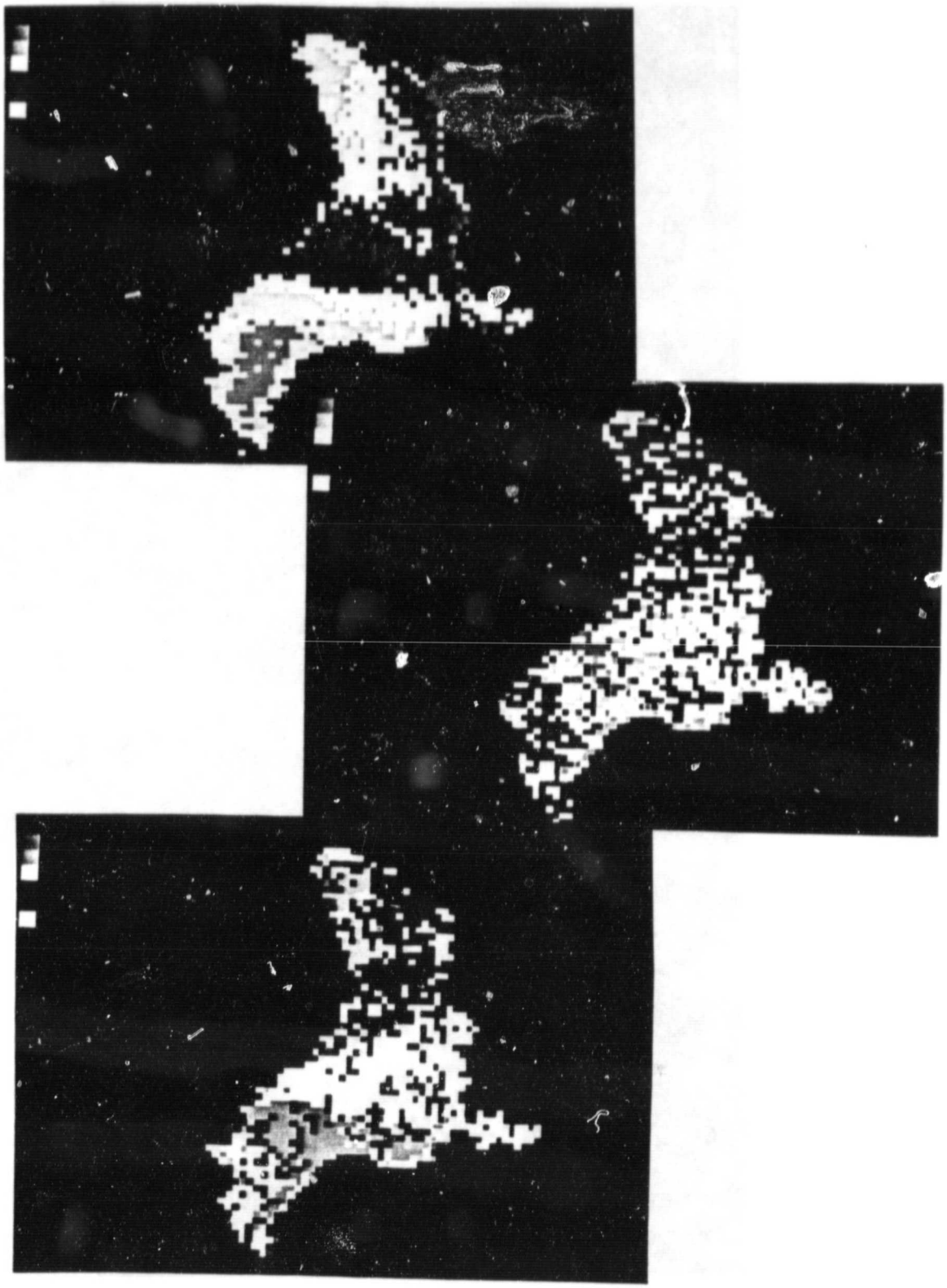

Figure 10.7 Day Infrared, Day Visible and Correlation Images, 16 September 1979.

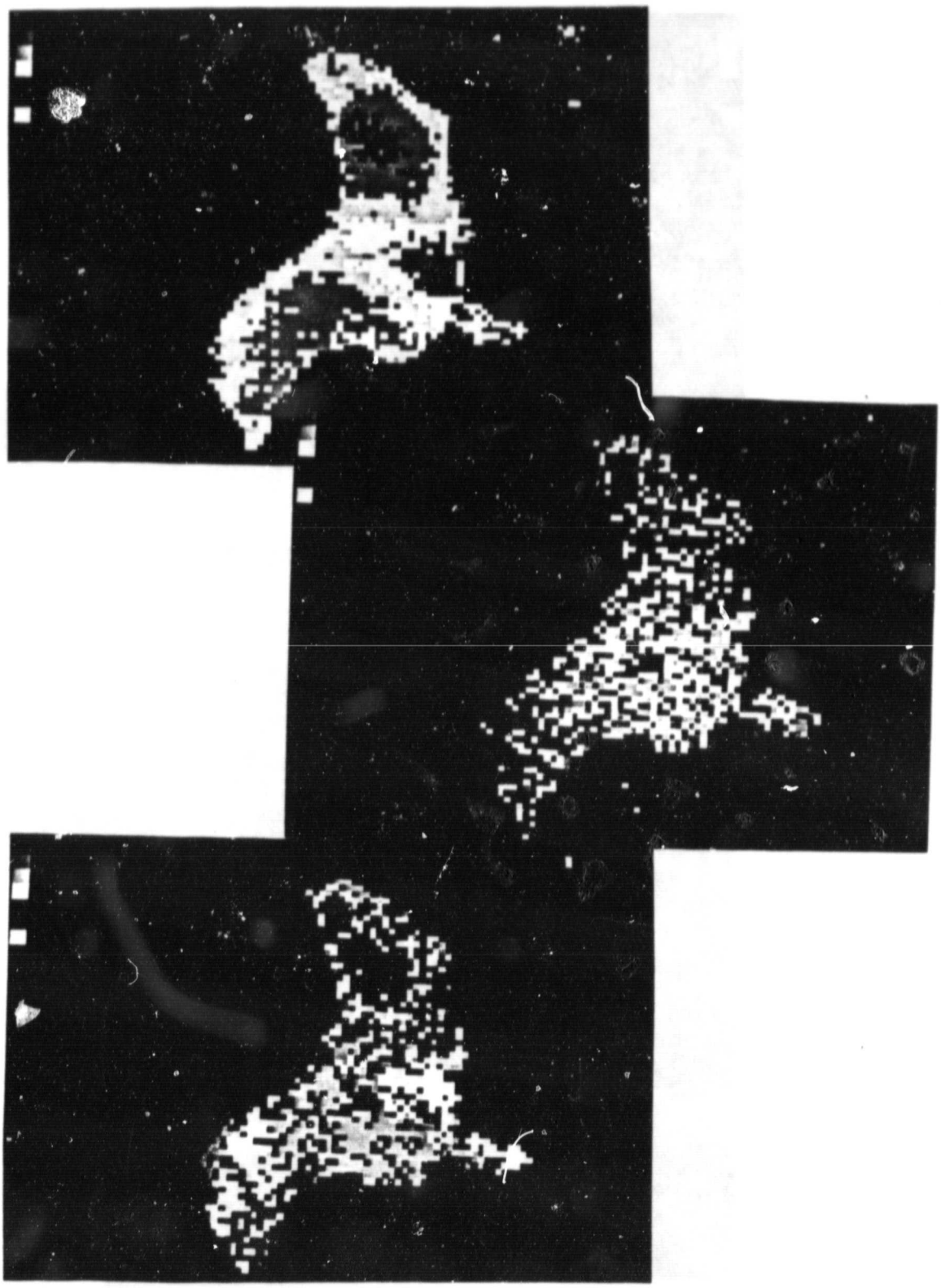

Figure 10.8 Day Infrared, Day Visible Correlation Images, 21 September 1979.

as great as the 11 September image. The change between the 11 September and 16 September is marked and indicates a dispersal of the bloom that is equally as rapid as the build-up from 4 September to 11 September.

The correlation image for 16 September shows the center of the lake as pink, M-L. The east side of the north lake has a M-H and M-M pattern, which could be the algae remaining from the bloom. The boundary of the center lake and Goshen Bay displays a mixing pattern from M-L in the center lake to L-L in Goshen Bay. The algae bloom has been dispersed over the north lake and that from the center lake to Goshen Bay there is a drop in water temperature across a mixing zone.

The 21 September image (Figure 10.8) shows a more normal pattern. The only anomaly in the 21 September image is that where the algae bloom once was is a large area of low infrared, medium visible, and therefore L-M correlation. It is possible that the dying or dispersing algae are of such low concentration that there is little heat produced from the photosynthetic effect and that the relatively high reflectance causes less heating by solar radiation, resulting in a condition of low temperature and middle reflectance.

The degree of statistical correlation between the reflectance and plankton concentration data decreased sharply from a very strong negative relationship during the early summer to practically no relationship by October. The reason for this loss of a statistical relationship appears to be that algal blooms begin to form in the late summer and increase in number and size through the latter part of October. These blooms are characterized by large floating masses of algae which appear whitish due to the large number of entrained air bubbles produced by the photosynthetic processes of the plankton. These light colored floating masses are very reflective and reduce the relationship between algae concentration in the water and the accompanying lower reflectivity of the earlier season.

11. EVAPORATION

11.1 Dalton Equation

The evaporation analysis first involved application of the so called Dalton type equation. The typical form is:

$$E = (e_s - e_d)f(u)$$

where E = evaporation
e_s = vapor pressure at the evaporating surface.
e_d = vapor pressure in the atmosphere above.
$f(u)$ = function of the horizontal wind velocity of the form $a + bu$, where a and b are constants and u is the windspeed.

This equation was used because of its simplicity and the ability to use satellite data directly in the calculation of the saturation vapor pressure term in the equation.

Lake temperatures were calculated with the HCMM equation (NASA, 1980) and given the predetermined 4.9 degree centigrade offset. The corrected temperatures were then used to calculate the saturation vapor pressure of the surface of the lake. Maximum air temperatures from the Lehi station were used in calculating the prevailing vapor pressure.

11.2 Windspeed Function

With the corresponding Lehi pan evaporation, the values for the windspeed function $f(u) = E/(e_s-e_d)$ were calculated. These values were plotted against both the Lehi and Provo Airport wind data. Insignificant correlation existed in both cases. A comparison of these preliminary plots with those of Penman (1948) showed that the windspeeds of the HCMM days did not have as great a range as those of Penman. This is probably because the HCMM images are only for days that are clear and relatively calm, being in between storms. Therefore days with high windspeeds did not have corresponding HCMM data and were not studied in this analysis.

Other ways were explored in which the HCMM data could be used in the evaluation of windspeed functions. The relationship between maximum pan temperature and maximum HCMM lake temperature is seen in Figure 11.1 This figure shows the result of two windspeed functions, from Lehi pan data and satellite data, being plotted on the same graph.

In the computation of the pan windspeed function the average air temperature and average humidity were used to calculate the dewpoint temperature. From this the vapor pressure of the air, e_s, was calculated. The maximum pan temperature yielded e_s (maximum pan), the water surface vapor pressure. Maximum pan temperature was chosen because it corresponds to the HCMM day measurement which was also a maximum temperature. These maximum pan windspeed function values, f(u), were calculated and plotted against the windspeed u in Figure 11.1.

The maximum HCMM windspeed function was calculated with the e_d as above and Lehi evaporation. The water surface vapor pressure, e_s (HCMM day), was obtained from the use of HCMM lake temperature data for the fourteen HCMM days. The windspeed functions were then also plotted on Figure 11.1. Superimposing the two windspeed functions in this manner reveals the differences.

The windspeed function values from the HCMM data are much higher than those form the Lehi pan data. This is caused by the difference in temperature of the lake and the pan. For the days studied the pan temperature ranged from seven to fourteen degrees centigrade hotter than the lake. This causes e_s for the HCMM values to be smaller and therefore gives a larger f(u). Analysis of this difference would be useful in the study of pan coefficients, but is beyond the scope of this study and would require much more frequent satellite coverage of the lake.

The same method of calculation used in Figure 11.1 was used in the plotting of Figure 11.2. Evaporation and e_d are the same as in Figure 11.1. However, the average pan temperature was used to calculate the water surface vapor pressure, e_s in the average pan windspeed function.

The average HCMM windspeed function is calculated as above except that the average of the HCMM day and night (DIR & NIR) lake temperature is used in the computation of e_s and hence f(u). Figure 11.2 is a plot of the average Lehi windspeed function and the average HCMM windspeed function on the same graph. The superimposed values show that the average lake temperature is

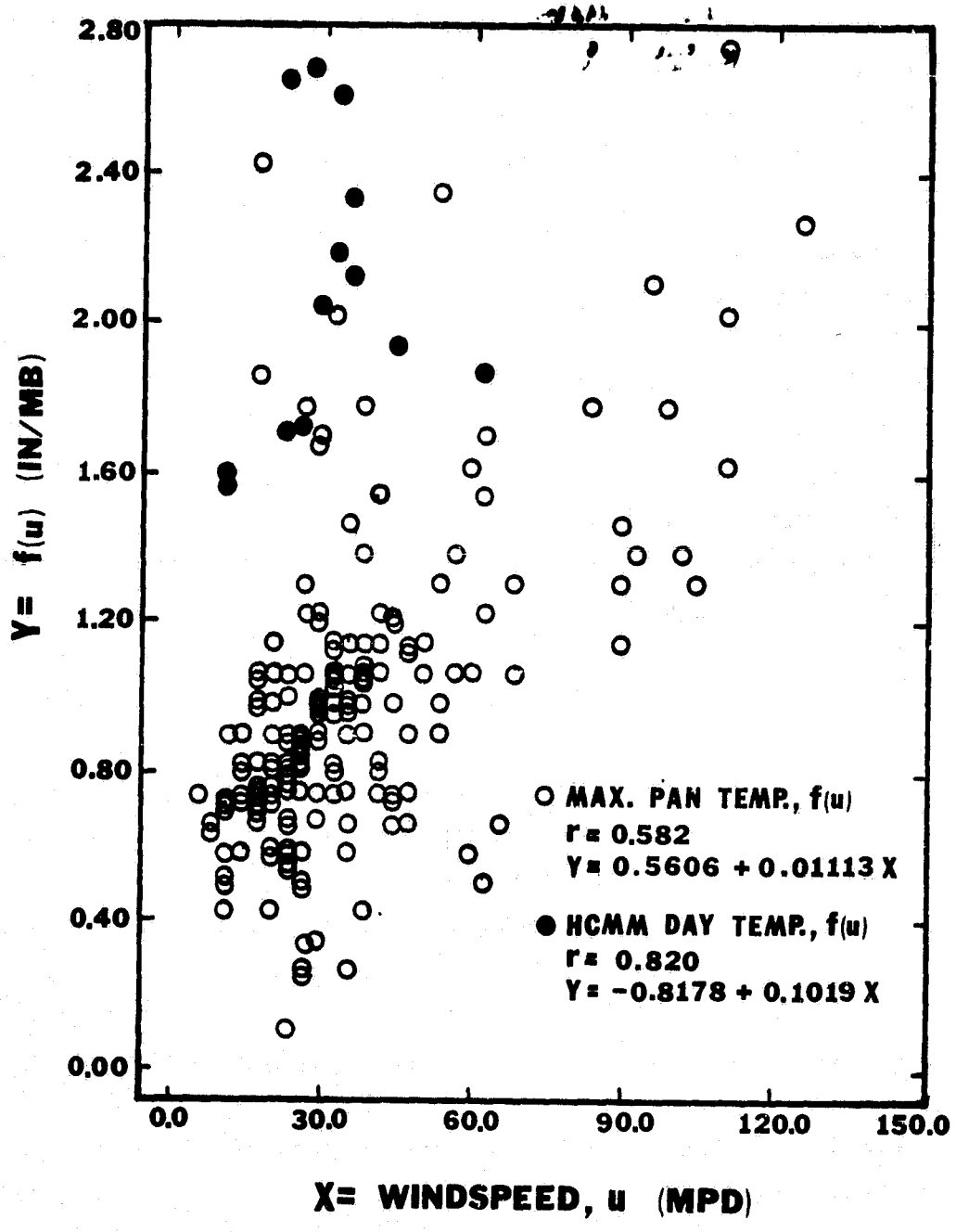

Figure 11.1. Windspeed Functions f(u) (in/mb) from Maximum Pan Temperature (^{O}C) and from HCMM Day Temperature (^{O}C) versus Lehi Evaporation Pan Windspeed U (mpd).

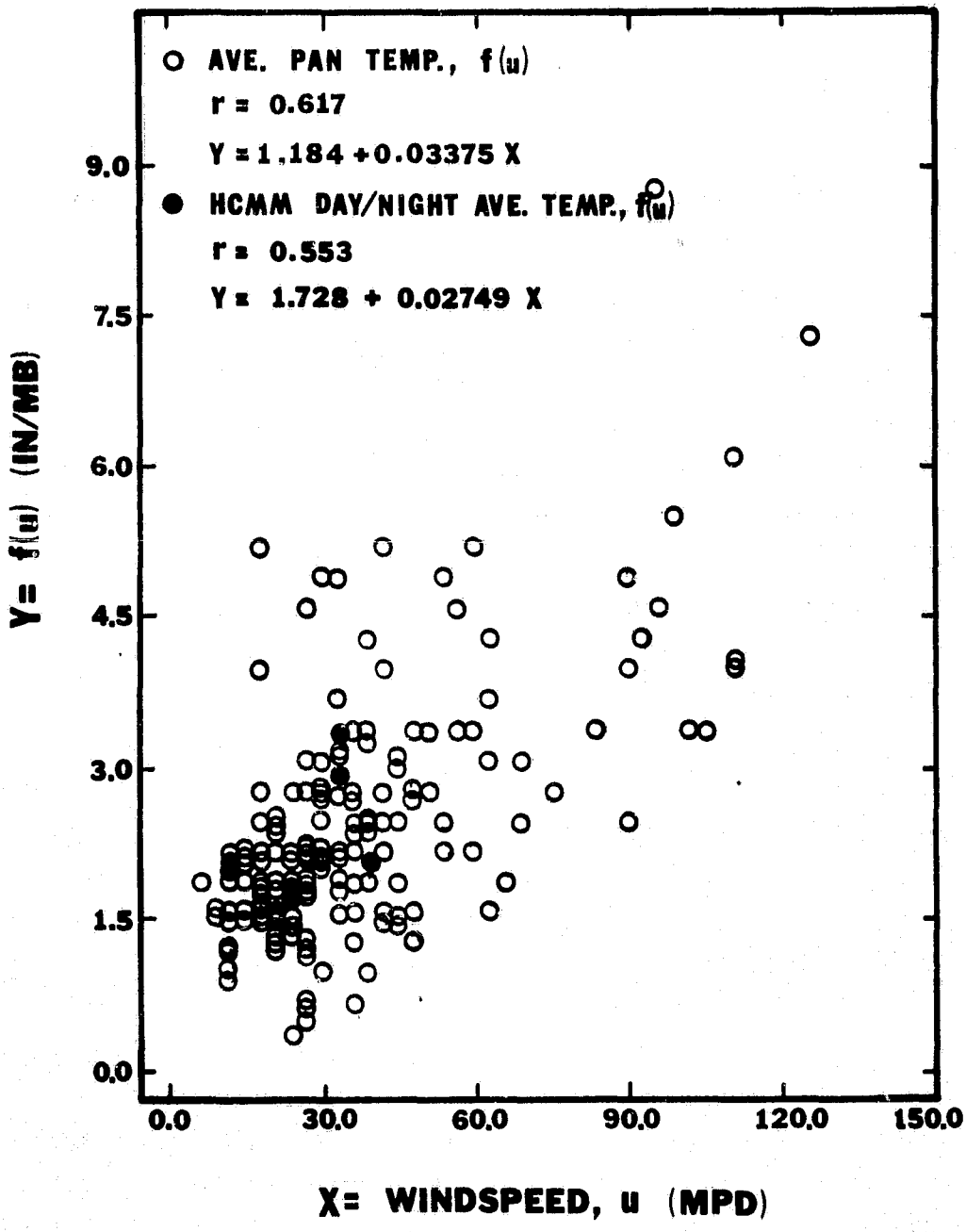

Figure 11.2. Windspeed Functions f(u) (in/mb) from Average Pan Temperature (^{O}C) and from HCMM Day/Night Average Pan Temperature (^{O}C) versus Lehi Evaporation Pan Windspeed u (mpd).

slightly lower than the average pan temperature. The average of the five day/night HCMM temperatures yields a windspeed function that plots in the same region of the graph as the Lehi pan data. The study of evaporation and windspeed functions should be made with the use of average HCMM temperatures.

11.3 Vapor Pressures

An interesting relationship is shown in Figure 11.3. Three plots are superimposed on the same graph. The first plot is of e_s (maximum pan) derived from the maximum pan temperature versus e_s (average pan) derived from the average pan temperature. The second set of points plotted is of e_s (maximum pan) versus e_s (HCMM day/night) calculated from the HCMM day/night (DIR/NIR) average temperatures. The final plot is of e_s (maximum pan) versus e_s (HCMM day) from the HCMM day infrared (maximum) temperatures.

A comparison of the three sets shows that the e_s values for the HCMM average temperatures are lower than those calculated from average pan temperature. The vapor pressure calculated from the HCMM day temperature corresponds very well with the vapor pressure calculated from the average pan temperature. It is possible then to use HCMM day data instead of the day/night average.

The agreement between the average pan and the HCMM day values is very useful. Other researchers have shown that a pan 12 feet in diameter has the same evaporation as does a lake. This allows the use of the relatively abundant day infrared satellite data for the study of evaporation.

11.4 Evaporation Model

Miller (1980) gives comparisons of evaporation from several different pans. The pan coefficients were derived using the water budget for the years 1970-1973. The pan evaporation was compared to evaporation calculated from a model developed by F.I. Morton. These data were plotted with respect to the HCMM intensities. Model and pan evaporation was by month; therefore, monthly HCMM averages were calculated using the average lake intensity from the HCMM images. This data, for the years 1978 and 1979, was then plotted against the DIR and the NIR HCMM intensity as seen in Figure 11.4 and Figure 11.5.

The correlation for both day and night intensities was excellent. The plot of monthly model and pan evaporation versus DIR showed that 93 and 94 percent respectively of the variation in evaporation could be accounted for by

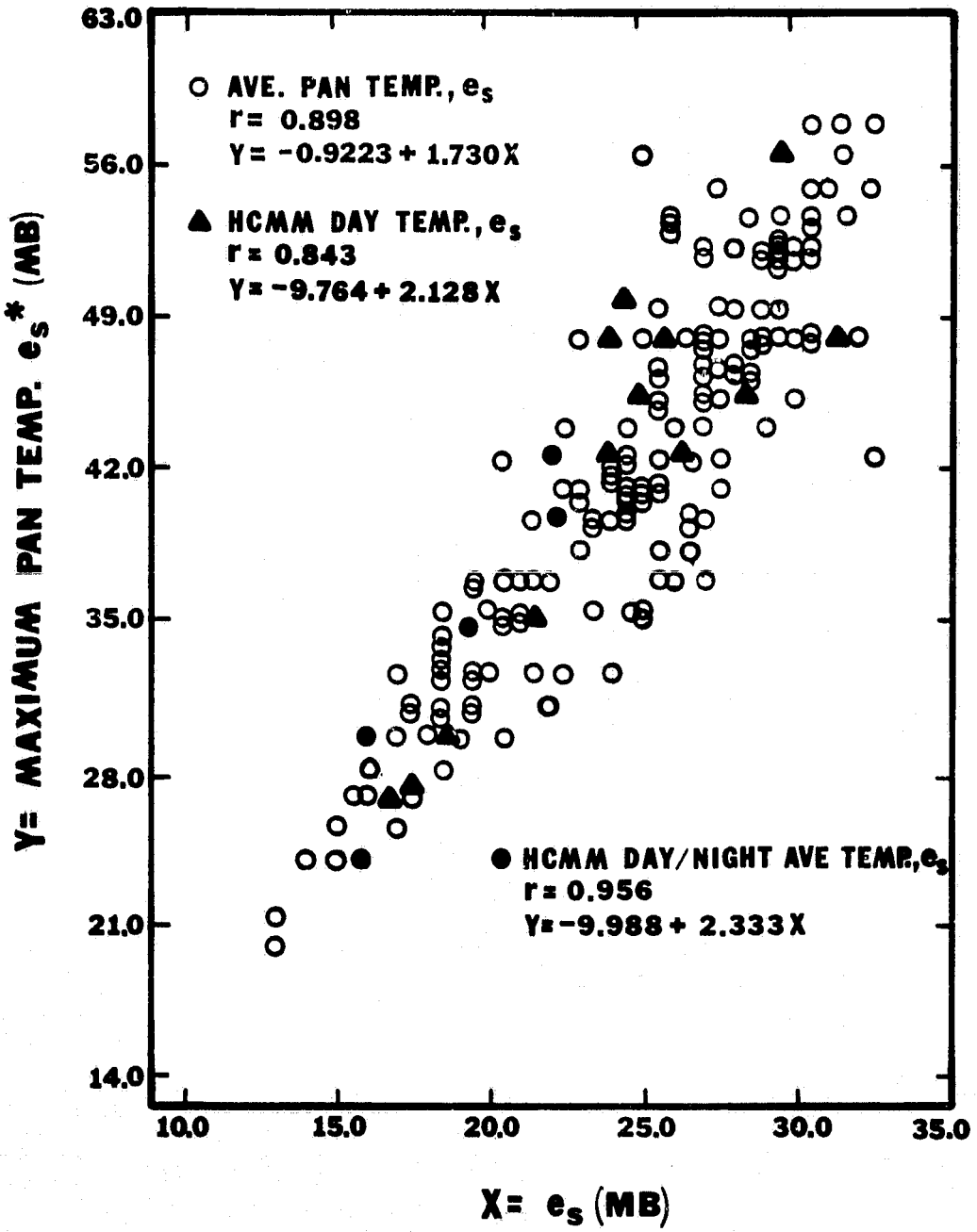

Figure 11.3. Saturation Vapor Pressures e_s (mb) for Maximum Pan Temperature (^oC) versus Saturation Vapor Pressure e_s (mb) for Average Pan, HCMM Day, and HCMM Night Temperatures (^oC).

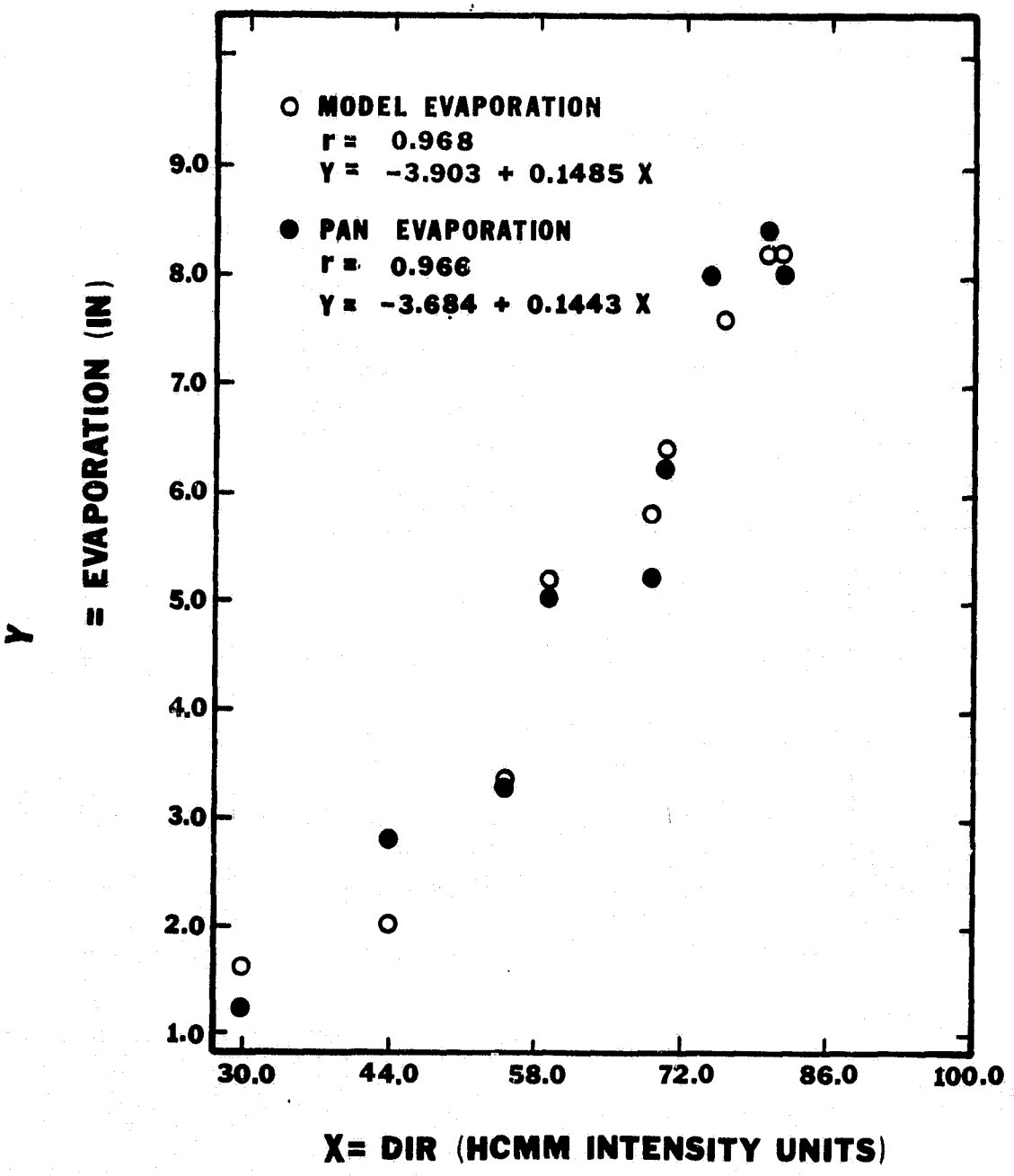

Figure 11.4 Pan and Model Evaporation (in) Versus HCMM DIR from Monthly Data.

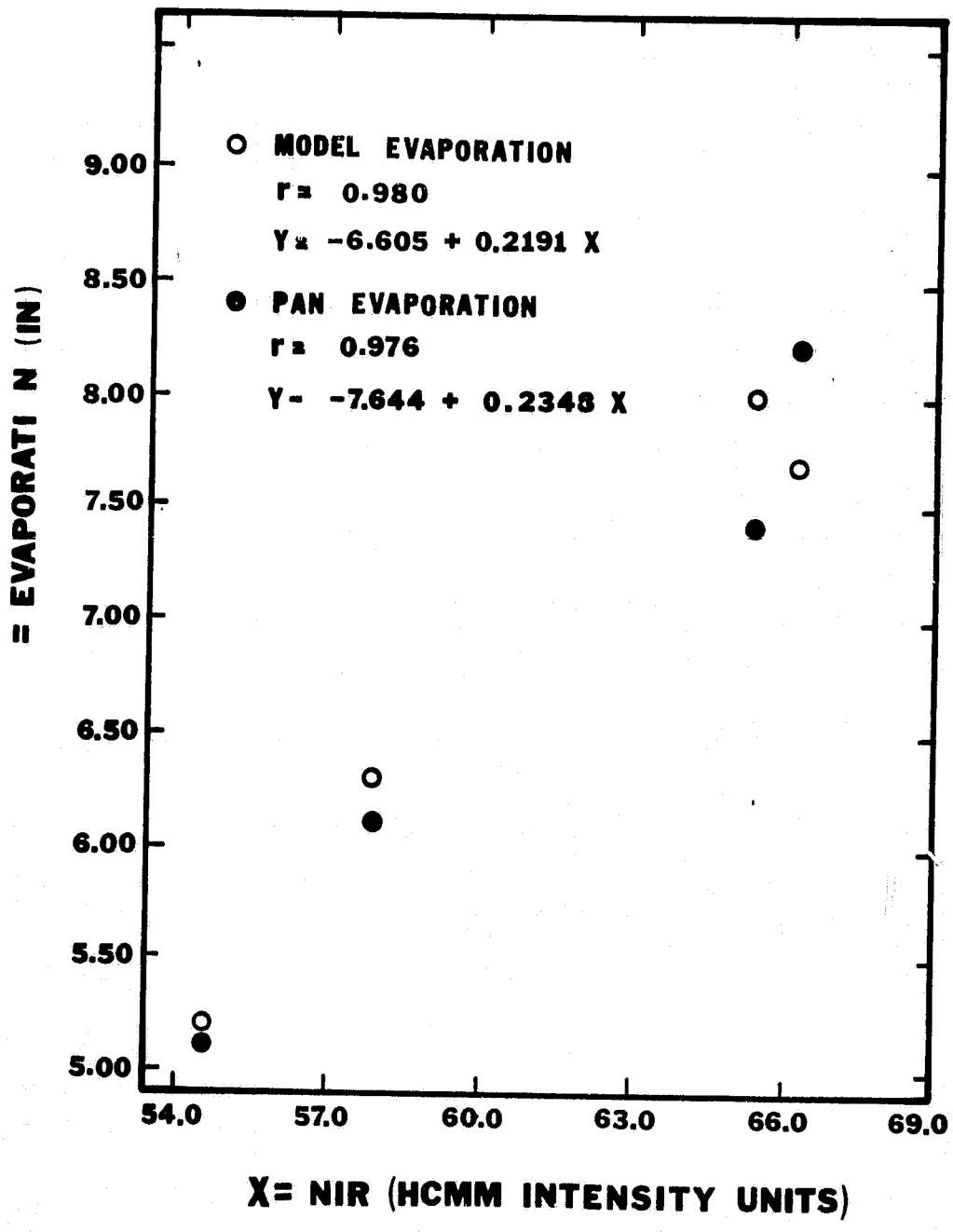

Figure 11.5. Pan and Model Evaporation (in) versus HCMM NIR from Monthly Data.

HCMM day intensity. DIR versus daily evaporation gave correlations of only 0.8 to 0.86 (see Table 12.1, Section 12) as compared to 0.97 for monthly values. As with other methods of evaporation estimation, the shorter the time interval the less accurate are the results.

The plot of evaporation versus NIR shows similiar results (Figure 11.5). The HCMM night intensity accounts for 95 and 96 percent respectively of the variation in model and pan evaporation. However, the increase in accuracy by using the larger monthly period for night infrared is very small, from r = 0.95 to r = 0.98. This small change in accuracy indicates that estimates of evaporatation for any time period much shorter than a month should be made with the use of HCMM NIR. For periods longer than a month the day intensity is as accurate.

12. CLIMATOLOGICAL ANALYSIS

12.1 Parameters

The HCMM data were compared to the climatological data of 1978 and 1979 in order to analyze and document the relationship to the hydrology of the study area. HCMM temperature data included day, night, day/night average, and day/night difference. Several parameters were evaluated to determine if any significant correlations existed. These included HCMM day and night data to pan evaporation and to miniumum and maximum pan temperatures, and wind to evaporation and surface temperature, and surface temperatures in different parts of the lake to each other.

12.2 Pan Evaporation

The four types of HCMM temperatures, day, night, day/night difference and day/night average, were plotted against the Lehi same day evaporation and the average Lehi evaporation for the two days before the satellite overpass. A typical plot is shown in Figure 12.1. This is of HCMM night temperature versus Lehi average evaporation. The correlations and regressions of all the evaporation relationships are given in Table 12.1. Heat is a main cause of evaporation of water and the expected high correlation was observed.

The data for Provo Airport evaporation in Table 12.1 shows a difference in correlation from that of the Lehi evaporation data. One reason is that Provo airport evaporation is an average evaporation. Measurements were taken only when the pan was filled, which varied from two to six days. The effect of this is unknown and the Provo Airport evaporation data was largely discounted.

The two day average of Lehi evaporation versus HCMM temperatures gave better correlations than the same day Lehi evaporation versus HCMM temperatures except in the case of the HCMM day/night temperature difference. The use of a pan coefficient does not have an appreciable effect on the correlation coefficient and has only a small effect on the regression equation. Two of the cases in Table 12.1 were of particular interest in this study. They were HCMM temperature difference versus evaporation and HCMM night temperature versus evaporation.

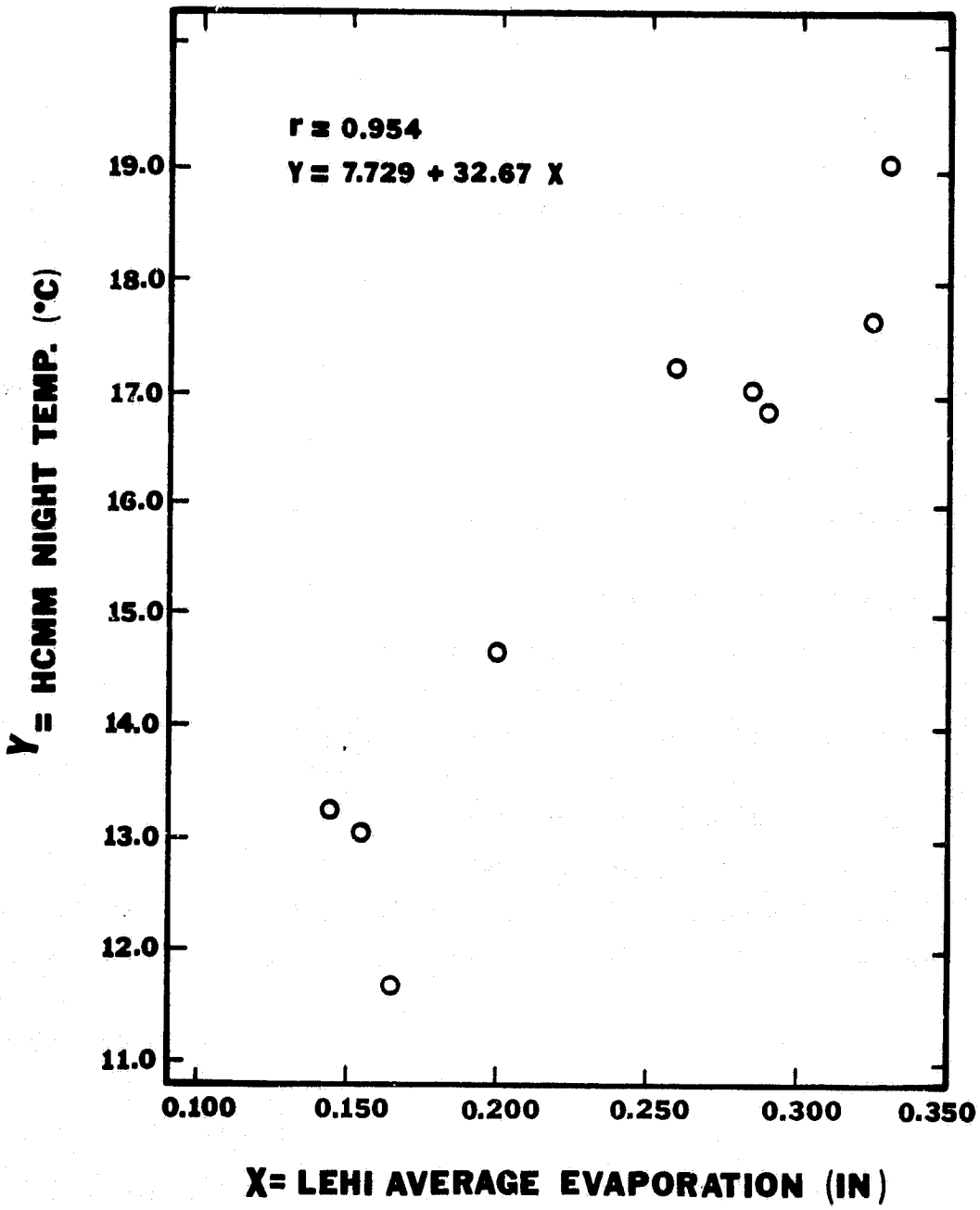

Figure 12.1. HCMM Night Temperatures (°C) versus Lehi Average Evaporation (in).

Table 12.1. Correlation Coefficient, r, and Regression Coefficients, a and b, for Temperature versus Evaporation, where Temperature (^{o}C) = a + b x Evaporation (in).

	Lehi Evaporation (in)				Provo Airport Evaporation
	Same Day		Two Day Average		
	w/o pan coef.	w/pan coef.	w/o pan coef.	w/pan coef.	w/o pan Coef.
HCMM Day	r = .823 a = 14.02 b = 24.41	r = .806 a = 13.99 b = 25.19	r = .859 a = 10.98 b = 34.12	r = .834 a = 10.91 b = 35.27	r = .875 a = 11.53 b = 31.11
HCMM Night	r = .653 a = 11.74 b = 15.69	r = .658 a = 11.79 b = 15.34	r = .954 a = 7.729 b = 32.67	r = .952 a = 7.249 b = 34.23	r = .803 a = 9.575 b = 24.19
HCMM Day/Night Difference	r = .751 a = 4.684 b = 23.89	r = .744 a = 4.852 b = 22.97	r .297 a = 6.900 b = 14.70	r = .294 a = 7.038 b = 14.00	r = .564 a = 4.900 b = 22.49
HCMM Day/Night Average	r = .759 a = 12.65 b = 19.52	r = .761 a = 12.73 b = 19.02	r = .942 a = 8.333 b = 37.65	r = .938 a = 8.627 b = 36.09	r = .858 a = 10.55 b = 27.65

The comparison of HCMM temperature difference versus evaporation showed high correlation for the same-day Lehi evaporation but a much lower correlation with the two day Lehi average. This is explained by the fact that the two day Lehi average evaporation masks the effect on evaporation of sudden temperature changes. The same day evaporation is more sensitive to temperature changes. HCMM data for this study were from August and September of 1978 and 1979. For these months there is a large variation in day and night temperature.

The heat storage of the lake maintained the water temperature as the air temperature fell during September and evaporation decreased by more than half during the month. The high correlation of the two is expected but is probably a measure of the increasing temperature difference occuring at the same time as the evaporation decreased in early autumn.

The best results were obtained from HCMM night temperature versus average Lehi evaporation. The correlation coefficient was 0.95 (Table 12.1). With proper calibration of the water body it would be possible to generate good evaporation estimates from the night infrared temperatures. Night temperatures on the lake are near minimum temperatures. There are two possible reasons for the good results. First, the average Lehi evaporation effectively masks any sudden changes in pan evaporation due to the changing local weather. Second, the night temperature readings were unaffected by the surface heat gain that is registered by the day readings. This means that the night temperatures are a much better gage of the average temperature and therefore heat storage of the lake. If night infrared data become common it could very well be possible to use those measurements for energy budget calculations.

12.3 Wind and Surface Temperature

The surface of the lake is where energy is absorbed and released and much of this energy is released through evaporation. The air-water interface is acted upon by the wind and the heat flux caused by sunlight. With the satellite imagery the effect of wind on surface temperature and hence evaporation was investigated. Table 12.2 gives the results of the study of various HCMM temperatures versus the wind. Wind measurements were from a continuous recorder at a height of 11.5 m that was maintained by the Bureau of

Table 12.2. Correlation Coefficients, r, and Regression Coefficients, a and b, for Wind, Evaporation and Temperature Relationships where Evaporation (in) = a + b x Wind (mph), 24 Hour Average.

	Lehi Average Evaporation	HCMM Day	HCMM Night	HCMM Average	HCMM Difference
	r = .276	r = -.002	r = .533	r = .355	r = -.617
Wind (mph)	a = 5.243	a = 6.684	a = 6.319	a = 10.78	a = 24.52
24 Hr. Avg.	b = 4.965	b = -.00071	b = 1.504	b = 1.074	b = -2.308

Table 12.3. Correlation Coefficients, r, and Regression Coefficients, a and b, for Utah Lake HCMM Temperature versus Air Temperature, where HCMM Day Temperature (^{o}C) = a + b Air Temperature (^{o}C).

	Ta Max	Ta Average	Ta min	Ta min	
	r = .868	r = .818	r = .693	r = .886	
HCMM DAY	a = 1.215	a = 4.046	a = -9.037	a = 9.226	HCMM NIGHT
	b = 1.405	b = 1.221	b = 1.036	b = .5751	

Reclamation. Hourly wind speeds were read from the graph and averaged for the 24 hours before the HCMM image, 2 p.m. to 2 p.m. A typical graph, wind versus HCMM day/night temperature difference, is shown in Figure 12.2.

The correlation of wind to evaporation is small, but significant, and confirms what has already been suggested. That is, wind effects evaporation only slightly on large lakes. The comparison of wind to HCMM temperatures gave mixed results. There is virtually no correlation between wind and HCMM day temperatures. One reason for this is that the HCMM data is only for periods of relative calm before and after storms. At these times the windspeed is usually within the range of only four to seven miles per hour. The night temperature showed a significant correlation. However, the night temperature of the lake is also very constant during July, August, and September. The combination of a constant wind and temperature would give a significant correlation only true for the specific conditions and not generally applicable to the lake.

The effect of wind on changing temperatures was investigated using a plot of 24 hour wind versus the HCMM temperature difference between day and night. This is shown in Figure 12.2. The high negative correlation of -0.617 means that the regression line has a negative slope. That is, there is a smaller temperature difference with increasing wind. Thirty-eight percent of the variation in the HCMM temperature difference is caused by wind. During a windy day the daytime temperature of the lake rises less than on a comparable calm day. The wind increases the amount of energy removed by advection. Radiation and mixing of the warm upper layer in the water column accounts for the remainder of the loss. Further studies could be made using several night images. The correlation of the thermal images with extensive wind measurements made simultaneously on and around the lake could be the basis for additional studies.

12.4 Air Temperature

Tables 12.3, 12.4, and 12.5 show the results from comparisons of air temperature to HCMM temperature. In Table 12.3 the HCMM day and night temperature is compared with the maximum, minimum and average overland air temperatures. The maximum air temperature correlates very well, as the HCMM day temperature was designed to be a maximum at the earth's surface.

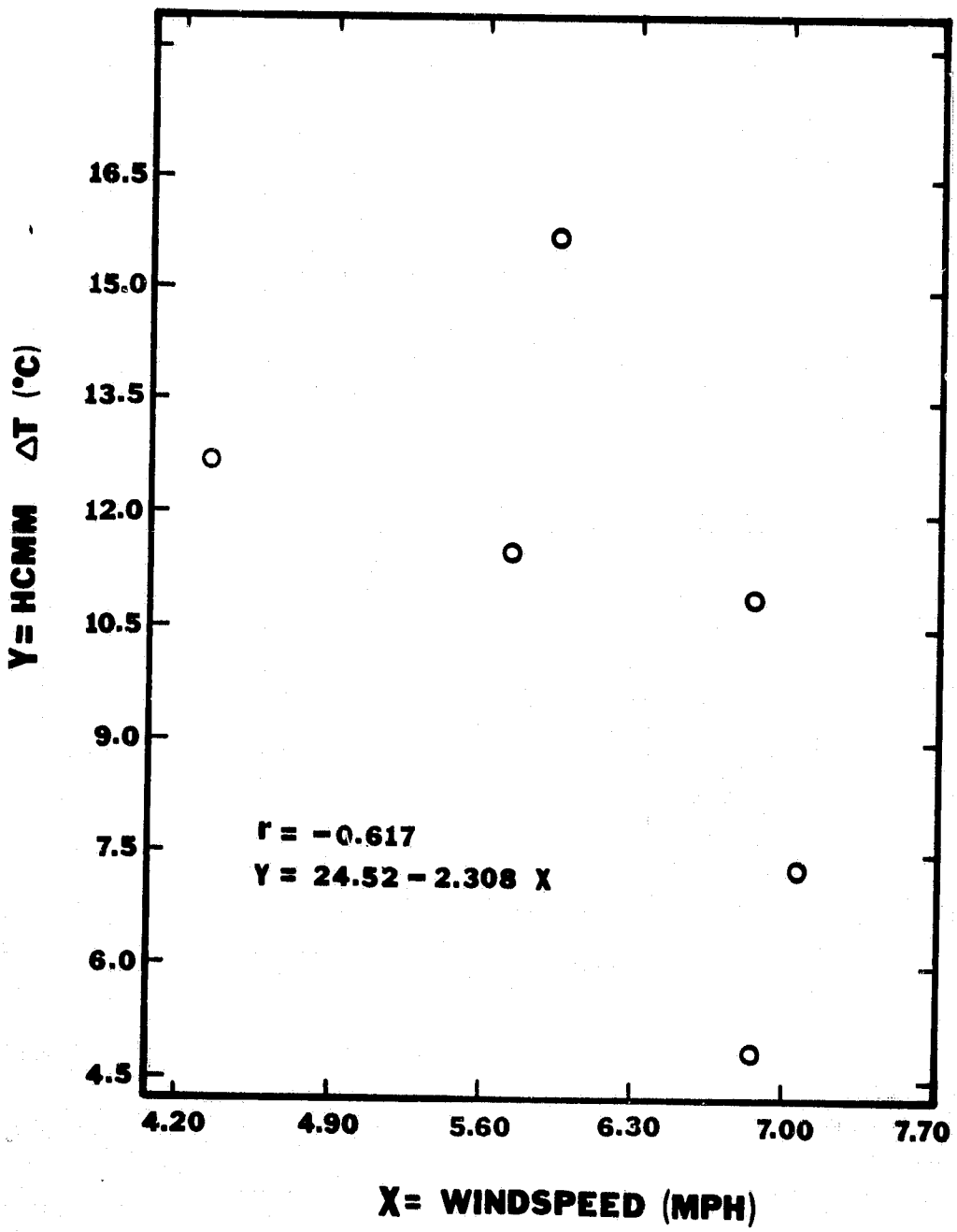

Figure 12.2. HCMM Day/Night Temperature Difference T (^{o}C) versus Windspeed u (mph).

Table 12.4. Correlation Coefficients, r, and Regression Coefficients, a and b, for Air Temperatures versus HCMM Day Temperatures for Sectors of the Lake, where Air Temperature (°C) = a + b x HCMM Day Temperature (°C).

	HCMM Day Temperature				
	Utah Lake	North Lake	Center Lake	Goshen Bay	Provo Bay
Ta max	r = .868 a = 1.215 b = 1.405	r = .746 a = 6.026 b = 1.150	r = .857 a = 2.060 b = 1.348	r = .888 a = 1.372 b = 1.446	r = .813 a = 2.407 b = 1.249
Ta min	r = .693 a = -9.307 b = 1.036	r = .563 a = -4.734 b = .8009	r = .682 a = -8.597 b = .9902	r = .756 a = -8.923 b = 1.038	r = .703 a = -10.14 b = .9971

Table 12.5. Correlation Coefficient, r, Regression Coefficients, a and b, and Standard Deviation, σ, for Utah Lake Average HCMM Day Temperature versus HCMM Day Temperatures for Sectors of the Lake, where UL HCMM Average Temperature (°C) = a + b x Lake Sector Temperature (°C).

	HCMM Day Temperature			
	North Lake	Center Lake	Goshen Bay	Provo Bay
Utah Lake Average HCMM Day Temperature Std. Deviation	r = .945 a = 1.696 b = 0.9001 σ = 1.03	r = .991 a = .5209 b = .9631 σ = .421	r = .994 a = .02350 b = 1.045 σ = .353	r = .938 a = 0.8167 b = 0.8902 σ = 1.09

Likewise, the minimum air temperature correlates well with the HCMM night temperature. Had air temperatures been taken over the lake even higher correlations would probably have resulted.

Utah Lake was broken into its main sectors and the HCMM temperatures of each sector were compared to the average HCMM temperatures of the lake. Table 12.4 shows the correlation of maximum and minimum overland air temperatures with the HCMM day temperatures of the sectors of the lake. The results displayed in Table 12.4 are an extension of that given in Table 12.3. The temperature differences among parts of the lake were consistent over the three months of HCMM data. This is also shown in Table 12.5. Figure 12.3 shows the good temperature correlation between the center sector and the entire lake. The summer months that the HCMM data covered, July, August, and September, are the most productive months for Utah Lake. The close agreement in temperature among the different parts of the lake during the summer should hold during the rest of the year when the lake is less active biologically.

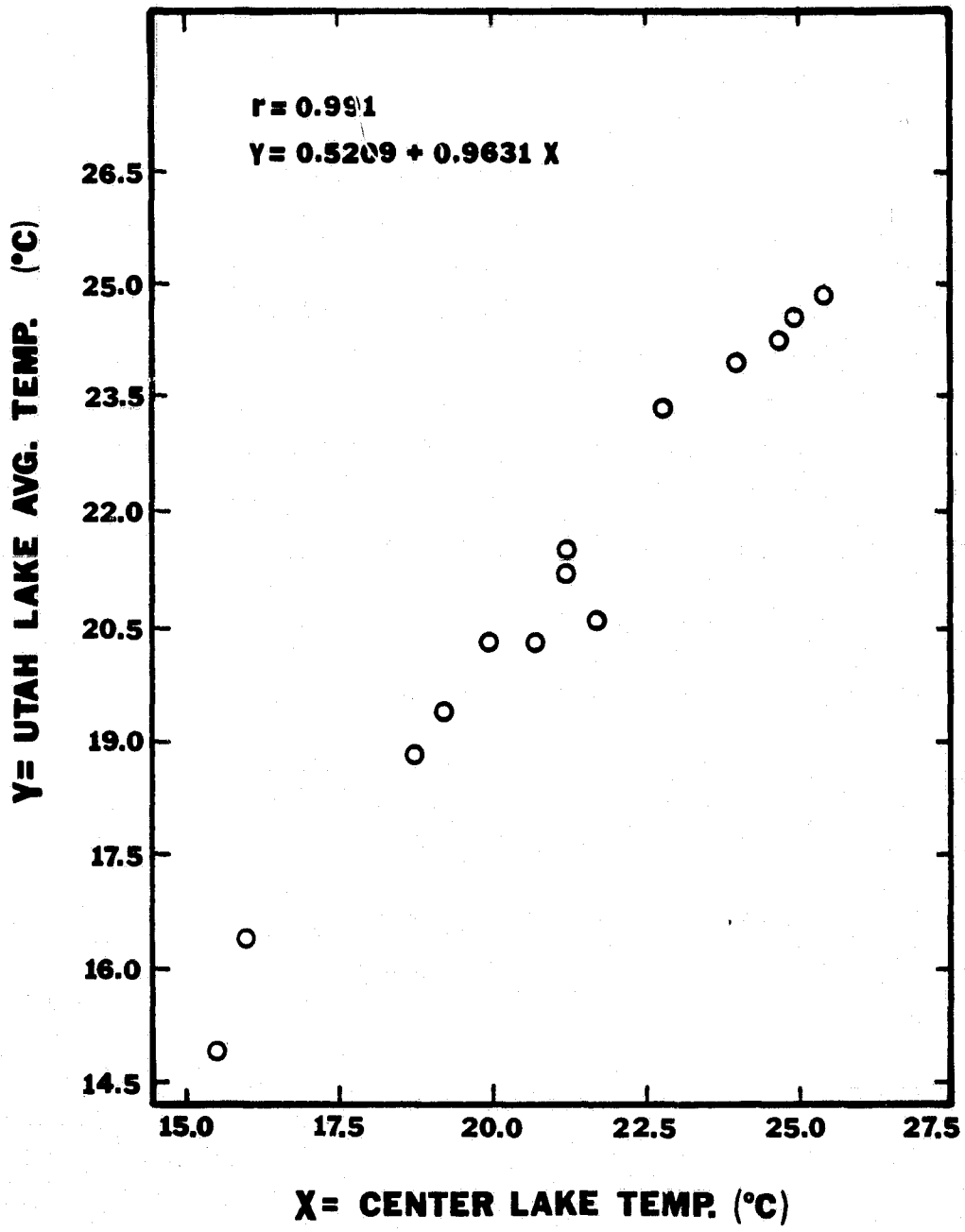

Figure 12.3. Utah Lake Temperature (°C) versus Center Lake Temperature (°C).

13. ALGAE AND EVAPORATION

13.1 Hypothesis

During the summer of 1981 research was conducted to study the effect of algae on evaporation. Class A evaporation pans were seeded with algae and evaporation, temperature and biomass measurements were taken. Results of this were used to determine the extent to which algae altered pan evaporation. The conclusions from this study might be applied to the lake to give an indication of the effect of algae in the natural environment.

There are several processes blocking or driving evaporation that were of interest. The first consideration was that of the increased pan temperature due to photosynthesis by the algae. This would elevate the water temperature. The reflectivity of the algae affects the amount of energy absorbed in the pan. The blocking effect of a large mass of floating algae was the third consideration. The photosynthetic effect and the increased absorption were expected to increase evaporation noticeably from that of a clean class A evaporation pan while the blocking action of the algae was expected to be minimal.

13.2 Location and Methodology

The Bureau of Reclamation (USBR) evaporation pan is located at the Provo Airport. The enclosure where the algae pans for this study were located, is adjacent to the USBR site. Therefore the wind, rain and evaporation data to be used in this study were available from the Bureau of Reclamation.

The size of the enclosure allowed three pans to be placed inside. The construction of the stands and their installation were in accordance with U.S. Weather Bureau instructions and matched that of the Bureau of Reclamation (USBR) pan nearby. By this method any error due to difference in installation was climinated and the USBR pan measurements was used as a control in the experiment.

Measurement of evaporation was made with standard stilling wells installed in every pan and the use of a hook gage. The hook gage gave readings to the nearest thousandth of an inch. The same hook gage was used for reading each pan, eliminating error in the use of different instruments. The measurements were read and the pans were filled at 10 a.m. each day.

Thermometers were used in two of the pans to record the high and low temperatures. The 10 a.m. check of evaporation was late enough in the day that the thermometers could be reset to a low enough temperature that the next nights minimum and the day's maximum would move the indicators and give a correct reading. The thermometers rested in the bottom of the pan and were usually read in place and then lifted out and reset. When the algae was thick the thermometers had to be lifted out and read immediately. The south side of the bottom of the pan was shaded during most of the day and was where the thermometers were placed in order to give on accurate reading of the water temperature.

13.3 Sampling

Evaporation from the pan occurs at the air-water interface and the algae studied was a floating variety. The samples were taken from the surface. Concentration of algae varied over the surface of the pan. In addition, the wind would on occasion cause the algae to concentrate on one side of the pan. Sampling was done with a one quart plastic bottle. The mouth of the bottle was lowered into the water to a depth of about 5 mm and the bottle was drawn across the pan at a uniform rate. The pattern used to sample was that of several straight lines. This ensured that the sample would be representative regardless of the variation in concentration. On those days that the concentration of algae was uniform a triangular pattern was used.

The samples were taken to the B.Y.U. Environmental Analysis Laboratory and frozen. They were later thawed and tested for biomass. Each sample was homogenized and a part put into a vial and centrifuged. The supernatant was drawn off and the algae washed into an evaporation dish. The water was driven out by heating to 103 ^{o}C for at least eight hours. The dishes were weighed and the biomass calculated as mg/l.

13.4 Algae Growth

The early summer algae growth was from an innoculation. The pans were prepared by filling them with water and adding a nutrient solution. A standard Allen's nutrient solution was considered to be satisfactory (Bold, 1978 and Starr, 1978). Allen's solution was added to the pan at the same time as the water and allowed to set overnight. A sample of Anabaena flos-aqua, another prominent algae species in Utah Lake, was introduced into one of the pans in order to obtain a unialgal culture. The algae did not grow. A larger sample of Anabaena was reseeded into the same pan while the other two pans were seeded with algae taken from Provo Bay.

The object of this proceedure was to grow algae in the pan and take samples as it grew from a small to a large concentration. The water turned green and the algae mixed in the water column, but no large surface concentration was formed. The Anabaena flos-aqua grew even less than the algae in the pans seeded from lake water. During the later part of the summer when the lake was very active, algae was collected and the pans were stocked with this lake algae once a week using a quantity large enough to cause a high surface concentration.

13.5 Errors

Several phases of the data collection could have introduced errors into the study. The sampling time of 10 a.m. was just before the major evaporation of the day took place. Variation in the time that the evaporation in the pans was sampled would give erroneous readings. However, due to careful monitoring the error resulting from the variation in the sample time was minimized. Any sample time that differed from 10 a.m. was noted and the evaporation of the USBR control pan was extended for that period from the continous forms.

The use of the USBR pan as the control pan was in itself a major source of error. The pan was filled with water approximately once a week and the measurements of evaporation and rain were recorded on charts with a continuous recorder. The varying water level of the pan effected the amount of evaporation. Calculating evaporation from the strip charts was fairly reliable except during periods of rain. Because of this, all data during times of precipitation was disregarded.

Sampling and determination of biomass was standardized as much as possible. The collection of the sample was the least reliable proceedure. The mouth of the bottle had to be immersed the same amount each time and the speed with which it was drawn across the water had to be held as constant as possible. To reduce the amount of error, the same size bottles were used to obtain all samples. Also the same person took all the samples so that variation caused by different techniques would not be present.

The centrifuge used to concentrate the algae would sometimes leave small pieces floating in the supernatant. Care was taken in this process and finally another more powerful machine was used. Error introduced in this proceedure was considered minimal.

13.6 Results

Temperature was known to be increased by masses of algae in the lake. Pan temperatures were taken infrequently in the USBR pan. A comparison of the temperatures of the pans showed that the pans with algae had a smaller change in temperature from minimum to maximum. The amount of evaporation during this period did not vary significantly from pan to pan. The lack of difference in total evaporation indicated that the amount of algae in the pans had no significant effect on evaporation. The top of the pans were covered with algae when many of the samples were taken. Table 13.1 shows a histogram of the middle of the interval of the log of the algae biomass concentration and the number of observations in each interval. The range of biomass data is large enough that any effect on evaporation would have been shown.

The amount of evaporation did not depend on the amount of algae present. The separate effects of differing albedo, photosynthesis, and blocking could not be determined. Figures 13.1 and 13.2 show the change in evaporation versus the log of the algae biomass concentration using both the USBR pan and the B.Y.U. weather station pan on the B.Y.U. campus. The correlation coefficients were almost zero and the regression lines were virtually horizontal.

The plots from the B.Y.U. and the USBR pans are similar except for the differing intercepts of the Y-axes. From this it is concluded that any of the effects of algae on evaporation cancel each other with no net effect on evaporation. The use of B.Y.U. data results in a different intercept because

Table 13.1. Histogram of the Middle of the Interval and the Number of Observations of the Logarithm of the Algae Biomass (mg/l).

MIDDLE OF INTERVAL	NUMBER OF OBSERVATIONS	
1.6	1	*
1.8	1	*
2.0	6	******
2.2	6	******
2.4	7	*******
2.6	10	**********
2.8	5	*****
3.0	8	********
3.2	3	***
3.4	5	*****
3.6	1	*
3.8	0	
4.0	1	*

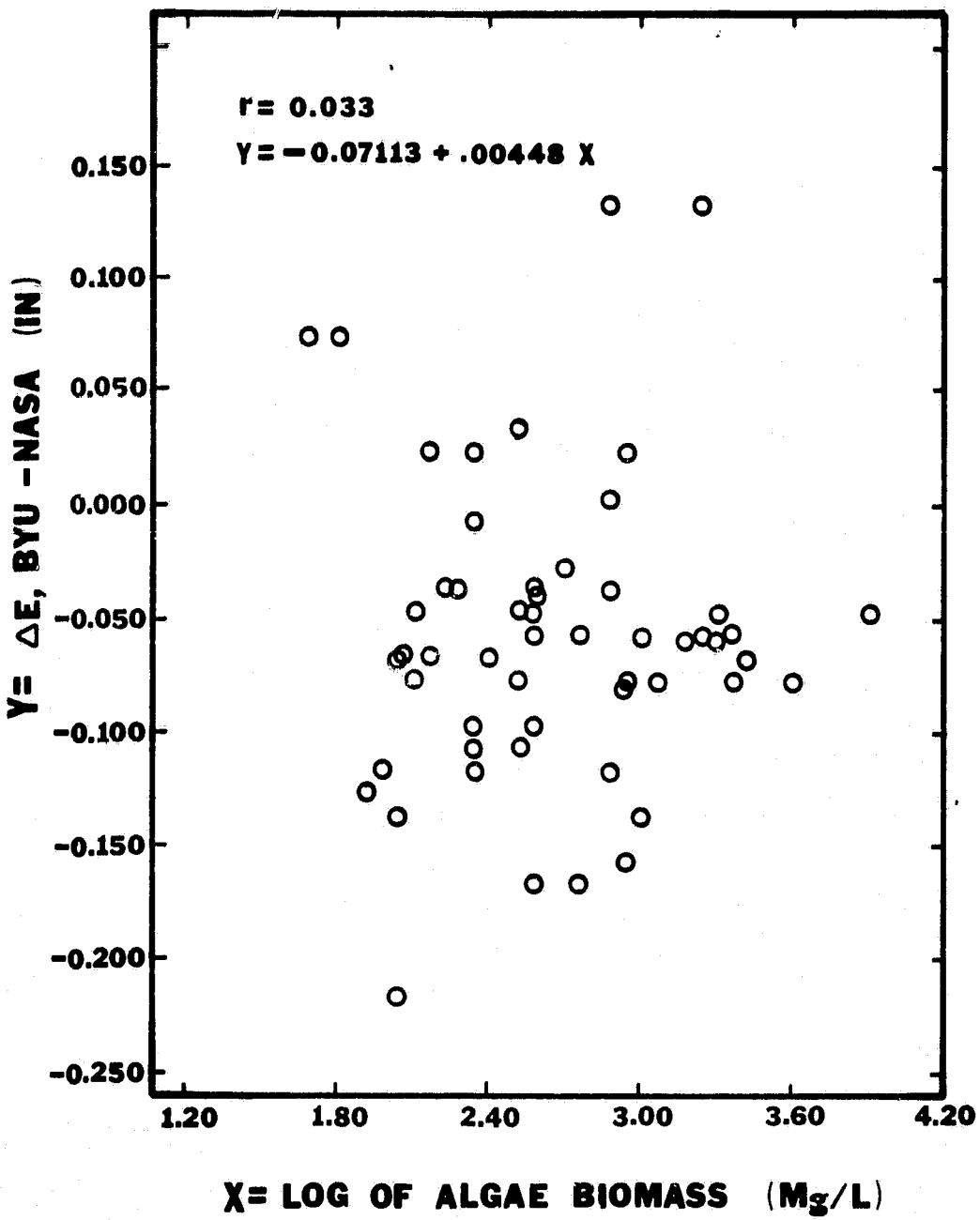

Figure 13.1. Difference in Pan Evaporation (in), BYU Weather Station Pan minus NASA Pan, versus the log of the Algae Biomass (mg/l).

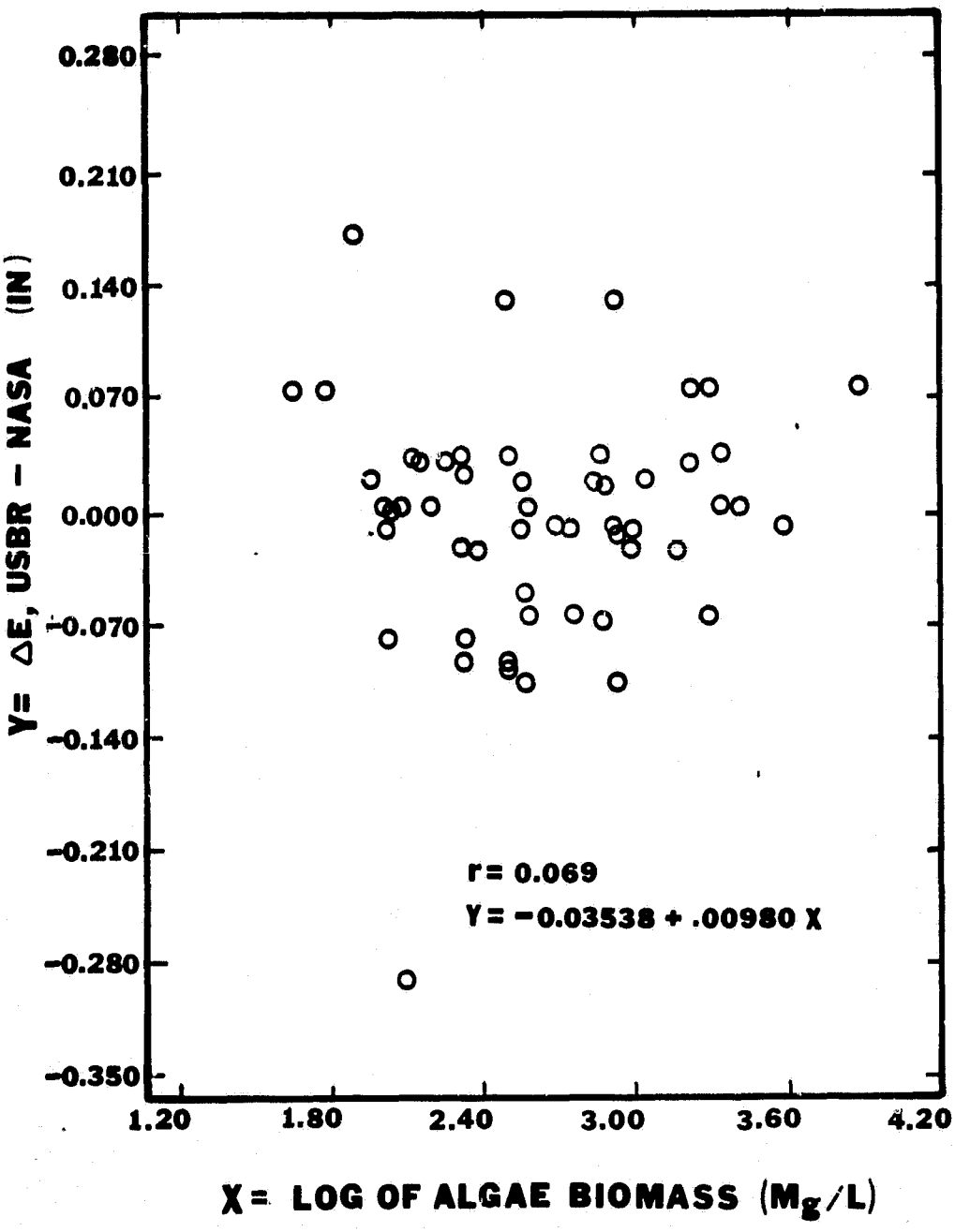

Figure 13.2. Difference in Pan Evaporation (in), USBR Pan minus NASA Pan, versus the log of the Algae Biomass (mg/l).

the B.Y.U. pan is located over 5 miles from the lake. This shows that though the location of the pan may be different, the regression line is virtually horizontal, showing no correlation of algae and evaporation in both cases.

14. THERMAL SPRINGS

14.1 Ground Identification

It is estimated that approximately 20 percent of the floor of Utah Lake more than one kilometer offshore is spiked with springs or seeps (Brimhall, et al, 1976). A large portion of these springs, including those in the Goshen Bay area, are either known or suspected to be thermal in nature. During the summer 1975 a semi-intensive study of Utah Lake was made by means of a sonarlike device. The acoustical reflection pattern obtained from numerous profiles imaged the thickness distribution and character of the underlying sediments. Using these profiles,it was possible to infer the existence and location of underground seeps and springs (Dustin and Merritt, 1980). Figure 14.1 depicts the location of suspected spring and seep areas in the lake bottom.

Two years later, in 1977, aerial thermal scans were made by the Idaho Air National Guard. An RF-46 aircraft was used, flying at 5,000 ft. (Dustin, 1978). A large number of surface anomalies were present on the imagery, showing small areas of thermal discontinuity. Figure 14.2 shows the location of the suspected areas.

An observation made during the HCMM study period that warrants mention was the marked deviation of two boat measured surface temperature from the daily average on the 10th of July, 1979. Generally, the data obtained from different parts of the lake followed a fairly predictable pattern, with Provo Bay being the warmest area and Goshen Bay the coolest. On the above date, however, two stations in Goshen Bay were significantly warmer than the remaining part of the lake. This corresponded to an atmospherically stable period substantiated by the lack of deviation of all other points sampled that same day. Upon close examination, it was found that the area containing these points quite often corresponded to a dissimilarity in surface temperature as sensed by the HCMM.

Figure 14.3 shows an enlarged view of the Goshen Bay area, also depicting the location of the two deviant points. The close proximity of these two points to the strongest suspected spring area in Goshen Bay raised the question of a possible connection between the two. For the springs to

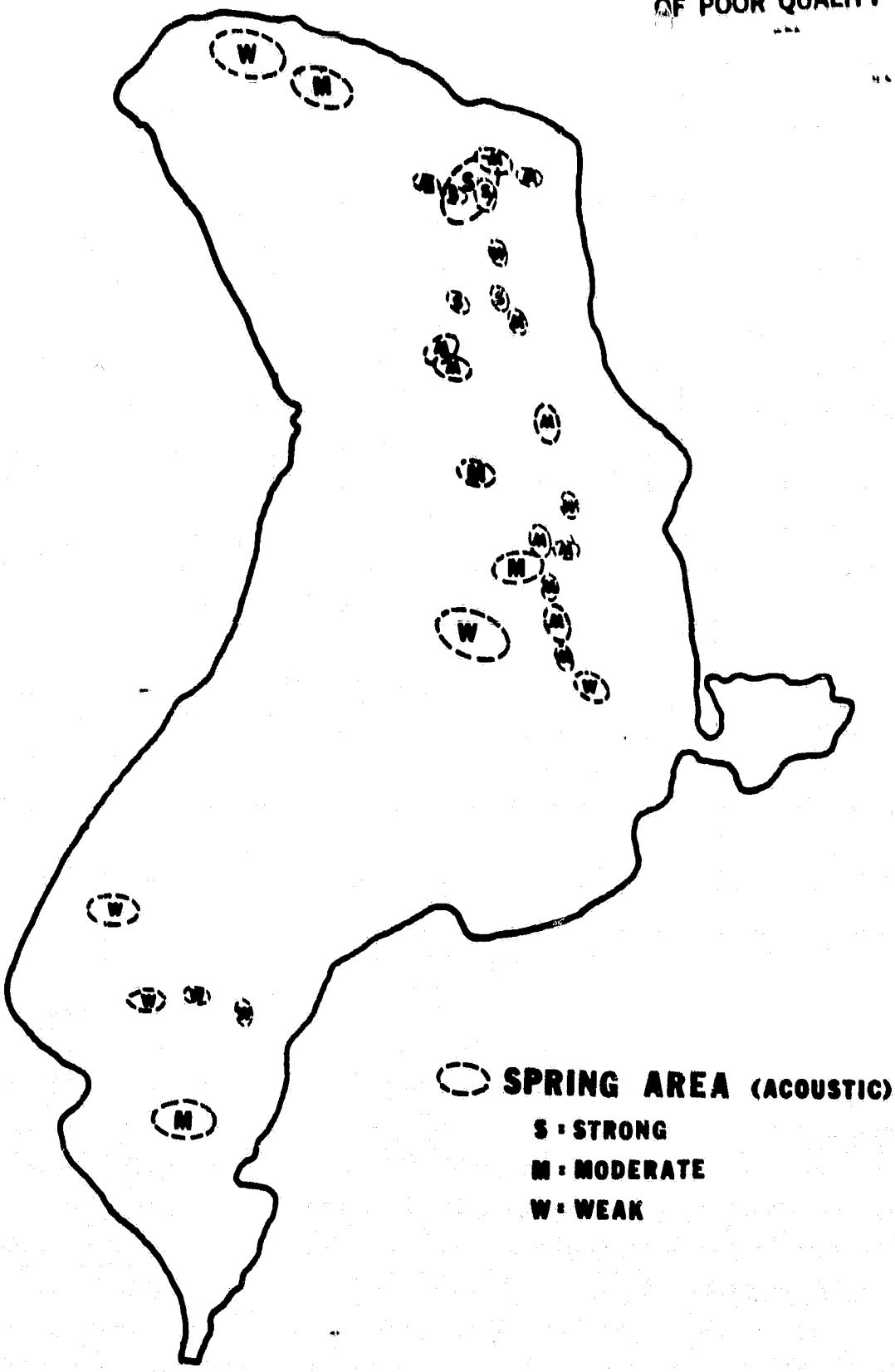

Figure 14.1. Suspected Subsurface Spring Areas: Acoustic Method (Dustin, 1978)

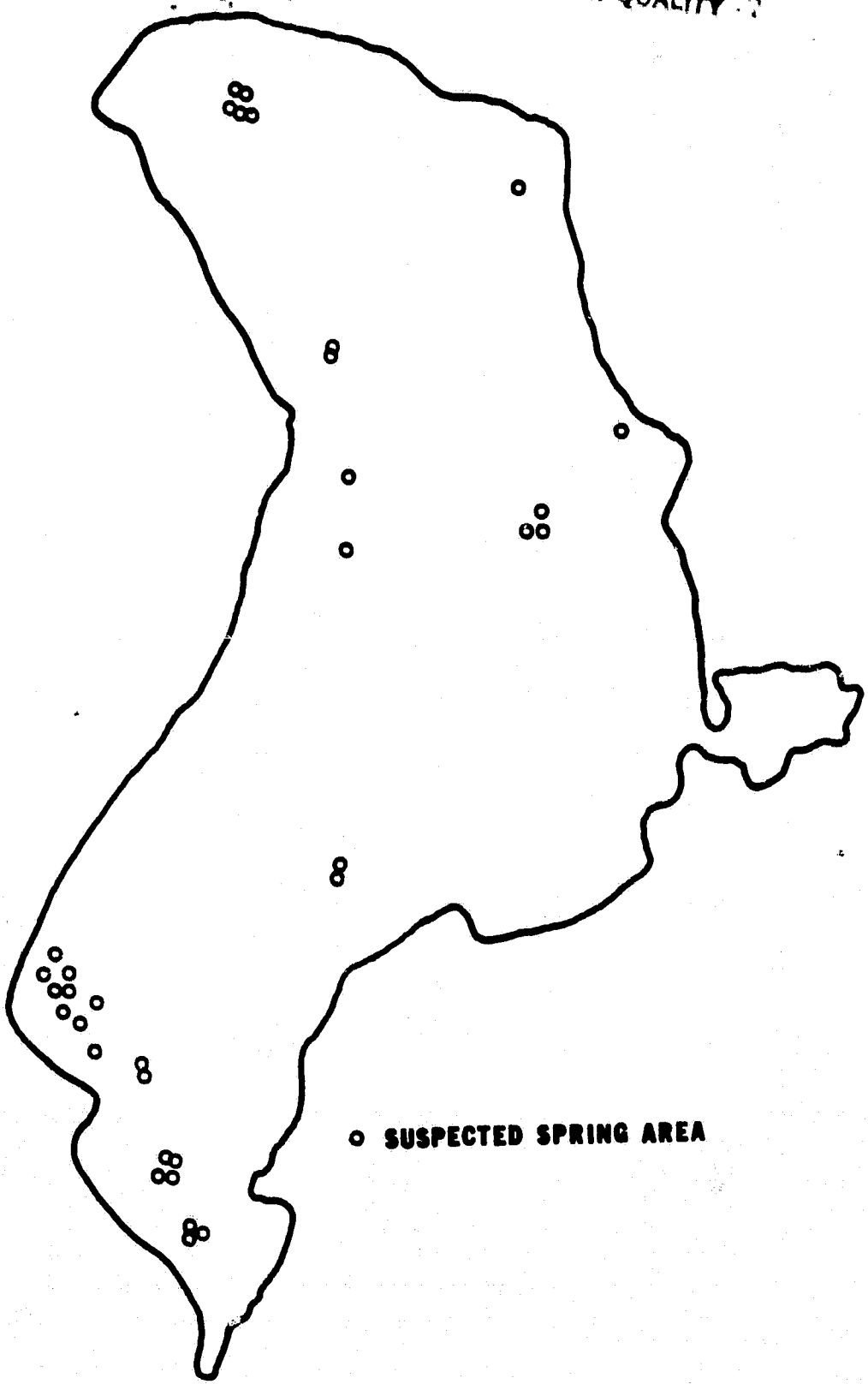

Figure 14.2. Suspected Subsurface Spring Areas: Aerial Thermal Scans (Dustin, 1978)

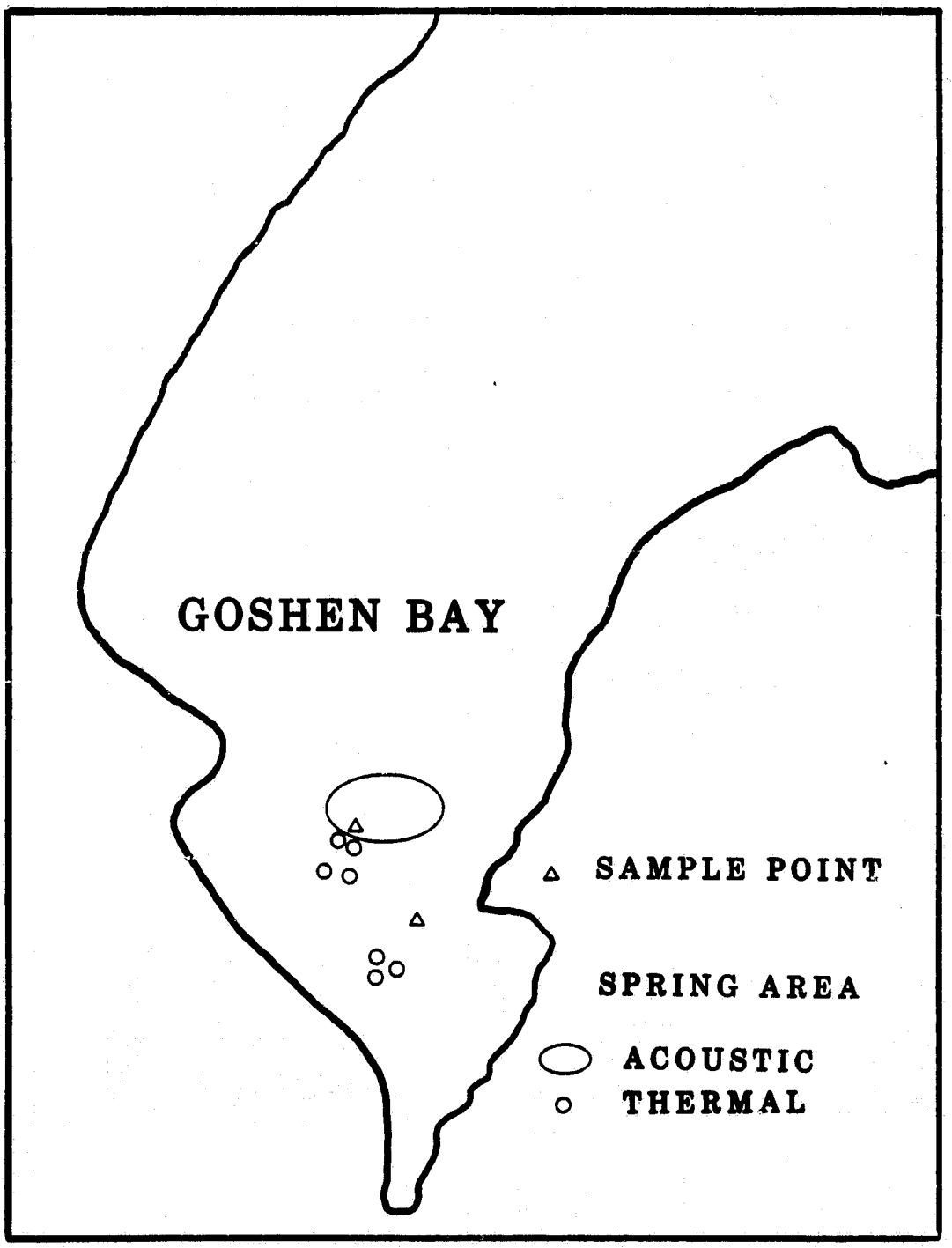

Figure 14.3. Proximity of Deviant Data to Suspected Spring Areas

have this noticed effect on the HCMM imagery, one explanation would be that they have a somewhat sporadic, surging nature, releasing moderate amounts of warmer water upon occasion and being relatively inactive the remainder of the time. However, this was not the suspected nature of the spring, but rather it was felt to have an essentially continuous flow.

Another possible explanation was the development of a thermal "plume" emanating from the spring area. In atmospherically stable and windless periods, this plume might be established and measurable. Periods of high wind, conversely, would tend to mix and distribute the warm water with that of the surrounding area, making it's detection from the surface impossible. A review of existing wind conditions at that time showed that for several days preceding the lake surface temperature measurement, winds were relatively calm. The next few days, however, between the lake surface measurement and the HCMM overflight, showed a marked increase in wind activity, which was sufficient to have a mixing effect on the lake surface waters. This explains why the warm spots didn't show up in the HCMM data of 14 July 1979.

14.2 HCMM Identification

One of the most interesting and useful applications of the color graphics of the DIR and NIR HCMM data has been the identification of these thermal areas within Utah Lake. The late summer and fall NIR color images and the late fall DIR images were used in an attempt to locate areas within the lake where significant thermal sources exist.

As the temperature of the lake water cooled in the late summer an area of consistently higher NIR intensities developed in the southwestern quadrant of the main lake body. Several other areas of two or three pixel groups consistently indicated warmer temperatures as well. However, the southwestern quadrant area is by far the largest and most easily observed. Figure 14.4, the color representation of the HCMM NIR intensities measured on Utah Lake for September 4, 1979, shows the location and intensity of this thermal area (green and yellow).

By November the daytime temperatures of the lake had dropped to a level where some thermal areas could be seen in the DIR color prints. By this time the algae in the lake have been removed by the cold evening temperatures or have been carried to the northern end of the lake by the wind or with the flow toward the Jordan River outlet. Observed warm areas (yellow and pink)

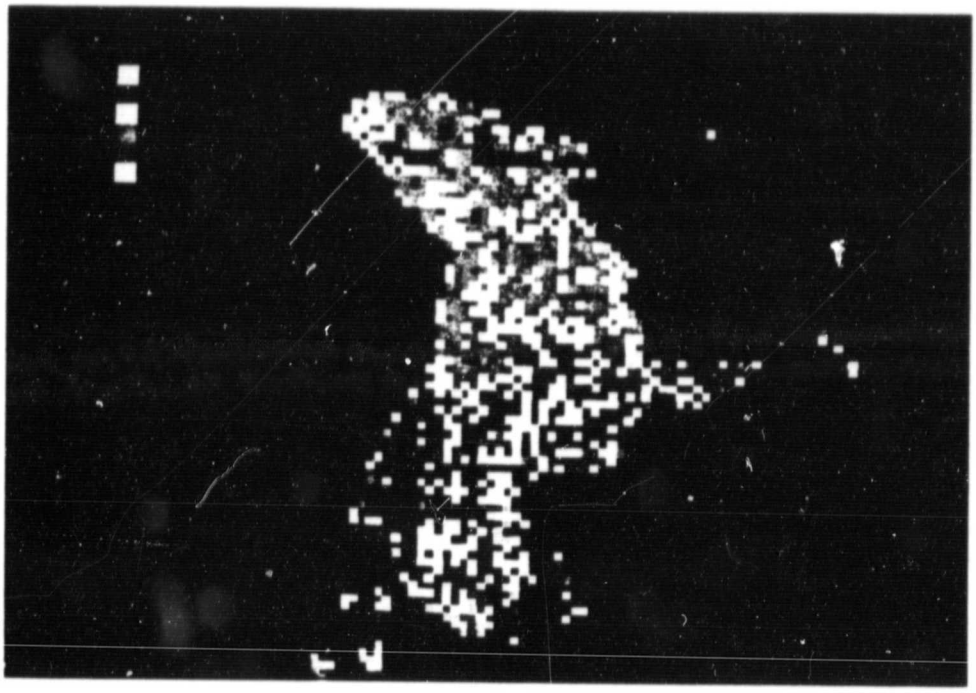

Figure 14.4. NIR on Utah Lake, September 4, 1979.

Figure 14.5. DIR on Utah Lake, November 14, 1979.

are therefore most likely a result of sources within the lake. In Figure 14.5, HCMM DIR for November 14, 1979, the warmer pixels are in the same general area which showed warmer waters in Figure 14.4. This apparently substantiates the presence of thermal sources.

15. GROUNDWATER

15.1 Data Availability

Initially, this research was to be done using chiefly quantitative data, obtained from various Federal and private organizations having conducted studies within the study area. A more thorough analysis of the available data, however, led to the realization that the vast majority of previous studies had been done on the three deep aquifers and had virtually ignored the near surface water table. The only available data was from county percolation testing done in the application for building permits. This data, in addition to being somewhat sketchy, was also subject to some question as to accuracy.

The distinct lack of what was felt to be a significant volume of usable data prompted the decision to expand the originally planned research into the qualitative area. The data search had turned up several well documented maps covering the study area and showing regions of characteristically high and low groundwater.

15.2 Quantitative Groundwater Analysis

The quantitative portion of the groundwater study was procedurally similar to the development of the linear model for predicting surface temperature. The groundwater model was not restricted to a linear fit, however, so more advanced regression techniques were needed. These techniques are still matrix operations, however, and were done with the aid of the Minitab II statistical package.

Since no base model for this type of system was found in the literature, a variety of different types of curves were tried, using the correlation coefficient as the chief indicator of the best fit. After the best curve was determined, the groundwater data was also extensively examined, through the use of the residual plots, in order to locate any unaccounted for parameter affecting the model.

The quantitative data was obtained from unpublished records of county percolation tests performed in the study area. Twenty-two tests were recorded of which seven were unsupervised by county personnel. During the study period, a procedural change was made that required a county official to

directly supervise the percolation testing. The reason for this change was the inaccuracy of reported results when testing was not overseen by a county official. Although data obtained from unsupervised tests were not immediately rejected, they were closely examined as to their impact on any results obtained through their incorporation into the data base.

15.2.1 All Data

Figure 15.1 depicts the relationship between depth to groundwater and the HCMM sensed surface temperature, using both supervised and unsupervised data. As can be seen, no obvious strong correlation exists. It appeared that a best fit curve would possibly be a third or fourth order polynomial. Only 0.394 was the best correlation coefficient for the fourth order equation given below:

$$d = a + bT^4 \quad ,$$

Where d = depth to groundwater

and T = HCMM temperatures

It is recommended, however, that polynomials of 3rd order and higher be avoided, and that models of a different type i.e. log, exponential, etc., be used (Ryan, et al, 1976). After extensive analysis of several recommended models and combinations, it was determined that the best fit to the curve was given by the following equation form:

$$d = \left[\frac{1}{a + bT^2}\right]^2$$

The correlation coefficient of the above equation was 0.411. This model, however, has absolutely no theoretical basis. It simply provided the best fit curve to the available data.

15.2.2 Separated Data

The data base was next separated into two sets corresponding to the supervised and the unsupervised test. Figures 15.2 and 15.3 show the respective relationships between depth to groundwater and the HCMM sensed surface temperature. Again, no strong correlation exists.

By using the same approach as above, several types of curves were examined in an attempt to find the "best fit". Several equations yielded a correlation coefficient of 0.37 for the supervised test data, the simplest of which was a straight line:

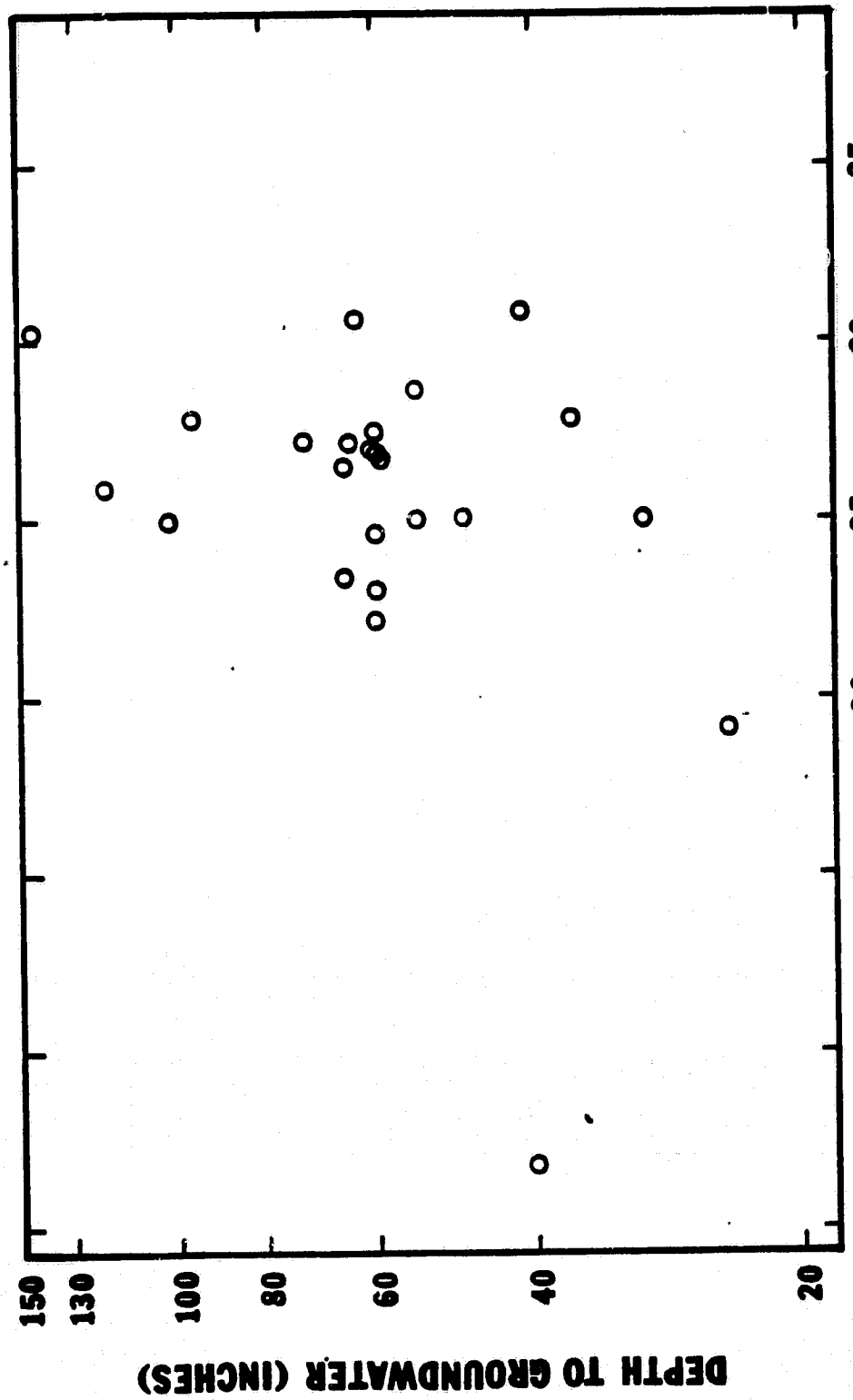

Figure 15.1. Depth to Groundwater vs. HCMM Surface Temperature

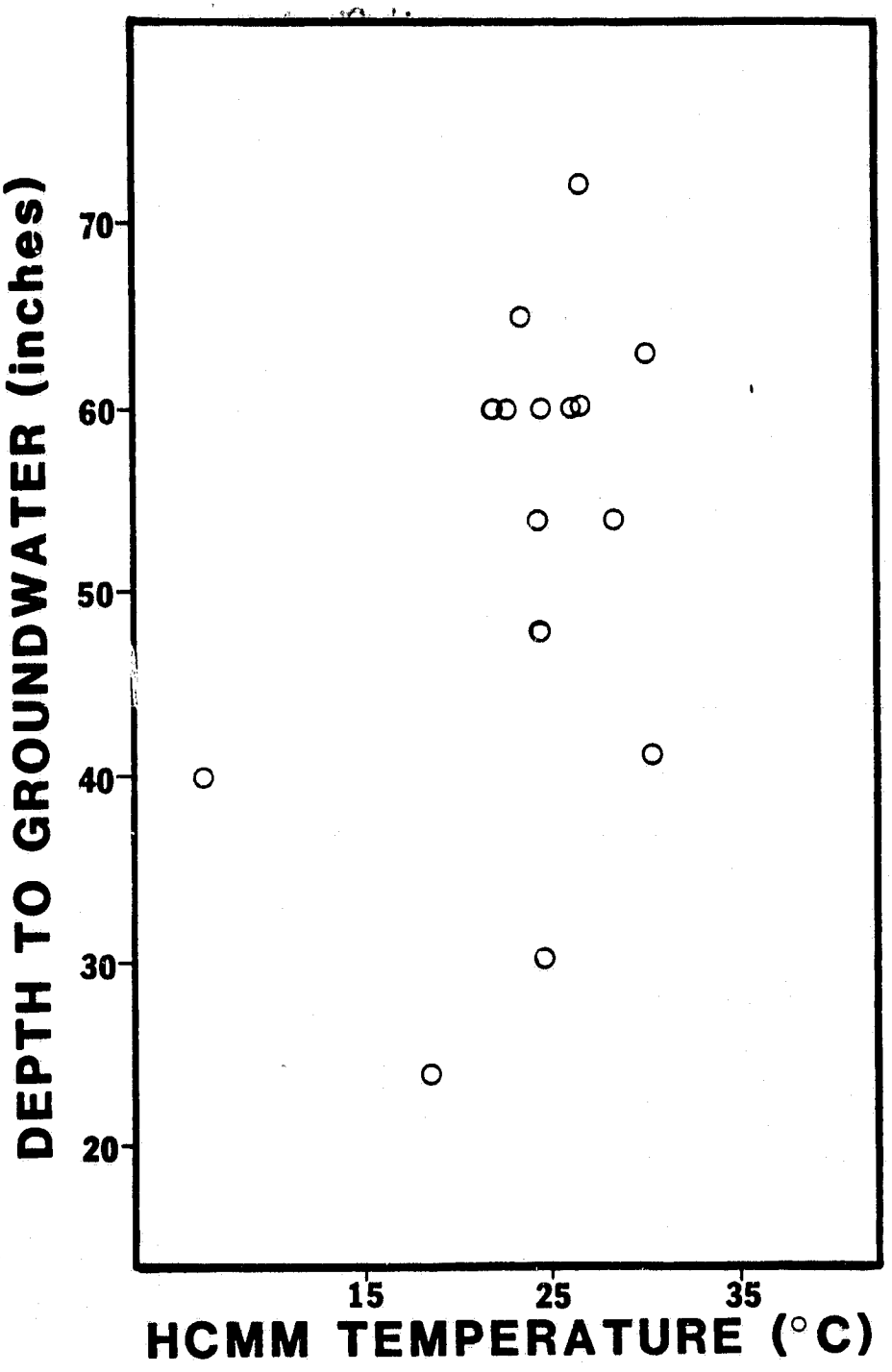

Figure 15.2. Depth to Groundwater vs. HCMM Temperature for Supervised Tests

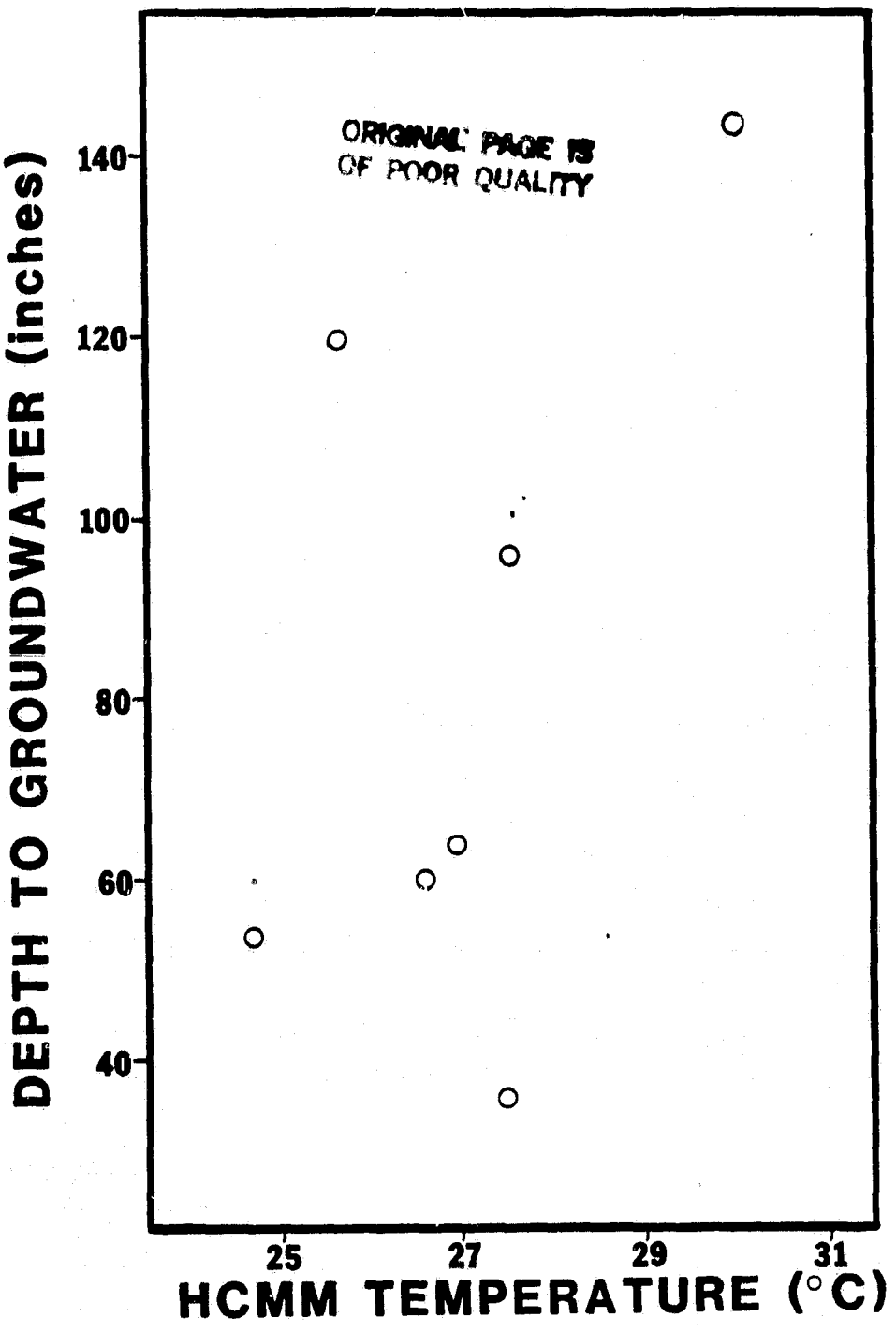

Figure 15.3. Depth to Groundwater vs. HCMM Temperature for Unsupervised Tests

$$d = a + bT$$

Surprisingly, a correlation coefficient of 0.678 was obtained through the use of the following model with only the unsupervised test data:

$$d = a + bT^{4}/_{3}$$

Possible explanations as to why the more questionable unsupervised data yielded the superior correlation coefficient are discussed later.

15.2.3 Seasonal Variation

Non-vegetated areas are preferred for this type of study for a variety of reasons. Therefore, the mid-summer values were deleted from the groundwater data base, leaving only the spring (April and May) and fall (November) data. It was hoped that through this approach the majority of the vegetation season could be eliminated, or at least the effect minimized.

Table 15.1 lists the off season groundwater data used in the above correlation. As can be seen, the data is essentially from 3 HCMM overpasses. Of the nine measurements, four are from May of 1978, four from April of 1979 and one from November, 1979. Although the last data is quite late in the season, an examination of National Weather Service data for the area showed no indication of snow on the ground.

Figure 15.4 shows groundwater depth plotted against HCMM temperature for the non-summer data only. The linear correlation of the groundwater depth to HCMM sensed temperature increased to 0.61, which for some natural systems is considered acceptable

Groundwater depth was then correlated with the HCMM intensity value as opposed to the computed surface temperature. With an exponential curve applied to the data a correlation coefficient of 0.64 was obtained. This higher correlation which was possibly due to the slight curvature of the relationship between HCMM Intensity and HCMM Temperature, yielded the following relationship:

$$d = 10.827e^{0\ 01743\ I\ (HCMM)}$$

Of the off season data, all depths of greater than 60 inches were measured in May, while those depths less than 60 inches were the April and November values. Since ground temperature would naturally be expected to rise as the spring season progressed, a measurable rise in sensed surface temperature would be expected regardless of groundwater fluctuation. This trend would likely have a significant impact on the relationship to be

Table 15.1

Off Season Groundwater Data

Ground Measurement Date	Depth to Groundwater	HCMM Intensity	HCMM Overflight Date
May 3, 1978	96	111	May 13, 1978
May 10, 1978	64	109	May 13, 1978
May 10, 1978	120	105	May 13, 1978
May 17, 1978	144	120	May 13, 1978
April 10, 1979	54	102	April 15, 1979
April 13, 1979	24	84	April 15, 1979
April 18, 1979	48	102	April 15, 1979
April 20, 1979	54	102	April 15, 1979
November 15, 1979	40	49	November 14, 1979

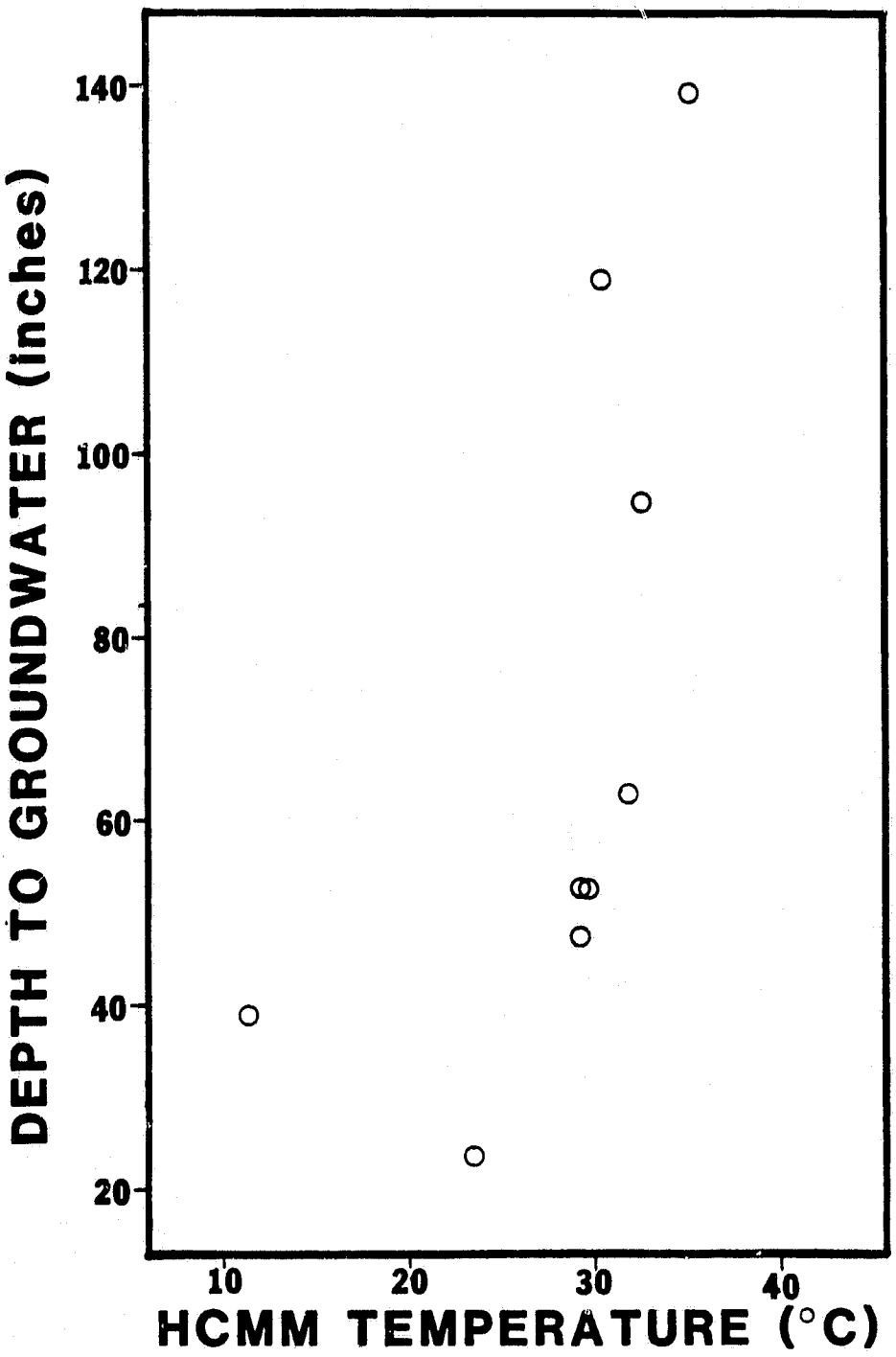

Figure 15.4. Depth to Groundwater vs. HCMM Temperature for Off Season Data

developed. Therefore, two independent approaches were taken in an attempt to remove its effect. First, on attempt was made to factor the seasonal temperature variation out of the data, reducing it to standardized, and therefore comparable, values. Second, the different overflight dates were examined independently.

15.2.3.1 Temperature Standardization

The first step in attempting to factor out seasonal variation was to find a suitable parameter that could be used to reduce the data to seasonally independent values. The temperature of dry soil at each of the data sites would have been ideal, but no such data existed. The most reasonable approximation to this data that could be located was the recorded 8 inch soil depth temperature at the Salt Lake City Airport Weather Station. As this was sufficiently far away (50 miles) from the study area to be quite questionable, the average daily air temperature for the study area was also recorded. Both the soil and air temperatures were each subtracted from the HCMM predicted surface temperatures. The resulting values, reflected the soil surface temperatures while minimizing the possible influence of seasonal variation.

This procedure had the effect of generally moving the four higher points to the left in relationship to the lower values as shown in Figures 15.5 and 15.6. Although any significant correlation was essentially eliminated, it is felt that in subtracting the seasonal variation, the true ground water/surface temperature relationship was more accurately established.

15.2.3.2 Independent Overflights

The separation of data into individual overflight days totally eliminated the seasonal variation. However, it reduced the number of data points for each set to four, making significant results difficult to obtain. The two groups of data are shown in Figures 15.7 and 15.8.

Figure 15.7 shows an slight indication of higher surface temperature with deeper groundwater, but the spread of the data is quite broad and results are somewhat questionable. Figure 15.8 shows much better correlation between deeper groundwater and higher surface temperature. A curve through the points further substantiates that the relationship between groundwater depths and surface temperatures may follow an exponential curve of the form:

$$d = ae^{bT}$$

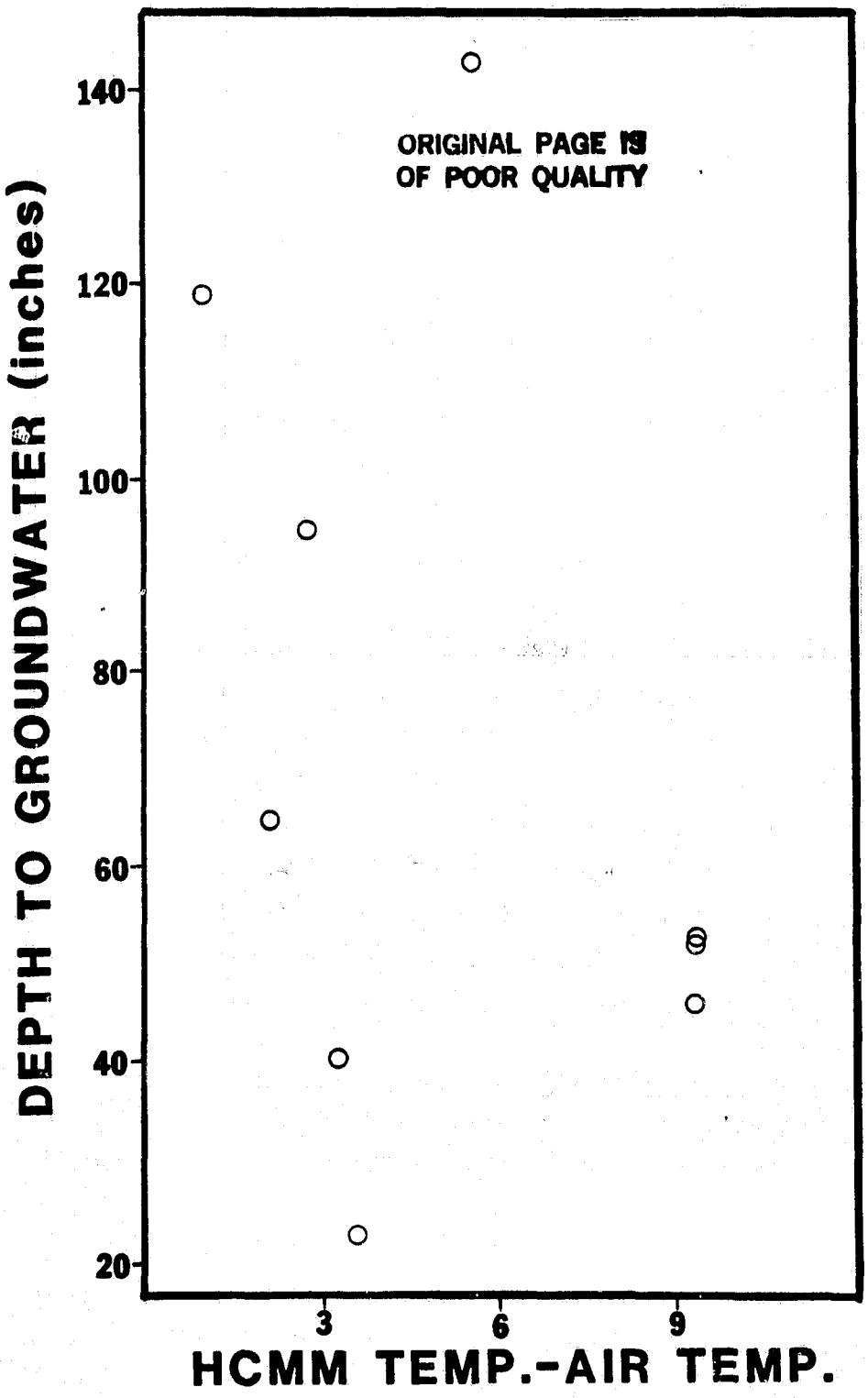

Figure 15.5. Depth to Groundwater vs. HCMM Temperature - Ambient Air Temperature for Off Season Data

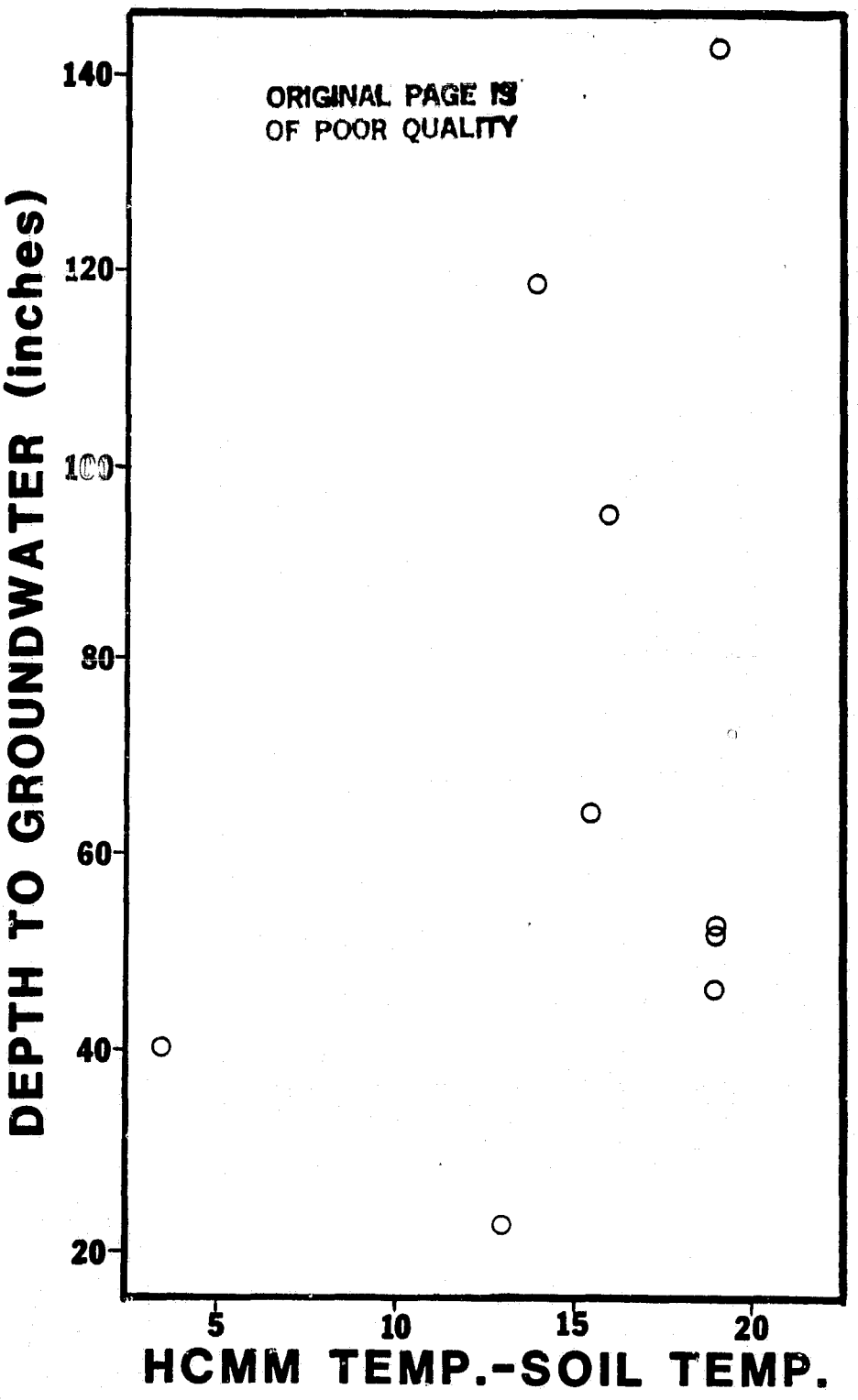

Figure 15.6. Depth to Groundwater vs, HCMM Temperature - Soil Temperature for Off Season Data

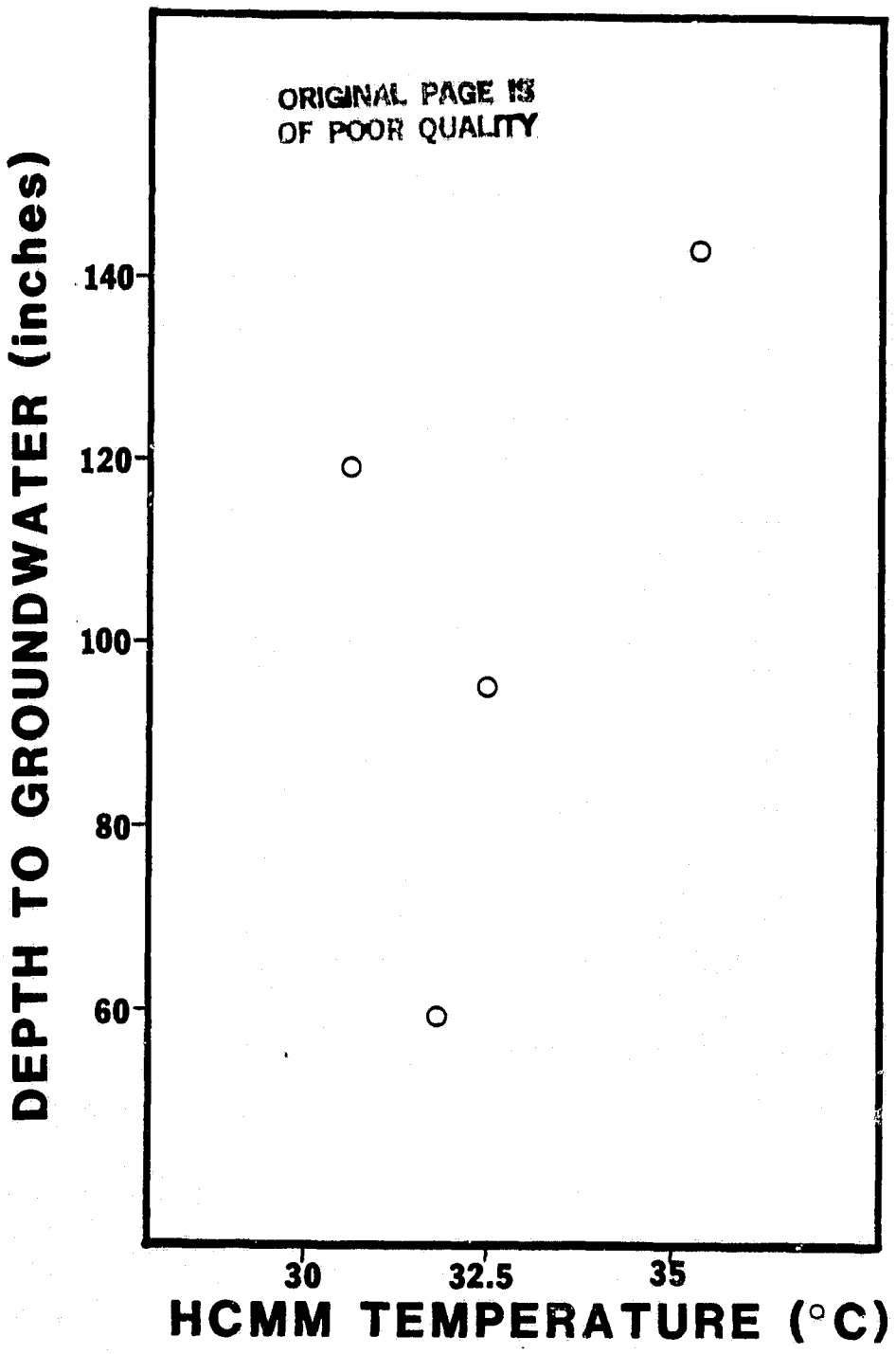

Figure 15.7. Depth to Groundwater vs. HCMM Temperature for May, 1978 Data

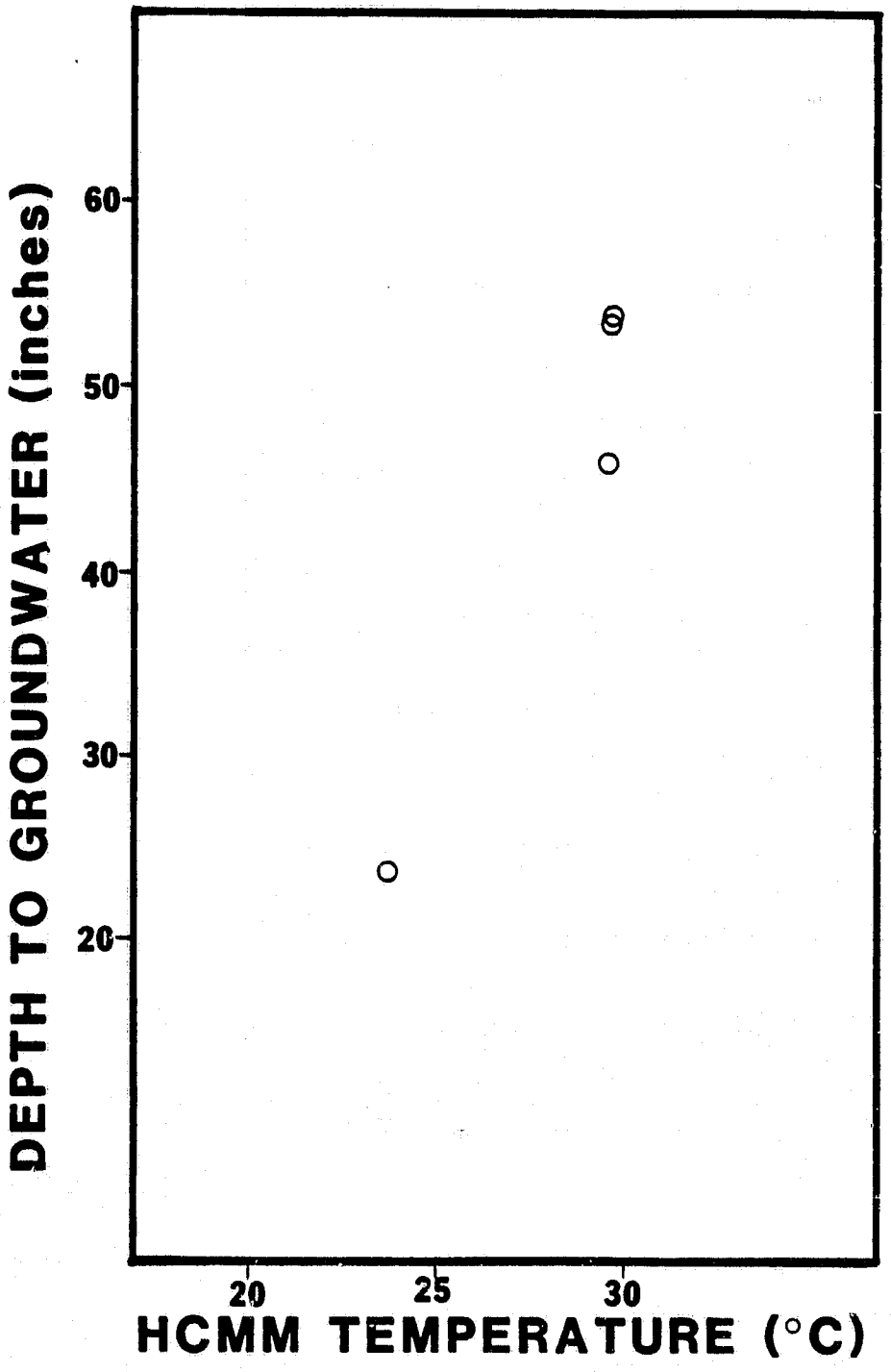

Figure 15.8. Depth to Groundwater vs. HCMM Temperature for April, 1979 Data

15.3 Qualitative Groundwater Analysis

15.3.1 Methodology

The qualitative portion of the groundwater study took a much broader approach. Figure 15.9, 15.10 and 15.11 depict sketches of the maps obtained from the Utah State Geological and Mineral Survey(UGMS), Soil Conservation Service (SCS) Septic Tank Study, and SCS high water table study, respectively.

The method employed consisted of examining several transects through the study area. Transect location was based on several factors. Emphasis was given to areas of rapid change in groundwater depth. Nonvegetated areas were preferred, but as the study site was chiefly agricultural, this requirement was difficult to fulfill. Special attention was given to non-homogeneous areas, well defined shallow water table areas surrounded by deeper water table, etc. One problem encountered was disagreement among the three maps as to the location of some of the critical areas. Generally, this was resolved by taking transects based on a specific map, as opposed to constructing an aggregate map or using multipurpose locations. In all, ten transects were chosen. Transect locations on the groundwater maps are shown in Figure 15.12, 15.13 and 15.14.

After having determined the key locations, the chosen transects were plotted on the overlays of the study area. Due to the expanded east west scale of the HCMM line printer maps, distances along the transects were rather severely distroted, depending on their relative position on the overlay. An east west transect for instance, appeared roughly three times as long as a north south transect of similar actual length.

Also due to the skew angle difference between day and night images, the day/night lengths of the same transect varied. This variation in length became obvious as the overlays were used to obtain the HCMM sensed intensities from the line printer maps. As all data from the same transect was to be compared to the various groundwater map derived groundwater patterns, it was necessary to adjust the lengths of the varying transects to correspond to a specific base length. The longest transect was chosen as the base length. In using the longest, it was possible to insure that no critical data would be deleted. As transects needed to be lengthened, the number of additional intensity values were determined. The transects were then proportioned into

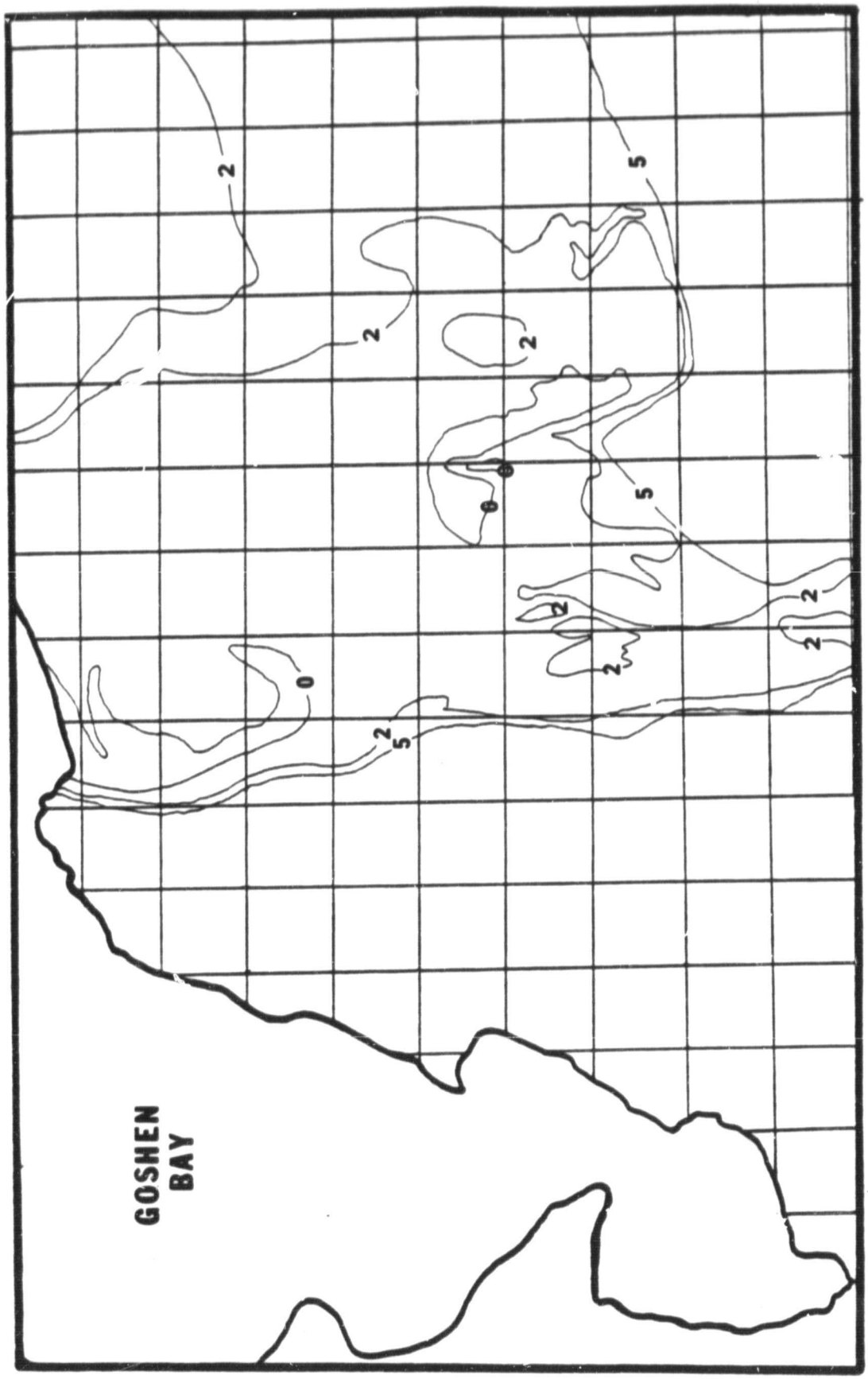

Figure 15.9. Utah Valley Groundwater Depth Contours According to Utah State Geological and Mineral Survey

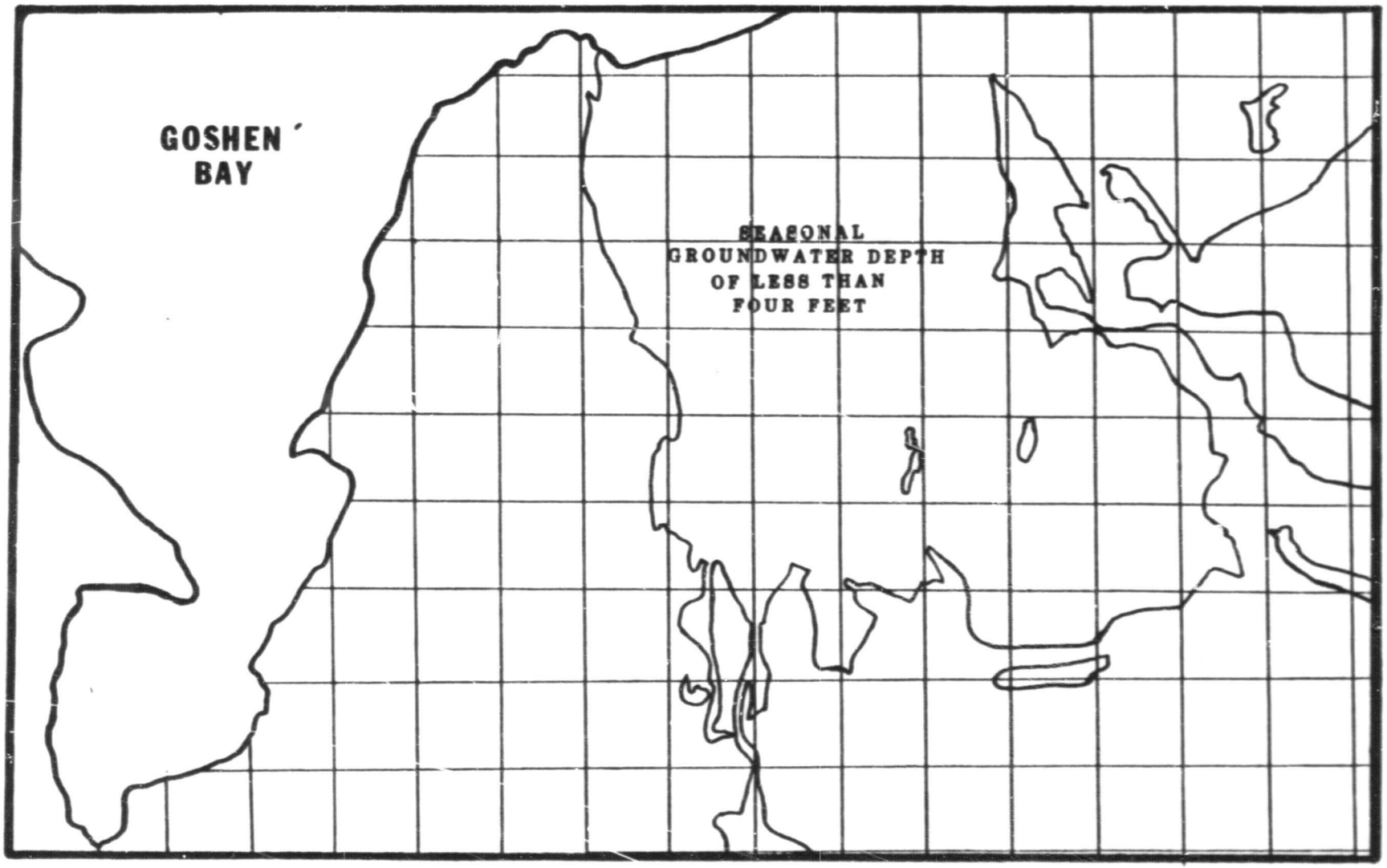

Figure 15.10. Utah Valley Areas of Seasonal Groundwater Depth Less than Four Feet (U.S. Soil Conservation Service Map)

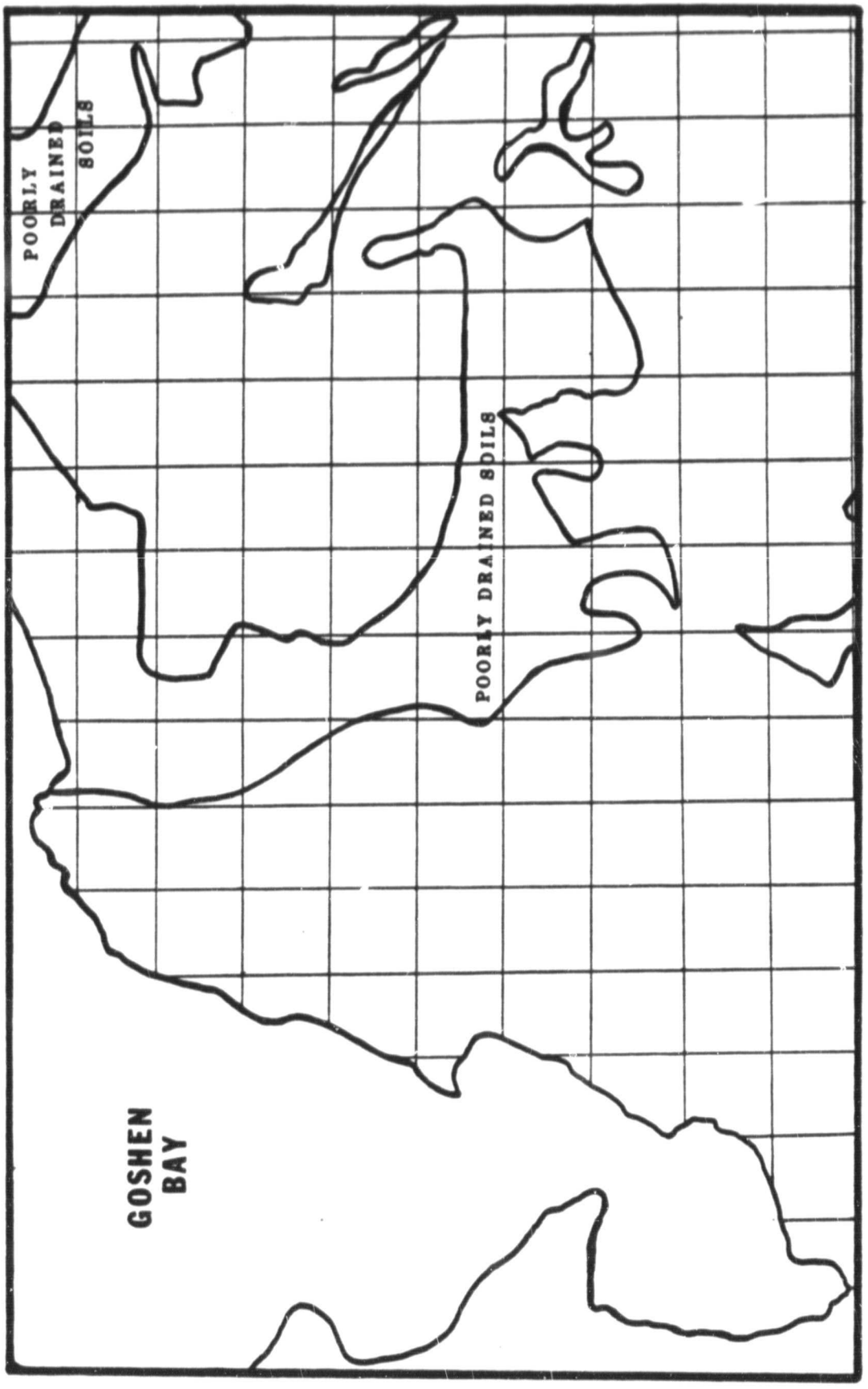

Figure 15.11. Utah Valley Areas of Poorly Drained Soils (Utah County Government Map)

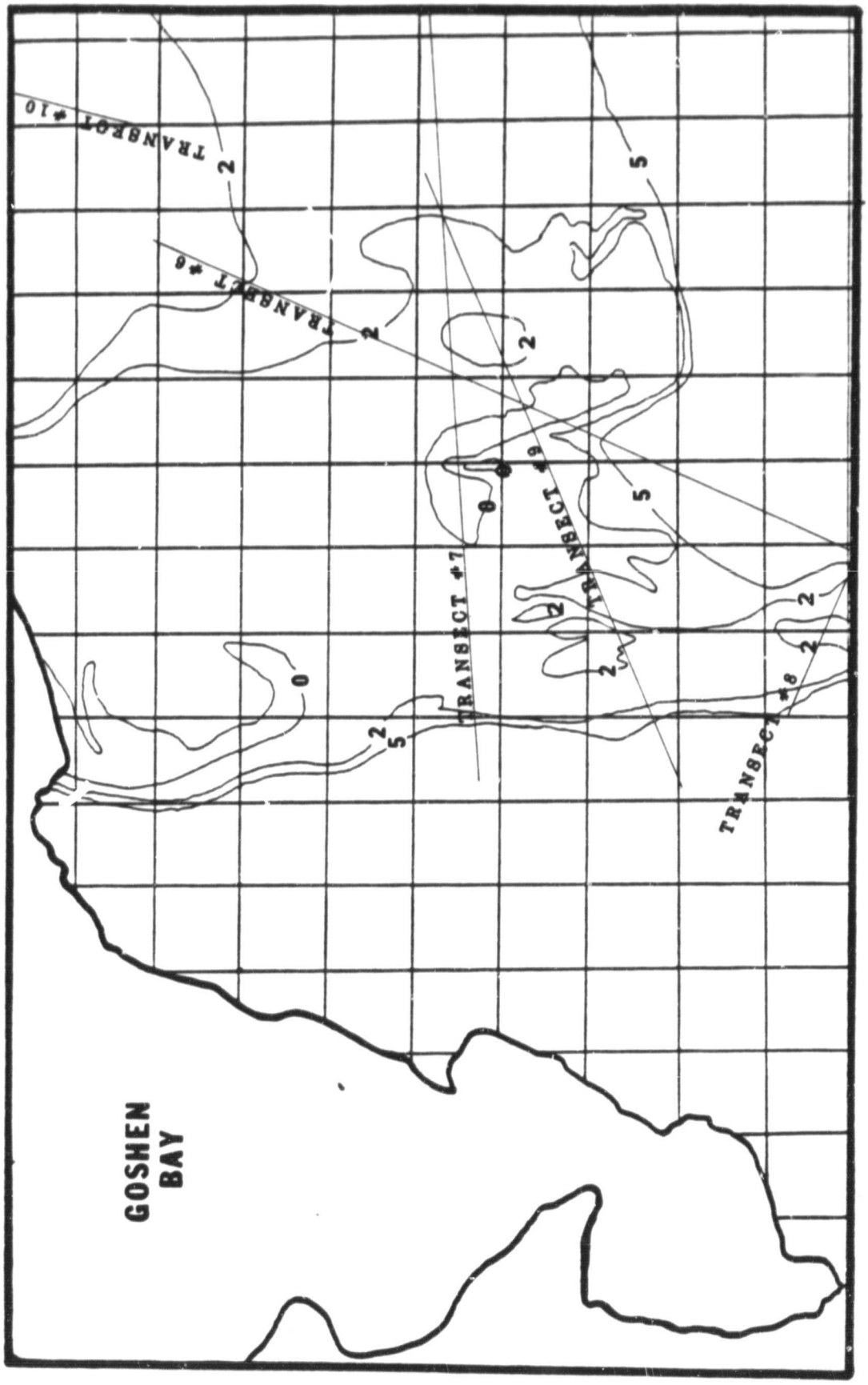

Figure 15.12A. Transects Examined as Compared to USGMS Groundwater Map

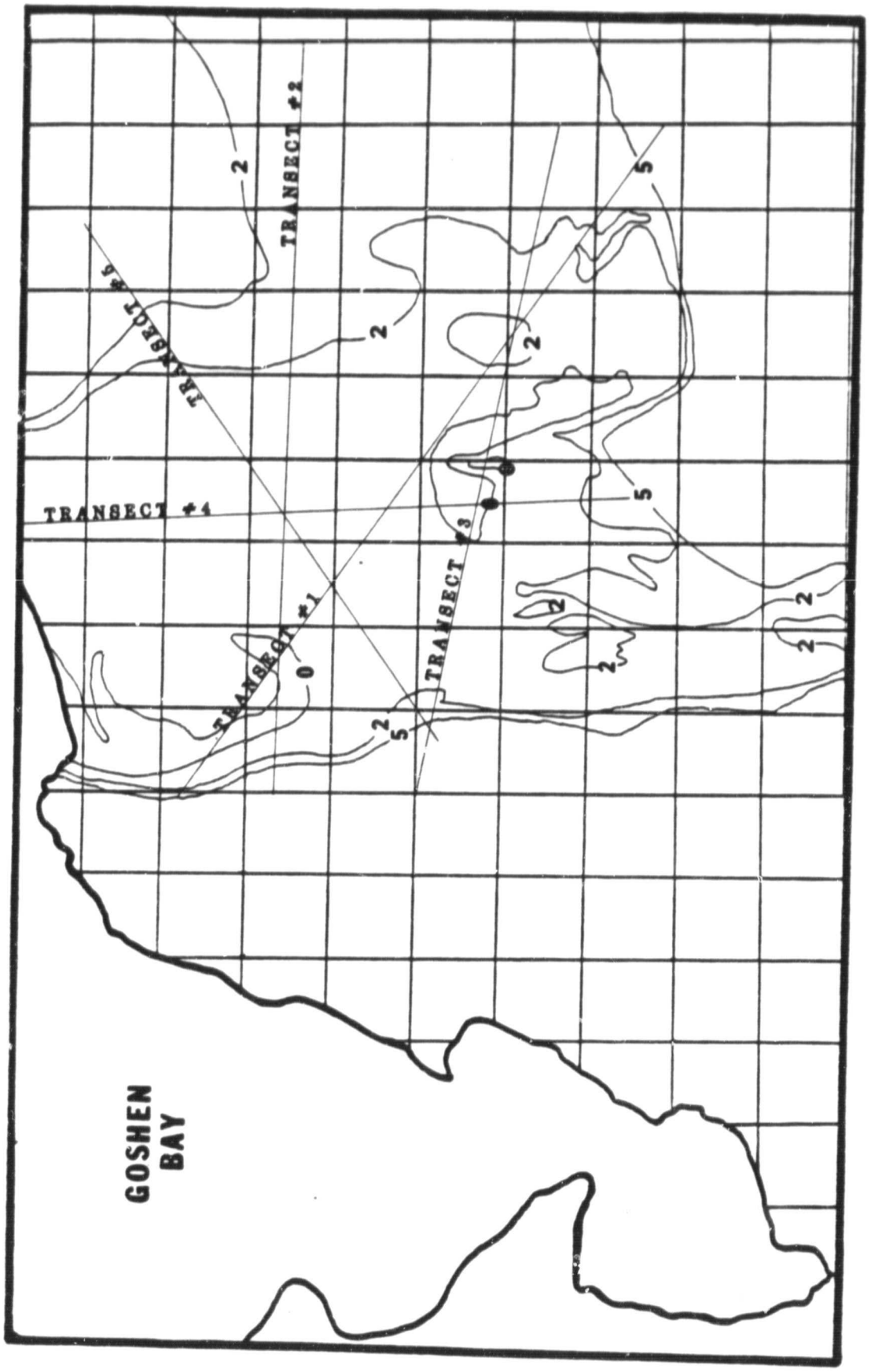

Figure 15.12B. Transects Examined as Compared to USGMS Groundwater Map

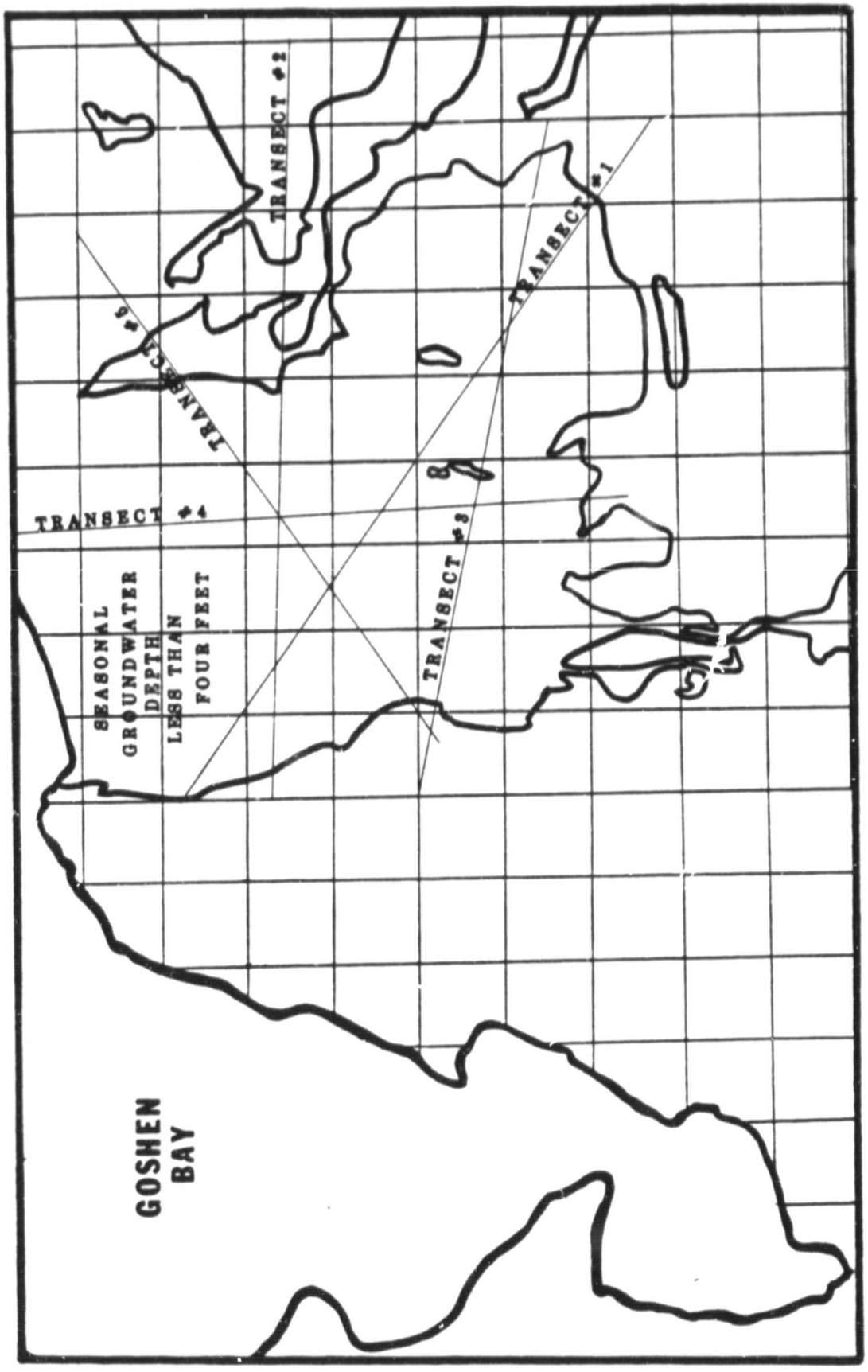

Figure 15.13A. Transects Examined as Compared to USSCS Groundwater Map

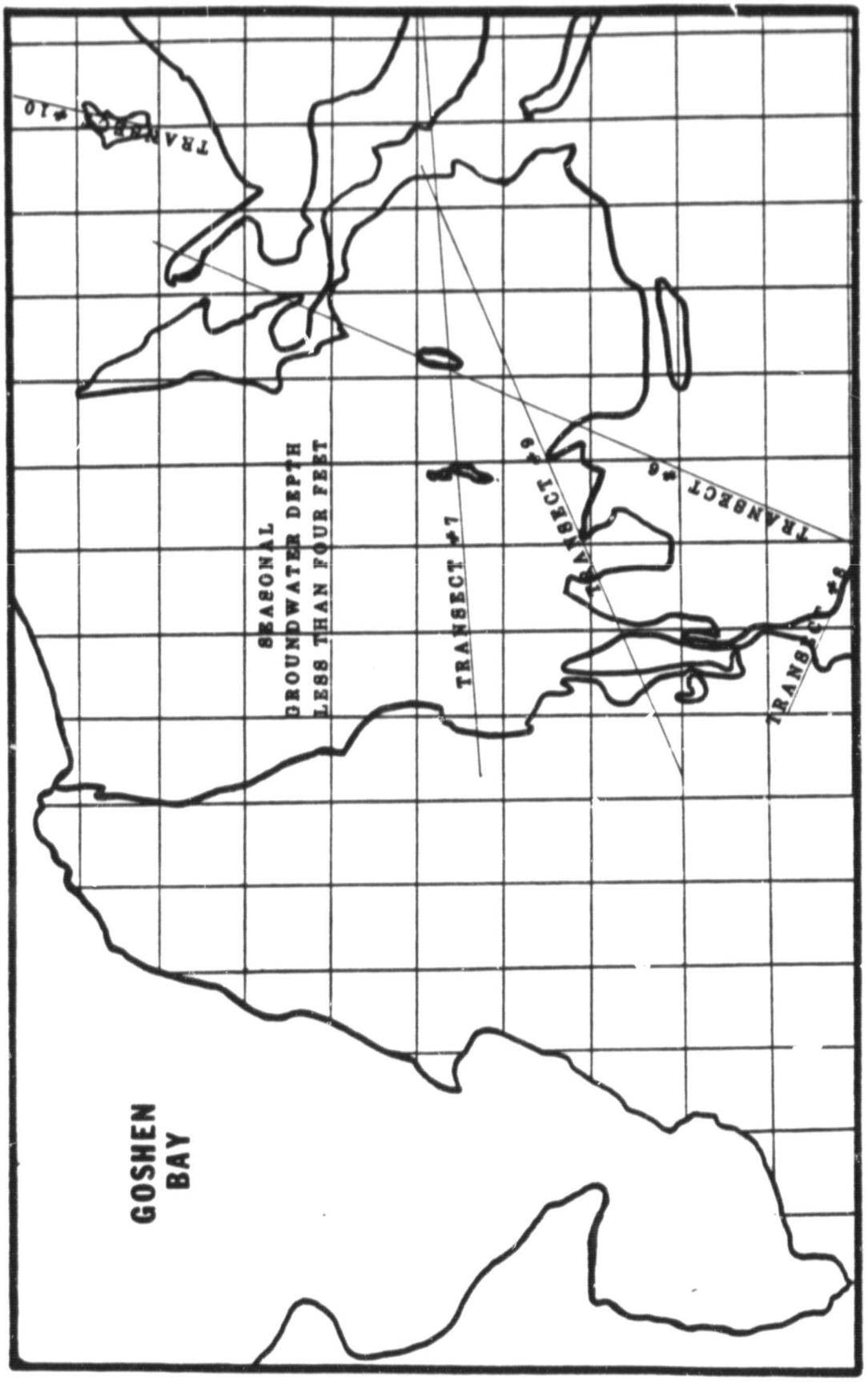

Figure 15.13B. Transects Examined as Compared to USSCS Groundwater Map

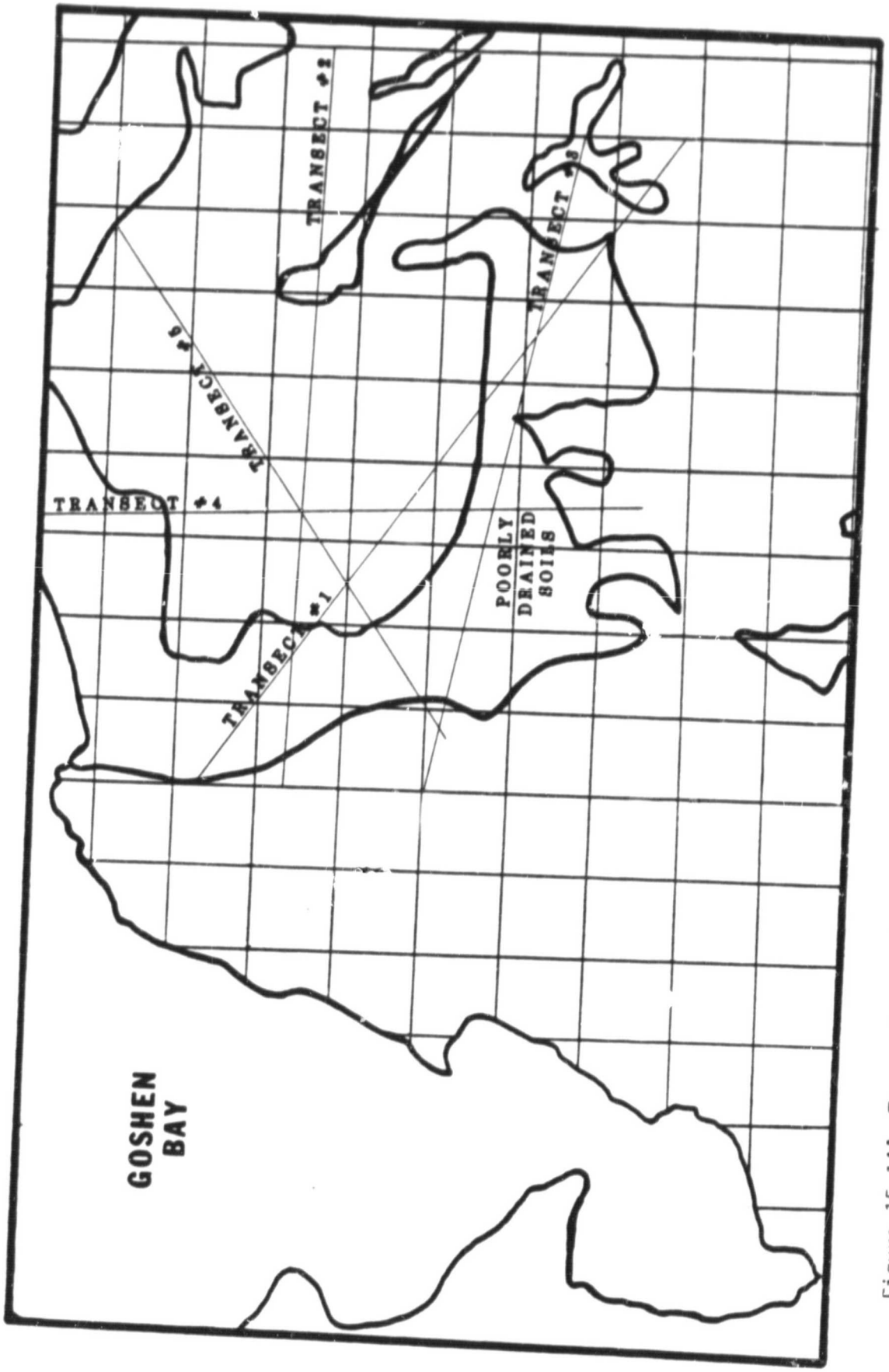

Figure 15.14A. Transects Examined as Compared to Utah County Government Groundwater Map

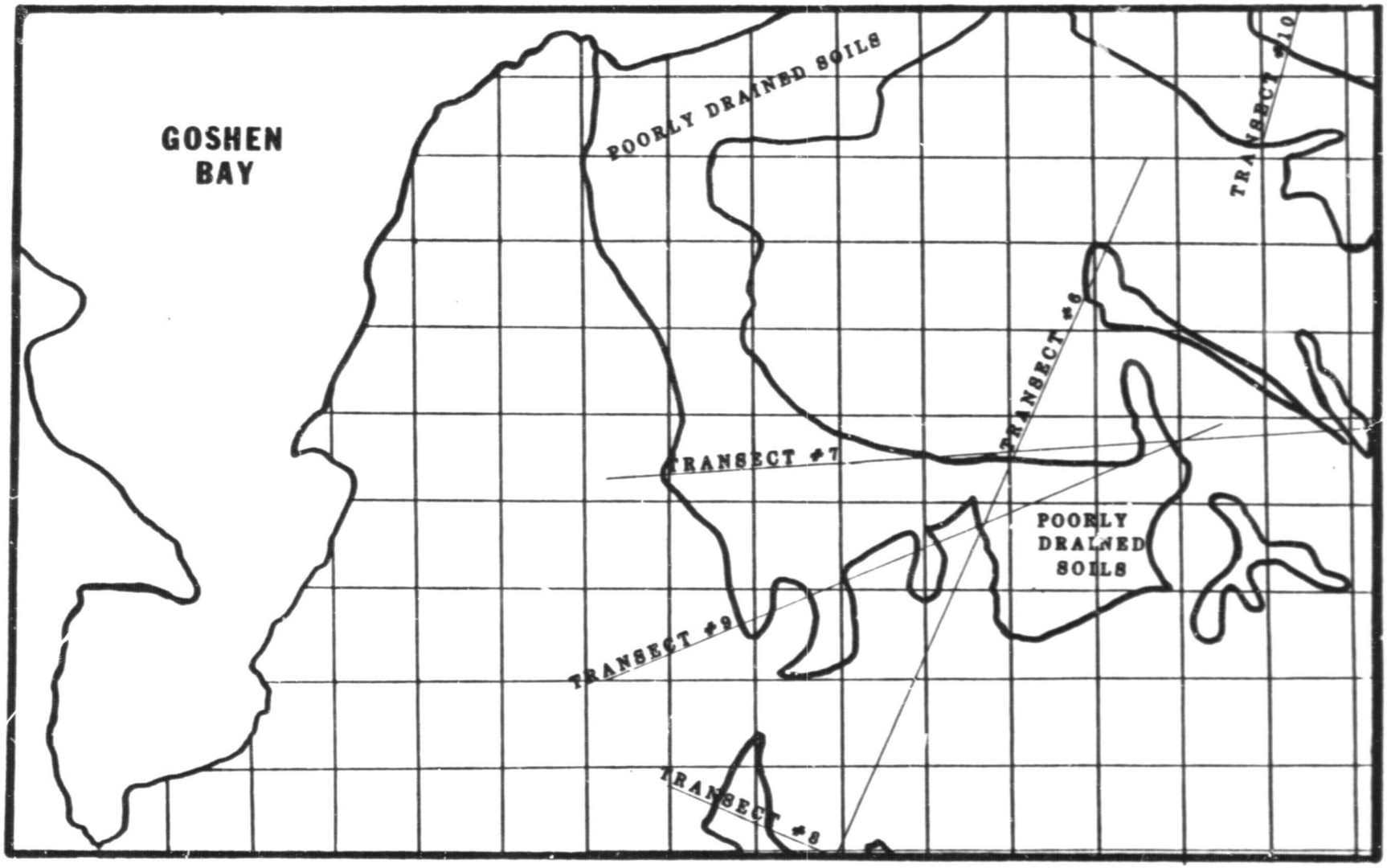

Figure 15.14B. Transects Examined as Compared to Utah County Government Groundwater Map.

that number of segments and additional intensity values were inserted between appropriate segments. The magnitude of the inserted value was the arithmetic mean of the two neighboring values.

After the ten best transects had been determined they were plotted as block diagrams, with the groundwater condition being the ordinate and distance along the transect being the absicissa. These transects were then overlayed on the HCMM DIR intensity maps for various seasonally representative days. The HCMM values were plotted as the ordinate, again with distance along the transect as the abscissa. These plots were then overlayed onto the block diagram of the transects previously obtained.

15.3.2 Results

A detailed comparison of the transects failed to lead to any conclusive results. Although some transects showed strong evidence of correlation, there existed a disturbing sign descrepancy. Le Shack et al (1975) had also experienced a similar discrepancy while doing work with soil moisture. Figures 15.15 and 15.16 represent two of the best correlations obtained. It was observed that as the groundwater approached the surface, the HCMM DIR intensities tended to rise, indicating higher ground surface temperatures. This result was opposite of what was expected, as well as opposite to the results obtained in the quantitative portion of the study. Apparently, what was being measured in the HCMM DIR intensities was some effect other than groundwater.

An examination of only early spring or late fall data failed to improve the situation. Figure 15.17 shows the correlation of transect 1 for May of 1978. Although a correlation seems to exist, it appears to change sign from one end of the transect to the other. The reason for this was unresolved.

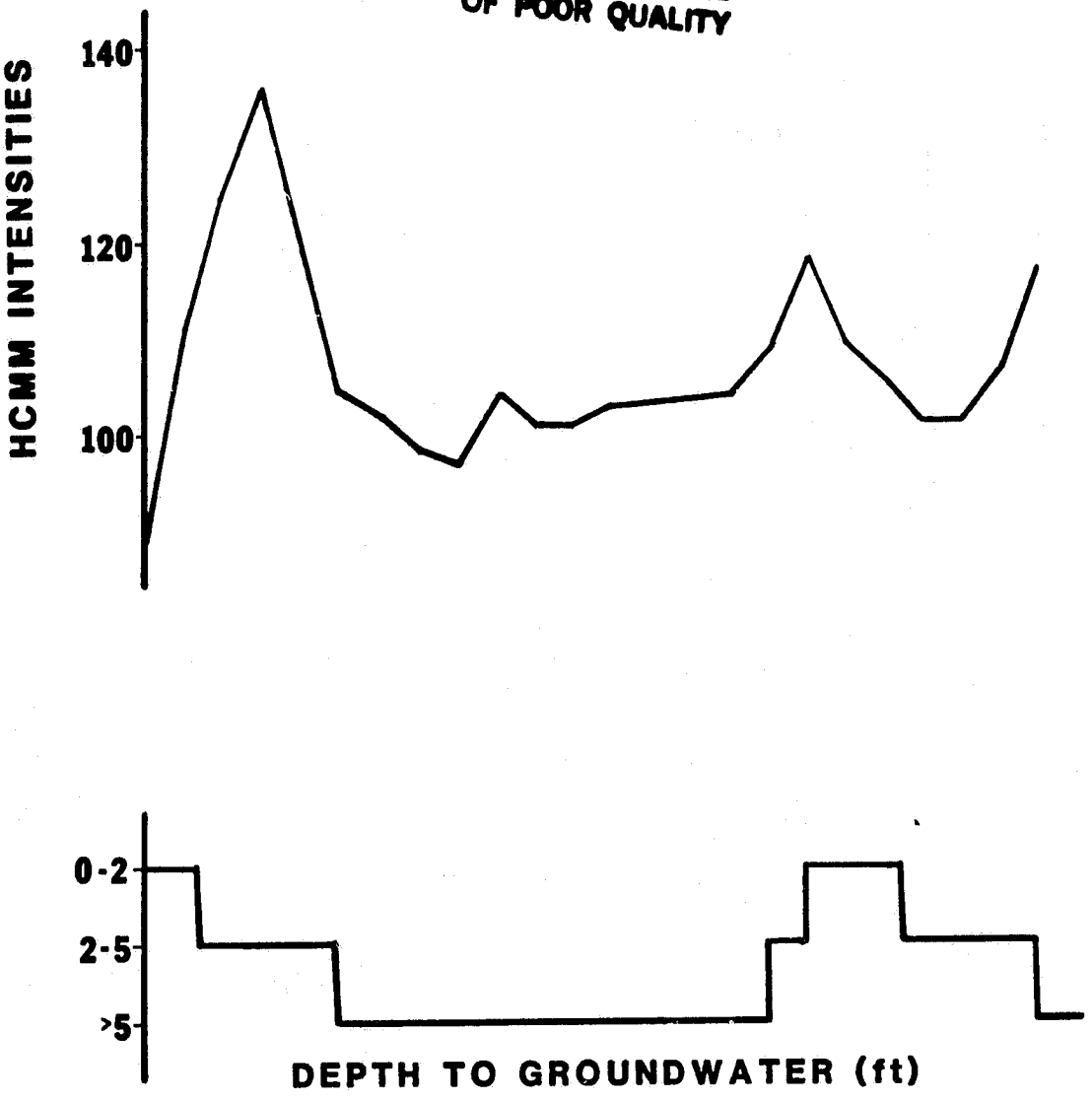

Figure 15.15. Comparison of Groundwater Profile to HCMM Intensities for 14, July 1979 (DAY INFRARED) Transect #5)

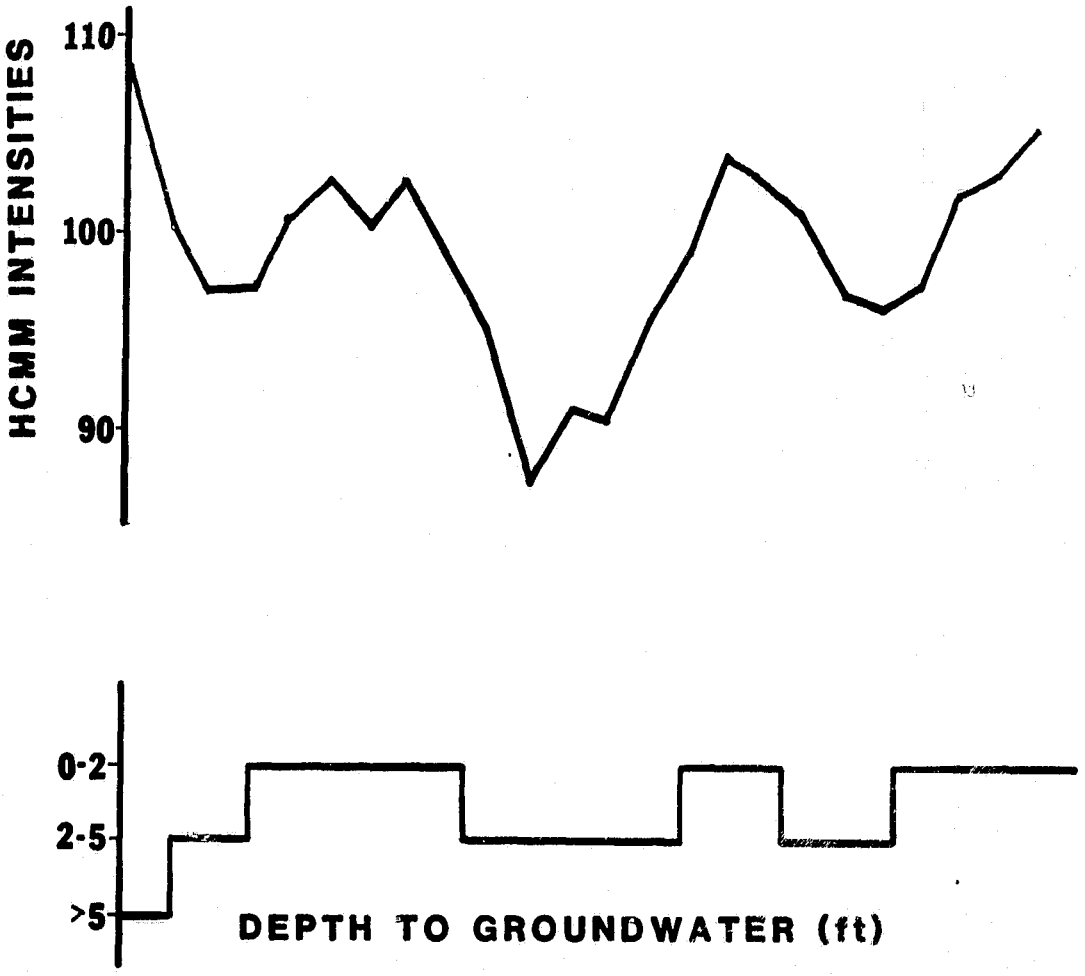

Figure 15.16. Comparison of Groundwater Profile to HCMM Intensities for 9, August 1979 (DAY INFRARED) Transect #4

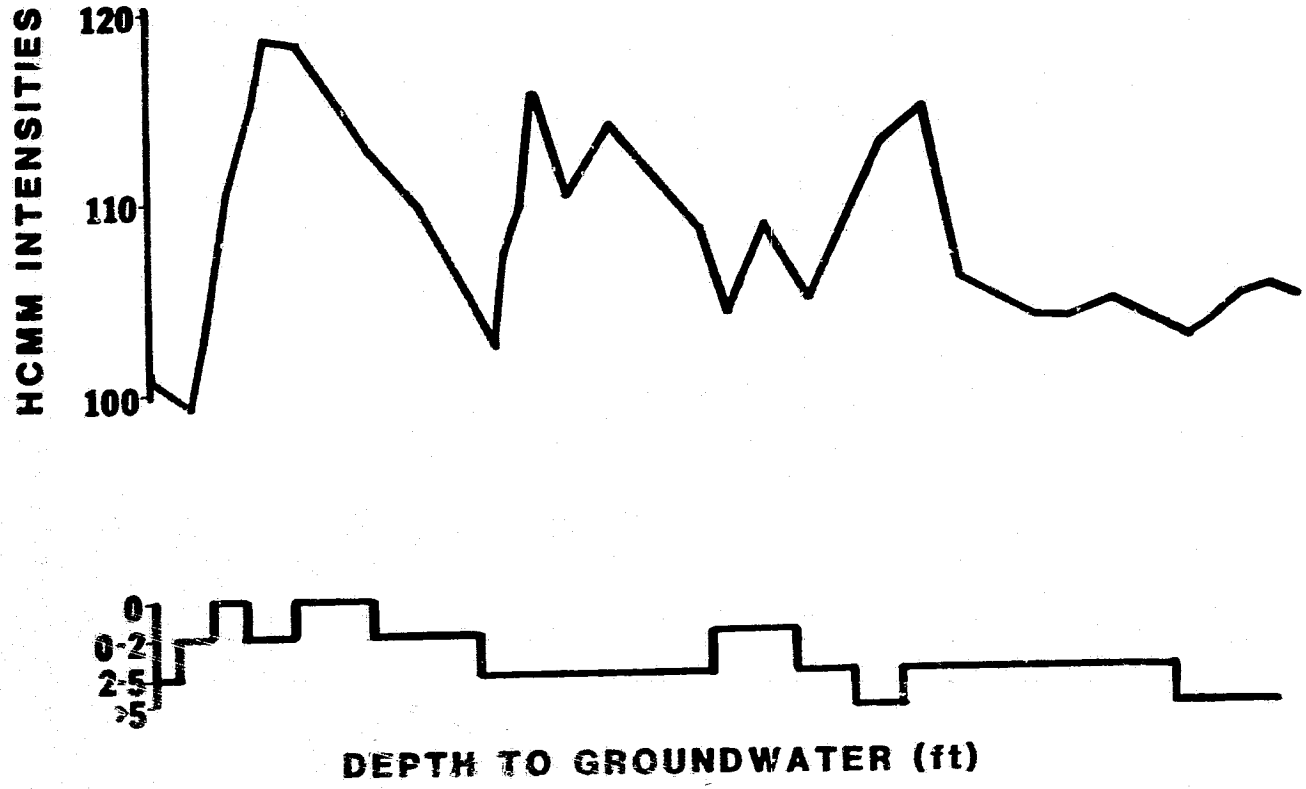

Figure 15.17. Comparison of Groundwater to HCMM Intensities for 13, May 1978 (DAY INFRARED) Transect #1

16. SUMMARY

16.1 Calibration

The study results indicate that the appropriate offset to be applied to calibrate the HCMM model to the Utah Valley area is + 5 degrees Celsius. The use of this offset yields radiative surface temperatures within approximately 1/2 degree Celsius of ground truth. This variation corresponds roughly to the accuracy of the combined sensing and telemetry equipment.

The lack of correlation between the required offset and the various examined atmospheric parameters indicates that the + 5 degrees should apply to any region of similar climate. The only significant parameter not examined was atmospheric transimissivity. This should be based on suspended particulate matter, and/or total atmosphere thickness above the study area. The 5 degree offset, therefore, may be restricted to areas of corresponding elevation (approximately 4,500 feet above mean sea level) and air quality.

In cases where a simplified relationship between HCMM sensed thermal IR intensities and surface temperatures is justified, it is felt that the linear relationship below yields sufficiently accurate values over the specified temperature range.

$$T = -7.172 + 0.3749\ I$$

where T = temperature in degrees Celsius ($0 < T < 30$)

and I = HCMM sensed thermal I R value

Although this is a fairly narrow temperature range, it essentially spans the range of water surface temperatures encountered in the study area. It should be emphasized that this model is entirely empirical, having no theoretical basis.

16.2 Water Quality

The statistical analyses performed on the data obtained from the Heat Capacity Mapping Mission and the water quality measurements made in Utah Lake in 1978 and 1979 yielded several significant relationships. The strong correlations identified between the DIR, VR and plankton concentration measurements provided the foundation for the use of the color prints to locate

areas of algae growth in Utah Lake. Several methods for identifying algae concentrations in the lake were determined, including the comparison of DIR and VR prints and the comparison of DIR and NIR prints.

Correlations between turbidity and the HCMM data were insignificant. This demonstrated that suspended algae in the lake were much more responsible for changes in the water's reflectivity than suspended sediments.

Relationships developed between algae concentrations in the lake and nutrient levels were inconclusive. This precluded the possibility of estimating nutrient concentrations in Utah Lake by assuming a relationship with algae growth and HCMM data.

16.3 Evaporation

Comparisons of wind and wind speed functions derived from HCMM data failed to yield significant correlations. This was mainly due to the small range of wind speeds on fair weather HCMM overflight dates. The HCMM day/night average temperatures, and likewise wind speed functions, compare well with average evaporation pan temperatures and extrapolation from pan data for larger wind speed ranges can be made. HCMM day temperatures are much lower ($7^{o}$to 14^{o}) than maximum pan temperatures yielding much higher windspeed functions. Vapor pressures calculated from the HCMM day temperatures correspond very well with the vapor pressure calculated from the average pan temperatures.

Utah Lake monthly modeled evaporation and pan evaporation correlated well with HCMM day and night temperatures. The correlation of daily evaporation with HCMM day temperatures was lower (0.8) than with HCMM night temperature (0.97). For short time intervals (days), the night data might be useful in estimating evaporation while for monthly evaporation either night or day data appears useful. The encouraging night data results are most likely because night temperatures are unaffected by surface heat gain that is significant during the day. That is, night temperatures are much better gages of the actual average temperature and heat storage of the lake.

16.4 Groundwater

The study relating off season groundwater depth to HCMM sensed thermal IR intensity yielded a model with an extremely good correlation to ground truth. However, further research is needed before it can be accepted as significant. The limited amount of data is the problem. Also, the influence of the extraneous parameters mentioned in the analysis of the quantitative groundwater data could be of equal or greater magnitude than the actual data being studied. It is felt, however, that there does exist a measurable relationship between HCMM sensed surface temperatures and depth to groundwater. This relationship appears to follow an exponential curve of the form:

$$d = ae^{bT}$$

where d = depth to groundwater

T = HCMM sensed surface temperatures

BIBLIOGRAPHY

Anderson, H. M. and Horne, A. J., 1975. Remote Sensing of Water Quality in Reservoirs and Lakes in Semi-Arid Regions, College of Engineering and School of Public Health, University of California, Berkeley.

Barnes, W. L. and Price, John C., 1980. "Calibration of a Satellite Infrared Radiometer", Applied Optics, Volume 19, Number 13.

Bartholic, J. F. Namken, C. N. and Wiegand, C. L., 1972. "Aerial Thermal Scanner to Determine Temperatures of Soils and of Crop Canopies Differing in Water Stress" Agronomy Journal 64: 603-608.

Bold, Harold C. and Michael J. Wynne, 1978. Introduction to the Algae, Structure and Reproduction. Englewood Cliffs: Prentice Hall Inc.

Bonn, Ferdinand J., 1977. "Ground Truth Measurements for Thermal Infrared Remote Sensing", Photogrammetric Engineering and Remote Sensing, Volume 43, Number 8.

Brimhall, Willis H., Bassett, Irvin G. and Merritt, Lavere B., 1976. Reconnaissance Study of Deep-Water Springs and Strata of Utah Lake; Implications for Resource Management. Mountainland Association of Governments, Technical Report Number 3, Provo, Utah.

Bukata, R. P., Harris, G. P. and Bruton, J. E., 1974. The Detection of Suspended Solids and Chlorophyll (a) Utilizing Digital Multispectral ERTS-1 Data, Proc. 2nd Canad. Sympos. Remote Sensing.

Chase, P. E. and Reed, Larry, 1973. Utilization of ERTS-1 Data to Monitor and Classify Eutrophication of Inland Lakes, Report on NASA Contract NAS 521810.

Dustin, Jacob D., 1980. Hydrogeology of Utah Lake with Emphasis on Goshen Bay, Doctoral Dissertation, Department of Civil Engineering, Brigham Young University, Provo, Utah.

Dustin, Jacob D. and Merritt, Lavere B., 1980. Hydrogeology of Utah Lake with Emphasis on Goshen Bay. Utah Geological and Mineral Survey, Water Resources Bulletin 23.

Egan, W. G., 1980. Optical Remote Sensing of the Sea -- A Carribean Example, Fourteenth International Symposium on Remote Sensing of Environment, San Jose, Costa Rica.

Eisenlohr, Win. S. Jr., 1966. "Water Loss from a Natural Pond Through Transpiration by Hydrophytes" Water Resourses Research, Vol. 2 No. 3: 443-453.

Everitt, Ben, "Depth to Wet Season Water Table, Utah, Goshen and Cedar Valleys, Utah County, Utah." Unpublished Research Report.

Fuhriman, Dean K., Merritt, LaVere B., Bradshaw, Jerald S. and Barton, James R., 1975. "Water Quality Effect of Diking a Shallow Arid-Region Lake," Environmental Protection Technology Series, EPA-660/2-75-007, Grant Number R-801400.

Hanson, B. J., Leslie, T. A., Murray, M., Roberts, K. A., St. Clair, L. L., Toole, T. W. and Whiting, M. C., 1974. Utah Lake Plankton Crop Estimation Incorporating ERTS-1 Imagery, Department of Zoology and Botany, Brigham Young University, NSF Project GY-11530.

Heckman, Richard A. and Merritt, LaVere B., 1981. "Utah Lake Monograph," Great Bain Naturalist Memoirs, Number 5. Brigham Young University, Provo, Utah.

Horne, A. J. and Wrigley, R. C., 1974. "Remote Sensing and Lake Eutrophication", Nature, Volume 250, Number 5463.

Idso, S. B. and Schmugge, T. J., 1975. "The Utility of Surface Temperature Measurements for the Remote Sensing of Surface Soil Water Status" Journal of Geophysical Research, Volume 80, Number 21.

Idso, Sherwood B., 1981. "Relative Rates of Evaporative Water Losses from Open and Vegetation Covered Water Bodies." Water Resources Bulletin, American Water Resources Association.

Ikeda, S. and Adachi, N., 1978. "A Dynamic Water Quality Model of Lake Biwa -- A Simulation of the Lake Eutrophication", Ecological Modeling, Volume 4.

Jackson, R. D., 1980. Heat Capacity Mapping Mission (HCMM). Science and Education Administration, Phoenix, Arizona, N81-1249716, NASA-CR-163506.

Kohler, M. A., T. J. Nordenson, and W. E. Fox, 1955. Evaporation from Pans and Lakes. U.S. Department of Commerce, Weather Bureau, Research Paper No. 38. Washington: U.S. Government Printing Office.

Kohler, M. A., and L. H. Parmele, 1967. "Generalized Estimates of Free-Water Evaporation" Water Resources Research, Vol. 3 No. 4.

LeShack, L. A., DelGrande, N. Kerr, Outcalt, S. I., Lewis, J., and Jenner, C., 1975. "Correlation of Dual Channel IR Data with Soil Moisture Measurements", Final Report Contract 4-35308 Development and Resources Transportation Co. Silver Spring, Maryland.

Linacre, E., B. B. Hicks, G. R. Sainty and G. Grauze, 1970. "The Evaporation from a Swamp." Agricultural Meteorology, Vol 7: 375-386.

Linacre, E., 1976. "Swamps", Vegetation and the Atmosphere, Vol. 2: 329-347.

Lindenlaub, John C. and Davis, Shirley M., 1978. "Applying the Quantitative Approach", Remote Sensing: The Quantitative Approach, McGraw Hill Incorporated.

Matson, M. and Berg, C. P., 1981. "Satellite Detection of Seiches in Great Salt Lake, Utah", Water Resources Bulletin, AWWA, Volume 17, Number 1.

Merritt, LaVere B., Miller, A. Woodruff and Fuhriman, Dean K., 1981. A Utah Lake WHAB Study-, Tabulation of Water Quality Data for Utah Lake and its Tributaries, Volume II, Lake Sites. Prepared for U.S. Bureau of Reclamation, U.S. Department of the Interior Contract 8-07-40-50616. Eyring Research Institute, Provo Utah.

Miller, A. W., L. B. Merritt, D. K. Fuhriman, 1980. Utah Lake Evaporation Study, Prepared for USBR, U.S. Department of Interior, Eyring Research Institute, Provo, Utah.

Morton, F. I., 1975. "Estimating Evaporation and Transpiration from Climatological Observations." Journal of Applied Meteorology, Vol. 14.

Morton, F. I., 1979. "Climatological Estimates of Lake Evaporation." Water Resources Research, Vol. 15 No. 1: 64-76.

Morton F. I., 1980. Programs REVAP and WEVAP for Estimating Areal Evapotranspiration and Lake Evaporation from Climatological Observations, National Hydrology Research Institute, Inland Waters Directorate, Ottawa, Canada. Paper No. 12.

Munro, D. S., 1979. "Daytime Energy Exchange and Evaporation from a Wooded Swamp" Water Resources Research, Vol. 15 No. 5: 1259-1265.

Myers, Victor I., 1970. "Remote Sensing for Defining Aquifers in Glacial Drift", NASA Annual Earth Resources Program Rev., 3rd, Volume 3.

NASA, 1980. Heat Capacity Mapping Mission (HCMM) Users Guide, Second Revision NASA: Goddard Space Flight Center, Greenbelt, Maryland.

Penman H. L., 1948. "Natural Evaporation from Open Water, Bare Soil and Grass" Proceedings of the Royal Society, Vol. 193: 121-145.

Piech, K. R., Schott, J. R. and Stewart, K. M., 1978. "The Blue-to-Green Reflectance Ratio and Lake Water Quality," Photogrammetric Engineering and Remote Sensing, Volume 44, Number 10.

Reeves, Robert G., 1975. Manual of Remote Sensing, American Society of Photogrammetry, Falls Church, Virginia.

Rijks, D. A., 1969. "Evaporation from a Papyrus Swamp" Quarterly Jounal Royal Meteorlogical Society, Vol. 95: 643-649, 1969.

Rohwer, Carl, 1931. Evaporation from Free Water Surfaces. "U.S. Department of Agriculture, Technical Bulletin No. 271. Washington; U.S. Government Printing Office.

Rohwer, Carl, 1933. "Evaporation from Different Types of Pans." American Society of Civil Engineers, Transactions pg. 673-703.

Rosema, A. and Bijleveld, 1978. "'Tell Us': A combined Surface Temperature, Soil Moisture and Evaporation Mapping Approach", Proceedings of The Twelfth International Symposium on Remote Sensing of the Environment, Volume 3.

Ross, L. and Rushforth, S., 1980. The Effects of a New Reservoir on the Attached Diatom Communities in Huntington Creek, Utah. Hydriobiologia, Volume 68, Number 2.

Rushforth, S. R., Grimes, J. A. and Javakul, A., 1980. An Introduction to the Algal Floras of Utah Lake, Utah, WHAB Study Contract 8-07-40-50616, Eyring Research Institute.

Rushforth, S. R., Grimes, J. A. and Javakul, A., 1981. Study of the Phytoplankton Along Established Permanent Transects In Utah Lake, Utah, WHAB Study Contract 8-07-40-50616, Eyring Research Institute, Provo, Utah.

Ryan, Thomas A. Jr., Joiner, Brian L. and Ryan, Barbara F., 1976. Minitab II Reference Manual, Preliminary Edition, Statistics Department, Pennsylvania State University, University Park, Pennsylvania.

Schott, J. R., 1980. Remote Sensing of Thermal Loadings on Aquatic Systems, Fourteenth Congress of the International Society of Photogrammetry, Commission VII, Hamburg, Germany.

Shannon, C. and Weaver, W., 1963. The Mathematical Theory of Communication, University of Illinois Press, Illinois.

Shih, S. F. and Gervin, J. C., 1980. "Ridge Regression Techniques Applied to Landsat Investigation of Water Quality in Lake Okeechobee", Water Resources Bulletin, American Water Resources Association, Volume 16, Number 5.

Squires, L. E., Whiting, M. C., Brotherson, J. D. and Rushforth, S. D., 1979. "Competitive Displacement as a Factor Influencing Phytoplankton Distribution in Utah Lake, Utah", Great Basin Naturalist, Volume 39, Number 3.

Starr, Richard C., 1978. "The Culture Collection of Algae at the University of Texas at Austin," Journal of Phycology, Supplement Vol. 14.

Strong, A. E., 1974. ERTS-1 Observes Algal Blooms in Lake Erie and Utah Lake, Remote Sens. Environ. Volume 3.

Tanis, F. J., 1978. A Remote Sensing Technique to Monitor Benthia Algae, Environ. Research Inst. of Michigan Report.

Tunheim, Jerald A. and Beutler, Gerard A., 1980. Model Development for Predicting Soil Moisture by Thermography, Office of Water Research and Technology, U.S. Department of Interior, Project A-063-SDAK, Washington, D.C.

Walpole, Ronald E. and Myers, Raymond H., 1978. Probability and Statistics for Engineers and Scientists, Second Edition, MacMillan Publishing Company, New York.

Welby, C. W., Witherspoon, A. M. and Holman, R. E., 1977. Monitoring of Water Quality and Trophic States in Shallow Coastal Lakes and Estuaries -- A Use of Landsat Imagery, National Aeronautics and Space Administration, Contract No. NAS8-31984.

Whiting, J. M., 1976. "Airborne Thermal Infrared Sensing of Soil Moisture and Groundwater", Remote Sensing of Soil Moisture and Groundwater, Workshop Proceedings, The Canadian Aeronautics and Space Institute.

Whiting, M. C., Brotherson, J. D. and Rushforth, S. R., 1978. "Environmental Interaction in Summer Algal Communities of Utah Lake", Great Basin Naturalist, Volume 38, Number 1.

Wrigley, R. C. and Horne, A. J., 1975. Surface Algal Circulation Patterns in Clear Lake by Remote Sensing, NASA Technical Memorandum X-62,451.

Wrigley, R. C., Klooster, S. A., LeRoy, M. J., Horne, A. J. and Anderson, H. M., 1975. Field Measurement of Algal Biomass by Infrared Reflectance, NASA Technical Memorandum X-73,107.

Wrigley, R. C., 1980. Introduction to Coastal Zone Color Scanning, American Association for the Advancement of Science Annual Meeting, San Francisco, California.